COMMITTEE CERTIFICATION OF APPROVED VERSION

The committee for Aimalohi Esechie certifies that this is the approved version of the following dissertation:

MECHANISMS OF IMPROVEMENT FOLLOWING FUNCTIONAL INHIBITION OF NITROSATIVE STRESS AFTER BURN AND SMOKE-INDUCED ACUTE LUNG INJURY

Committee:

_____
Daniel L. Traber, Ph.D., Chair

_____
George C. Kramer, Ph.D.

_____
Simon Lewis, Ph.D.

_____
Hiroshi Saito, Ph.D.

_____
Hal K. Hawkins, M.D., Ph.D.

_____
Csaba Szabo, M.D., Ph.D.

_____
Dean, Graduate School

MECHANISMS OF IMPROVEMENT FOLLOWING FUNCTIONAL INHIBITION OF NITROSATIVE STRESS AFTER BURN AND SMOKE-INDUCED ACUTE LUNG INJURY

by

Aimalohi Esechie, B.S., M.S.

Dissertation
Presented to the Faculty of The University of Texas Graduate School of Biomedical Sciences at Galveston
in Partial Fulfillment of the Requirements
for the Degree of

Doctor of Philosophy

Approved by the Supervisory Committee

Daniel L. Traber, Ph.D.
George C. Kramer, Ph.D.
Simon Lewis, Ph.D.
Hiroshi Saito, Ph.D.
Hal K. Hawkins, M.D., Ph.D.
Csaba Szabo, M.D., Ph.D.

December, 2008
Galveston, Texas

Key words: inflammation, neutrophils, nitrosative stress, oxidative stress

I would like to dedicate this work to my parents, Dr. Humphrey and Jovita Esechie who are a continual source of strength and inspiration and encouragement.

And to my sister Emilomo, and brothers, Imonihke and Ohihoin, who have been my cheerleaders and my biggest fans throughout this process.

ACKNOWLEDGEMENTS

I wish to acknowledge the contribution of many in my training and the completion of this work. Specifically, I wish to recognize Dr. Daniel Traber for his dedication to his students and patient nurturing of my skills.

I wish to acknowledge the members of the Traber lab, Dr. Perenlei Enkbaatar, Dr. Don Deyo, Lillian Traber, Collette, Yoshi, Jainpu, Hama, Matthias, Nettie, Jeff and Randy for their support and the occasional good laugh.

I wish to acknowledge Drs. Csaba Szabo and Paul Hill at Ikaria for the generous supply of Sodium Hydrogen Sulfide for the completion of this work.

I would also like to acknowledge the other members of my dissertation committee, Dr. George Kramer, Dr. Hal Hawkins, Dr. Simon Lewis and Dr. Hiroshi Saito, for their advice and support.

MECHANISMS OF IMPROVEMENT FOLLOWING FUNCTIONAL INHIBITION OF NITROSATIVE STRESS AFTER BURN AND SMOKE-INDUCED ACUTE LUNG INJURY

Publication No._____

Aimalohi Esechie, Ph.D.
The University of Texas Graduate School of Biomedical Sciences at Galveston, 2008

Supervisor: Daniel L. Traber

Severe trauma, caused by flame burn and smoke (B + S) inhalation induces acute lung injury (ALI) and results in the loss of pulmonary function. A cascade of molecular and cellular events initiates the formation of reactive oxygen/nitrogen species (ROS/RNS) that in turn drives an inflammatory response and consequently cell death through hyper-activation of poly (ADP-ribose) polymerase (PARP-1). The purpose of this study was to investigate and counteract pulmonary dysfunction associated with nitrosative stress generated after B + S inhalation injury in an ovine and murine model of ALI.

In our time course experiment, sheep were sacrificed at 4, 8, 12, 18 and 24 hours post B + S injury. From 4 through 24 hours, there was a progressive increase in airway obstruction and lung edema formation. Furthermore, injury was associated with increased ROS/RNS generation, pro-inflammatory cytokine expression and neutrophil accumulation. Additionally, PARP-1 enzymatic activity increased in parallel with Hoechst 3324 nuclear staining in sheep lung sections.

Treatment after ALI with a hydrogen sulfide (H_2S) donor compound, a peroxynitrite scavenger, was tested to determine the effect on mortality, pulmonary shunt fraction and gas exchange. The H_2S donor increased animal survival. Additionally the rapid decline in PaO_2/FiO_2, reduced the pulmonary shunt fraction and elevated airway pressures were improved. Likewise, the lung histological assessment demonstrated marked increase in aerated areas in lung sections.

Burn and smoke injury generates reactive oxygen species and nitrogen species and influences inflammatory cytokine expression. Pro- and anti-inflammatory cytokine protein levels were measured in the lung parenchyma as well as 3-nitrotyrosine and protein carbonyl formation (indices of RNS and ROS generation, respectively). In our murine study, treatment with the H_2S donor significantly reduced the pro- inflammatory cytokine level and increased the anti-inflammatory cytokine concentration in the lung. Additionally, ROS and RNS generation were significantly lowered.

These results demonstrate the effectiveness of inhibiting nitrosative stress after burn and smoke injury using a H_2S donor and a possible mechanism for improved outcomes may be the altered the expression pattern of pro- and anti-inflammatory cytokines and ROS generation which may contribute to dysfunctional outcomes after B+ S inhalation injury.

TABLE OF CONTENTS

LIST OF TABLES

LIST OF FIGURES

CHAPTER 1

BACKGROUND

INTRODUCTION

The incidence of acute lung injury (ALI) affects nearly 200,000 patients annually in the United States, of which 74,000 people die each year [Pruitt *et al.*, 2002; Rubenfeld *et al.*, 2005]. ALI is commonly associated with severe trauma, such as burn and smoke inhalation, sepsis, and shock, and is clinically manifested as severe arterial hypoxemia and pulmonary edema in the absence of elevated left atrial pressure. In the United States alone, smoke inhalation injury causes over 6000 deaths annually and more than 23,000 injuries [Alcorta, 2004]. Combined cutaneous burn and smoke inhalation injury is a major determinant of mortality in this trauma [Moylan, 1981; Shirani *et al.*, 1987; Wolf *et al.*, 1997; Barrow *et al.*, 2004]. Together these statistics attributed to burn and smoke-induced ALI therefore warrants continued investigation to further our understanding.

The major physiological derangement of ALI is compromised gas exchange [measured as the ratio between arterial blood oxygen (PaO_2) and the fraction of inspired oxygen (FiO_2)] and severe hypoxemia. These functional alterations are associated with damage to the alveolar membrane, increased alveolar-capillary permeability, and accumulation of protein-rich fluid in the alveolar space. The alveolar epithelium plays a critical role in the pathogenesis of ALI. In a normal healthy lung, the alveolar epithelium forms a barrier to alveolar flooding. In an experimental setting, there is substantial evidence that indicates pulmonary transvascular fluid flux increases resulting in elevated

interstitial pressure that is due to fluid accumulation in the interstitium [Sakurai *et al.*, 1999; Soejima *et al.*, 2001; Enkhbaatar *et al.*, 2008]. These findings have also been described in patients with smoke inhalation and burn injury [Herndon *et al.*, 1987].

Patients suffering from ALI experience a fall in oxygen saturation of the arterial blood. Redistribution of blood in the lungs in response to alveolar hypoxia also termed hypoxic pulmonary vasoconstriction (HPV) is an adaptive vasomotor response. HPV diverts blood flow from poorly oxygenated areas to optimally ventilated lung segments by an active process of vasoconstriction, particularly involving the small resistance pulmonary arteries. The hypothesized mechanism involves hydrogen peroxide (H_2O_2) generation by oxygen sensor, NADH oxireductase. H_2O_2 acts as a diffusible redox mediator and interacts with the anti-oxidant enzyme catalase to activate soluble guanylate cyclase and increase cGMP to provide tonic vasorelaxation under normoxic conditions. However, under hypoxic conditions, H_2O_2 production is reduced, resulting to the loss of the vasorelaxant influence, thus leading to hypoxic inhibition of certain voltage-gated K+ channels (Kv) in pulmonary artery smooth muscle cells [Reeve *et al.*, 2001; Sham, 2002]. This response establishes ventilation-perfusion matching and results in increased arterial oxygenation.

Smoke inhalation injury alone impairs HPV and combined burn and smoke-induced ALI significantly attenuates HPV [Theissen *et al.*, 1989; Westphal *et al.*, 2006; Westphal *et al.*, 2008]. Research by Westphal *et al* and others suggests that the loss of HPV is associated with an increase in inducible NOS (iNOS) mRNA transcription, elevated plasma nitric oxide (NO) concentration as well as an increase in reactive

nitrogen species in lung tissue [Westphal *et al.*, 2006; Petersen *et al.*, 2008]. Whereas burn and smoke injury increase NO production via induction of iNOS with a subsequent loss of HPV, N^{ω}-monomethyl-L-arginine (L-NMMA), a general NOS inhibitor, improves HPV blunting in sepsis induced ALI [Fischer *et al.*, 1997]. Additionally the loss of HPV is associated with an exaggerated inflammatory response in the lung via tumor necrosis factor-alpha (TNF-alpha) production [Johnson *et al.*, 1993; Petersen *et al.*, 2008]. Taken together, these data suggests that the pathogenesis of ALI is mediated in part through iNOS generated NO and increased levels of inflammatory molecules.

Multiple organ failure (MOF) is reported in patients with ALI [Oba and Salzman, 2000; Ware and Matthay, 2000]. In fact, a recent study demonstrated that the onset of ALI, caused by lung injury, is essential to the development of post-injury MOF [Ciesla *et al.*, 2005]. A similar observation has been made in our ovine model of ALI, where renal failure (decreased urine output) was evident after burn and smoke injury [Soejima *et al.*, 2001; Murakami *et al.*, 2007]. Therapeutic intervention directed towards improving pulmonary dysfunction could therefore decrease progressive MOF associated with ALI.

SECONDARY ACUTE LUNG INJURY

The development of ALI can be divided into direct (pulmonary) or indirect (extra-pulmonary) injury leading to pulmonary inflammation. Direct lung injury includes those conditions such as toxic gas/smoke inhalation, pulmonary contusion, and aspiration of gastric contents [Traber *et al.*, 2007; Sutyak *et al.*, 2007; Hoag *et al.*, 2008] whereby toxic substances migrate from the trachea through the respiratory tree (bronchial and

bronchiole branches) and injures the lung parenchyma (Figure 1.1). Indirect injury involves blood-borne systemic inflammatory processes such as sepsis, acute pancreatitis and other clinical events including major surgery, multiple transfusions, and ischemia-reperfusion injury. Burn and smoke induced-ALI comprises both types of lung injury.

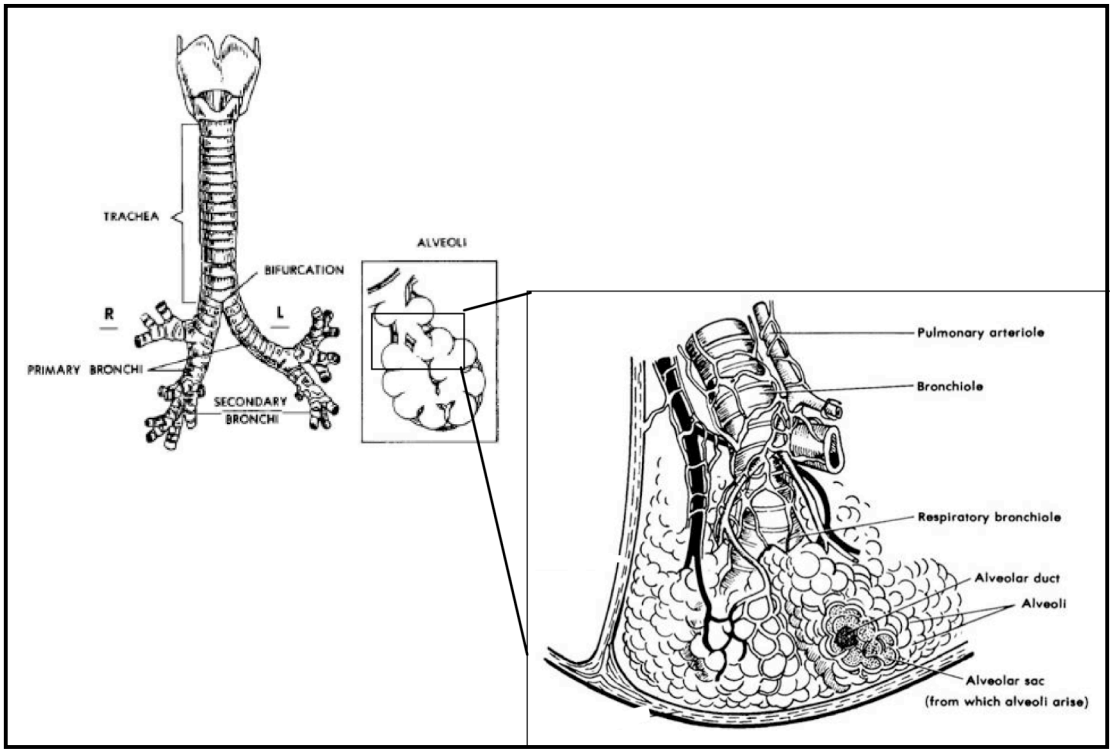

Figure 1.1 Diagram of the respiratory airways and lung lobule. Adapted from Respiratory Diseases and Disorders v1.0 Corpyright ©2006.

After the primary injury of cutaneous thermal injury with a concomitant smoke inhalation injury, there is a secondary injury that begins within hours of trauma. This is a

multifaceted process that includes the immediate release of neutrophils, elevated levels of cytokines, generation of reactive oxygen/nitrogen species, and subsequent lipid peroxidation at the injury site and in the systemic organs.

ACUTE LUNG INJURY AND INFLAMMATORY CELLS

Neutrophils play a central role in immune response during ALI as phagocytic white blood cells. These cells have characteristic multi-lobular, chromatin dense nuclei and cytoplasmic granules. Neutrophil adhesion and migration out of the vascular system and into the interstitial tissue occurs when there is inflammation or a need for an immune response. There are four steps associated with the adhesion cascade. The first step of the cascade is the rolling of neutrophils along the endothelial surface. In the second step, neutrophils are activated by signals present at the luminal surface of the endothelium. In the third step, neutrophils firmly adhere to the activated endothelial cell. Finally, in the fourth step, neutrophils emigrate into the injured tissue.

Neutrophils interact with specific receptors on the endothelial cells of the vessel wall, causing them to roll along the wall [Kogaki *et al*., 1999]. This is accomplished by selectins on the endothelial cell and their carbohydrate ligands. There are several types of selectins designated L-selectin (expressed on leukocytes), P-selectin (expressed on platelets and endothelial cells) and E-selectin (expressed on endothelial cells). P-selectin carried inside endothelial cells appears on the surfaces within a few minutes of exposure to cytokines or other inflammatory mediators [Lorenzon *et al*., 1998]. E-selectin on the other hand appears a few hours later. The selectins interact with neutrophil glycoproteins

and allows them to roll along the vessel wall, thereby permitting stronger and more stable adhesion [Tedder *et al*., 1995; Kogaki *et al*., 1999; Gardiner *et al*., 2001].

Neutrophil extravasation involves leukocyte functional antigen-1 (LFA-1) and Mac-1, intercellular adhesion molecules, ICAM-1 and ICAM-2 on the endothelium, as well as a further interaction involving an immunoglobulin-related molecule called platelet/endothelial cell adhesion molecule (PECAM), which is expressed both on the neutrophil and at the intercellular junctions of endothelial cells [Cooper, 2000; Janeway *et al*., 2001]. These interactions enable the phagocyte to squeeze between the endothelial cells. It then penetrates the basement membrane with the aid of proteolytic enzymes that break down the basement membrane proteins. The movement through the vessel wall is known as diapedesis, and enables neutrophils to enter the tissue [Janeway *et al*., 2001].

Patients suffering from ALI have a dramatic increase in neutrophils sequestered within the lung. These cells arrive in an activated state and display enhanced cytotoxic effects in the form of elevated levels of oxidants such as superoxide ($O\bullet_2$) and hydrogen peroxide (H_2O_2), elevated levels of reactive nitrogen species such as peroxynitrite (ONOO-), and release of neutrophil elastase, all of which act to disrupt the structure and architecture of the lung parenchyma [Sutter *et al*., 1992]. Damage to the epithelial and endothelial barriers in the lungs is associated with a massive increase in epithelial and endothelial permeability with accumulation of high-molecular-weight proteins that are normally excluded from the alveoli.

ACUTE LUNG INJURY AND MEDIATORS OF INFLAMMATION

The redox regulation of transcription factors, their target genes and gene products are important processes in the normal inflammatory response, as well as in the development of immune disorders. Nuclear factor-κB (NF- κB) is the major redox responsive transcription factor and it binds with a consensus sequence located in the promoters of nearly all genes involved in the initiation of an inflammatory response [Lavrovsky *et al*., 2002; Cheng *et al*., 2006].

The large influx of neutrophils during ALI is a hallmark of this injury and is largely mediated by inflammatory mediators. Clinical evidence suggests that cytokines play a role in the pathology of ALI. A recent study investigating bronchial inflammatory markers following smoke inhalation in burn victims, reported a marked temporal increase in concentrations of the pro-inflammatory cytokines interleukin -1 beta (IL-1β) and IL-8 in the tracheobronchial suction fluid during the first 6 hours following smoke exposure [Kurzius-Spencer *et al* 2008]. In fact, elevated levels of IL-8 and IL-1β are consistent findings in patients with the onset of ALI and sustained ALI [Miller *et al*., 1992; Villard *et al*., 1995; Goodman *et al*., 1996; Park *et al*., 2001]. Increase plasma and bronchial alveolar lavage fluid levels for cytokines such as IL-6, TNF-α and VEGF has also been reported [Goodman *et al*., 1996; Parker *et al*., 2005].

ACUTE LUNG INJURY AND NITROSATIVE AND OXIDANT STRESS

The cellular responses to oxidative stress are crucial for survival and essential for the normal function of the respiratory system in particular. The adaptive mechanism

includes induction of both intracellular antioxidant enzymes such as superoxide dismutase, catalase and gluthathione, as well as systemic free-radical scavengers such as vitamin E and vitamin C [reviewed by Cooper *et al.*, 2002]. However, oxidative stress does occur when the production of reactive oxygen species overwhelms that capacity of the cell to detoxify these oxidants using endogenous defense systems.

Reactive oxygen species (ROS) are produced by a variety of enzymes including xanthine oxidase (XO), NAD(P)H oxidase, and nitric oxide synthase (NOS) just to name a few. Physiologically, the NOS enzyme produces NO via the oxidative deamination of L-arginine to L-citrulline. This process requires the cofactors NADH and tetrahydrobiopterin (BH_4). In burn and smoke injury, it appears that these factors, in addition to L-arginine, are depleted resulting in the uncoupling of NOS and the generation of $O\bullet_2$ and H_2O_2. NO reacts with these ROS to form RNS such as peroxynitrite [Xia *et al.*, 1996]. The damage caused by ROS is attributed to the ability of this molecule to initiate a chain of reduction-oxidation reactions in the cell such that the production of one ROS often results in the production of other ROS. ROS such as the highly reactive hydroxyl radical rapidly attacks biological components, such as plasma membrane lipids [Hamahata *et al.*, 2008]. Protein oxidation also occurs due to the ability of molecules like hydroxyl radical to react with transition metals that are typically found in cellular proteins [Stadtman 1993; Shacter 2000; Esechie *et al.*, 2008].

Production of reactive nitrogen species (RNS) is related to a significant induction of iNOS transcription through NF-κB nuclear mobilization. iNOS produces a significant amount of NO in a relatively short period of time. Once NO is generated in close

proximity to superoxide, peroxynitrite (ONOO-) is formed. Accumulating evidence suggests that an increase in superoxide and NO at a 10-fold greater rate will increase peroxynitrite formation by 100-fold. Under pro-inflammatory conditions, NO and superoxide are simultaneously produced at a rate 1000-fold greater. This increases the formation of peroxynitrite by 1,000,000-fold [Pacher *et al.*, 2007]. Peroxynitrite, generated from this interaction nitrates proteins on tyrosine residues in a mechanism in which a hydrogen atom is abstracted from tyrosine to form an intermediate tyrosly radical that quickly combines with nitrogen dioxide to produce 3-nitrotyrosine [Beckman, 1996]. Tyrosine nitration affects protein structure and function, alters catalytic activity of enzymes and impairs cellular signal transduction. Peroxynitrite can also cause the oxidative modification of other amino acid residues, including methionine, trytophan, cysteine and phenylanaline [Ischiropoulos and al-Mehdi, 1995]. Therefore, nitrotyrosine formation can be considered a marker of 'nitrosative' stress.

ACUTE LUNG INJURY AND CELL DEATH

The pivotal role of peroxynitrite in ALI is increasingly recognized due to its ability to react with key components within the nuclear compartment thus affecting critical functions in this organelle. It is also known that in conditions of high NO production, there is an interruption in the transfer of electrons at cytochrome oxidase which markedly increases the leakage of electrons from the respiratory chain, resulting in enhanced formation of superoxide within the mitochondrial matrix and generation of significant amounts of peroxynitrite [Heck *et al.*, 2005]. In the nuclear compartment,

peroxynitrite-dependent DNA damage and activation of DNA repair enzyme poly (ADP ribose) polymerase-1 (PARP-1) are central in initiating cell death after injury. PARP-1 is a member of the PARP family. PARP-1 detects and signals DNA strand breaks induced by ROS and RNS. Upon binding to DNA strand breaks, PARP transfers ADP-ribose units from the coenzyme nicotinamide adenine dinucleotide (NAD^+) to various nuclear proteins (DNA polymerase and histones, for example) [Berger, 1985; Pacher *et al.*, 2007]. Over time, these units polymerize to reach up to 200 poly (ADP) ribose (PAR) units [Shall and de Murcia, 2000]. Upon severe DNA damage, over-activation of PARP-1 depletes the cellular stores of the NAD+ [Szabo *et al.*, 1996]. This leads to a marked decrease in the cellular pools of ATP resulting in cellular dysfunction and eventually cell death. PARP-1 is also involved in the up-regulation of inflammatory processes. In the absence of functional PARP-1, expression of pro-inflammatory cytokines, chemokines and enzymes is significantly attenuated via a mechanism involving NF-κB [Oliver *et al.*, 1999]. Included in this work are experiments designed to examine the earliest time point after burn and smoke inhalation injury, PARP-1 activity is up-regulated and NF-κB enters the nuclear compartment.

SUMMARY AND EXPERIMENTAL DESIGN

Cytokine production, in response to ROS/RNS, is tightly regulated by DNA-binding transcription factors such as NF-κB. Upon phosphorylation by IKK, the inhibitory κB proteins that sequester NF-κB to the cytoplasmic compartment, are

degraded, thus mobilizing NF-κB into the nucleus. NF-κB binds to its response element and begins transcription of inflammatory cytokines. Equally as important is the oxidative DNA damage, in particular to adenosine or guanine bases, after injury. In such instances, DNA repair enzymes such as PARP-1, recognize single strand DNA nicks and attempt to 'band-aid' the lesion by synthesizing PAR. These are general inflammatory phenomena and suggest that there indeed may be similarities of the inflammatory response in smoke and burn injury to other kinds of trauma that lead to ALI.

Our current understanding of the molecular events that occur in the lung after burn and smoke –induced ALI are gathered from studies conducted at 48 hours post injury in a clinically relevant ovine model (Fig 1.2) [Soejima *et al.*, 2001; Westphal *et al.*, 2006; Westphal *et al.*, 2008]. Here, we characterize the early molecular events in the lung after injury, a previously unconsidered time period in burn and smoke inhalation injury using a clinically relevant ovine model. In particular, we explore the role of peroxynitrite formation and protein oxidation after injury and correlate these findings with morphological alterations and functional changes such as gas exchange. We report the effectiveness of sodium hydrogen sulfide (NaHS), a H_2S donor and peroxynitrite "scavenger" in preventing the formation of 3-nitrotyrosine in the lung and the subsequent amelioration of deleterious sequelae. We support our findings from the ovine model using a murine model of burn and smoke-induced ALI.

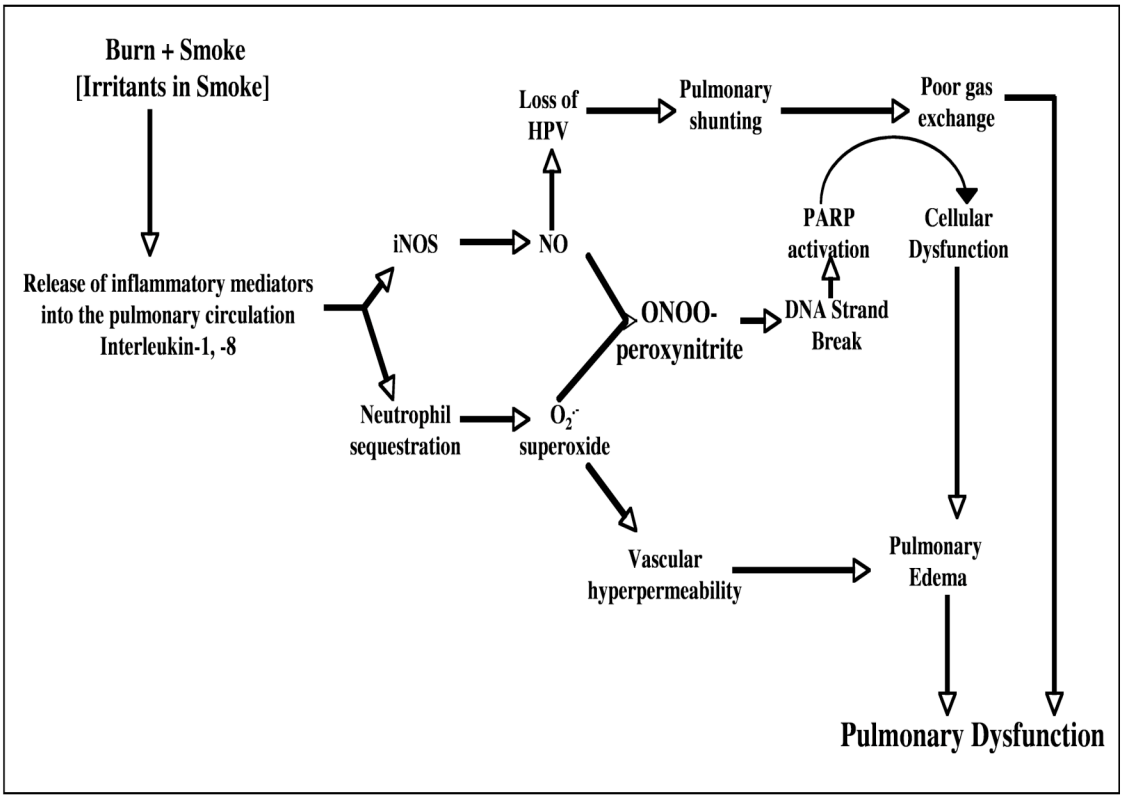

Figure 1.2 Schematic depiction of the ways in which burn and smoke inhalation injury leads to peroxynitrite and superoxide formation and consequently pulmonary dysfunction.

HYPOTHESIS

Burn and smoke inhalation injury results in an early and robust development of nitrosative stress response that attenuates pulmonary function and increase mortality.

This hypothesis will be tested in an ovine and murine model of burn and smoke inhalation injury following the experimental designed outlined below.

EXPERIMENTAL DESIGN

Hypothesis 1: Lung histological outcomes and pulmonary function are altered early after injury in an ovine model of burn and smoke induced ALI.

Specific Aim 1: To understand how the temporal changes in lung histology, after burn and smoke injury, affects pulmonary function, cardiopulmonary hemodynamics, neutrophil infiltration and lung cytokine expression.

Experiment: Using a scoring system, quantify septal edema formation, septal inflammation and degree of bronchial and bronchiole obstruction in masked serial histological sections of animals in the control group and at specific times after injury: 4, 8, 12, 18 and 24 hours post injury.

Experiment: Record the hemodynamic values and calculate the ratio between partial pressure of oxygen in arterial blood and the fraction of inspired oxygen (PaO_2/FiO_2). Blood-free wet-to-dry weight ratio will be calculated at the different experimental time points and compared to the control animals.

Experiment: Using a standard assay for myeloperoxidase (MPO), quantify MPO activity in lung samples from the lower right lobe taken at the same time points as the previous experiments.

Experiment: In parallel, samples from animals at the same time points as in the previous experiment will be homogenized and protein extracts will be assayed for cytokine expression using sodium dodecyl sulfate (SDS) gel electrophoresis followed by immunoblotting.

Hypothesis 2: Cell death in the lung correlates with the early presence of nitrosative and oxidative stress induced PARP activation.

Specific Aim 2.1: Demonstrate the presence of nitrosative stress and oxidative stress after injury.

Experiment: Lung tissue samples and plasma will be taken at specific times after injury: 4, 8, 12, 18 and 24 hours post injury. Plasma nitrite/nitrate, tissue iNOS and 3-nitrotyrosine will be analyzed.

Experiment: Using an assay to detect protein oxidation, lung tissue will be taken at the same time point and homogenized and dinitrophenylhydrazine (DNPH) will be used to derive carbonyl groups present on oxidized proteins. SDS gel electrophoresis followed by immunoblotting will be performed on each sample.

Specific Aim 2.2: Establish when burn and smoke exposure increases nuclear and cytoplasmic PAR polymers.

Experiment: Lung tissue samples will be homogenized, the nuclear fraction will be isolated, immunoblotted for PAR polymers.

Experiment: Determine the degree of PARP activity by immunohistochemistry in serial lung sections from animals at specific times after injury: 4, 8, 12, 18 and 24 hours post injury.

Specific Aim 2.3: Establish whether burn and smoke results in cell death in the lung.

Experiment: Determine Hoechst intensity in serial cyro-sections of animals from each experimental group after injury.

Hypothesis 3: Reducing nitrosative stress using a hydrogen sulfide donor improves pulmonary function and attenuates cytochrome C release in an ovine model of ALI, contributing to improved survival outcome.

Specific Aim 3.1: Establish whether diminished nitrosative stress improves gas exchange, pulmonary shunt fraction and airway pressure.

Experiment: Observe changes in pulmonary function by calculating PaO_2/FiO_2 and pulmonary function in the control and treated group.

Experiment: Measure changes in peak and pause airway pressure before and after injury in the control and the treatment group.

Specific Aim 3.2: Understand how diminished nitrosative stress affects downstream signaling cascade

Experiment: Plasma nitrite/nitrate will be measured using a colometric assay.

Experiment: Lung tissue iNOS and 3-nitrotyrosine will be analyzed using sodium dodecyl sulfate (SDS) gel electrophoresis followed by immunoblotting.

Experiment: Lung tissue samples will be homogenized, the nuclear fraction will be isolated, immunoblotted for PAR polymers

Experiment: In parallel, mitochondrial fraction will be isolated and assayed for cytochrome C using a commercially available enzyme linked immunoassay.

Hypothesis 4: Administration of peroxynitrite scavenger alters cytokine expression pattern and oxidative stress, and contributes to improved animal survival and lung histological outcomes in a murine model of ALI.

Specific Aim 4.1: Demonstrate the effectiveness of hydrogen sulfide as a free radical scavenger and alter the pro- and anti-inflammatory cytokine expression pattern in smoke injured lung.

Experiment: Lung tissue samples will be taken at 12 hours post burn and smoke injury and will be homogenized and protein extracted and analyzed for cytokine expression using an enzyme linked immunoassay.

Experiment: Using an assay to detect protein oxidation, lung tissue will be taken at the same time point and homogenized and DNPH will be used to derive carbonyl groups present on oxidized proteins. SDS gel electrophoresis followed by immunoblotting will be performed on each sample.

Specific Aim 4.2: Establish whether scavenging free radicals after hydrogen sulfide administration improves lung tissue histology and animal survival outcomes after burn and smoke injury.

Experiment: Using a masked scoring system for lung tissue sections, quantify the degree of epithelial disorganization, nuclear pyknosis and atelectasis 12 hours post-injury.

Experiment: Observe mortality for 120 hours in the injured/vehicle treated group, and the injured/hydrogen sulfide treated group.

CHAPTER 2

GENERAL METHODS

Animal Care

The following procedures were approved by the Animal Care and Use Committee of the University of Texas Medical Branch, and were in compliance with the guidelines for the care and use of laboratory animals of the National Institutes of Health and the American Physiological Society. Adult merino ewes (2 – 3 years old), weighing between 31 and 39 kg and were used. Ewes were used in these studies because of their docile nature compared to rams and the similarity of the lungs to that of humans.

Surgical Preparation

All animals were intubated and ventilated during the surgery while under ketamine and halothane anesthesia. Arterial catheters (16-gauge, 24 in., Intracath, Becton Dickinson, Sandy, UT) were placed in the descending aorta via the femoral artery. A Swan-Ganz thermal dilution catheter (Model 93A-131-7F, Edwards Lifesciences, Irvine, CA) was positioned in the pulmonary artery via the right external jugular vein. Through the left fifth intercostal space, a catheter (Durastic Silicone Tubing DT08, I.D.=0.062in, O.D.=0.125in., Allied Biomedical, Ventura, CA) was positioned in the left atrium. The sheep were given 5 to 7 days to recover from the surgical procedure with free access to food and water.

Burn and smoke inhalation injury

The animals were anesthetized using 10 mg/kg of ketamine (KetaVed, Phoenix Scientific, Inc., St. Joseph, MO.) and continued with halothane. A Foley catheter was placed in the urinary bladder to determine urine output after which the animals received a tracheotomy and a cuffed tracheostomy tube (10-mm diameter, Shirley, Irvine, CA) was inserted. The animal's wool was shaved and a 20% total body surface area (TBSA) third-degree flame burn was made on one flank. The burn was administered with a Bunsen burner, and flame applied until the skin is completely contracted and the nerve endings destroyed by the heat. Inhalation injury was induced using a modified bee smoker that was filled with 50 g of burning cotton toweling and connected to the tracheostomy tube via a modified endotracheal tube containing an indwelling thermistor from a Swan-Ganz catheter. During the insufflation procedure, the temperature of the smoke was monitored carefully not to exceed 40°C. The sheep was insufflated with a total of 48 breaths of cotton smoke. After smoke insufflation, another 20% TBSA third-degree burn was made on the contra-lateral flank.

Resuscitation protocol

After injury, anesthesia was discontinued and the animals were allowed to awaken but still mechanically ventilated with a Servo Ventilator (Model 900C Siemens-Elema, Solna, Sweden) throughout the experimental period. Ventilation was performed with a positive end-expiratory pressure (PEEP) of 5 cm H_2O and a tidal volume of 15 mL/kg. The respiratory rate was set to maintain normocapnia. For the first 3 hours the sheep

received an inspired oxygen concentration of 100%; thereafter, oxygen concentration was adjusted to maintain the arterial oxygen saturation above 90%. These settings allow a rapid disappearance of carboxyhemoglobin (CO-Hb) after smoke inhalation. Fluid resuscitation during the experiment was performed with Ringer's lactate solution following the Parkland formula (4 mL / % burned surface area / kg body weight for the first 24 hours and 2 mL / % burned surface area / kg body weight / day for the next 48 hours). The Parkland formula was started one hour after injury. One-half of the volume for the first day was infused in the initial 8 hours, and the rest infused in the next 16 hours. Urine was collected and urine output recorded every 6 hours. During this experimental period, the animals were allowed free access to food, but not to water, to allow accurate determination of fluid balance. The animals were resuscitated aggressively throughout the experimental period.

Measured Cardiopulmonary Variables

Measured physiological parameters were not considered valid until the animals were fully awake and standing. Mean arterial (MAP; in mm Hg), pulmonary arterial (PAP; in mm Hg); left atrial (LAP; in mm Hg), and central venous (CVP; in mm Hg) pressures were measured with pressure transducers (model P X 3 X 3, Edwards Lifesciences, Irvine, CA). The transducers were connected to a hemodynamic monitor (model M1205A, Viridia CMS 24/26, Philips Medical Systems, Andover, MA.). Zero calibrations were taken at the level of the olecranon joint on the front leg, which was considered to be the level of the right atrium. Cardiac output was measured with a

cardiac output computer (Model COM-1; Edwards Lifesciences, Irvine, CA.) using the thermodilution method with cold 5% dextrose as an indicator solution, for evaluation of cardiac function. The following derived hemodynamic variables were calculated: cardiac index, left ventricular stroke work index, pulmonary vascular resistance index and pulmonary shunt fraction. The standard equations used for these variables are listed in the Appendix. Arterial and mixed venous blood was measured with a blood gas analyzer (model IL Synthesis 15, Instrumentation Laboratory, Lexington, MA). The data was corrected for the body temperature of the sheep. Oxyhemoglobin saturation and carboxyhemoglobin concentration were analyzed with a CO-oximeter (Model IL482; Instrumentation Laboratory, Lexington, MA.). Hematocrit (Hct) was measured in heparinized microhematocrit capillary tubes (Fisherbrand; Fisher, Inc., Pittsburgh, PA).

Lung tissue preparation

Animals were sacrificed and lung tissue was sampled from the lower right lobe since the left lung lobe was handled during the surgical operative procedure. Tissue samples were immediately frozen in liquid nitrogen and stored at –80°C. Tissue preparation was performed using a modified protocol [Mineta *et al.*, 2002]. Lung tissue was weighed, suspended in 1 ml cold lysis buffer on ice (50 mM Tris-HCl [pH 7.4], 150 mM NaCl, 0.5% Triton X-100), 10 μL stock protease inhibitor cocktail (Sigma Aldrich, Saint Louis, MO) was added to produce a final 1 X concentration (AEBSF 1 mM, aprotinin 800nM, E-64 15 μM, leupeptin 20 μM, bestatin 50 μM, pepstatin A 10 μM). Additionally, 10 μL of stock phosphatase inhibitor (Pierce, Rockford, IL) was added to

produce a final 1 X concentration (sodium fluoride 50 mM, sodium orthovanadate I mM, sodium pyrophosphate 10 mM and β-glycerophosphate 10mM) and 1μL of 1 M dithiothreitol (Sigma Aldrich, Saint Louis, MO) was added to the lysis buffer mixture and homogenized with a LabGen 125 (Cole Parmer, Vernon Hills, IL). The lysate was clarified by centrifugation at 10,000 X g for 25 minutes at 4°C. The supernatant (cytoplasmic extract) was collected for total protein measurement. The pellet was saved for nuclear protein extraction.

Preparation of nuclear protein extracts

The pellet containing the nuclei was thawed on ice and resuspended in 250 μL cold nuclear extraction buffer containing 0.1 M DTT (Sigma Aldrich, Saint Louis, MO) and 1.5 μL stock protease inhibitor cocktail (Sigma Adrich, Saint Louis, MO) was added to produce a final 1 X concentration (AEBSF 1 mM, aprotinin 800nM, E-64 15 μM, leupeptin 20 μM, bestatin 50 μM, pepstatin A 10 μM). Samples were agitated vigorously for 15 seconds every 10 minutes for 30 minutes. The mixture is again centrifuged at ~ 20,000 X g for 5 minutes. The supernatant containing the nuclear proteins was collected and total protein was determined as outlined below.

Total protein quantification

Total protein in the supernatant (cytoplasmic and nuclear extract) was quantified using the Bradford method [Bradford, 1976]. Working Bio-Rad dye reagent (Biorad, Hercules, CA) was prepared by diluting 1 volume of the dye reagent concentrate in 4

volumes of ddH_2O. 1 mL of the working reagent was added to 12 X 75 mm tubes. 0 (reagent alone), 4, 8, 12, and 16 μL of 2 mg/mL bovine serum albumin (BSA; Pierce, Rockford, IL) was added to standard tubes and 4 μL of each sample were added to appropriate tubes. Each sample was vortexed and transferred to a disposable semi-micro cuvette and allowed to stand for 5 minutes. The absorbance of each sample was measured using a spectrophotometer (Beckman DU 640) at 595 nm against 0 mg/mL standard. The protein concentration of each sample was calculated by linear regression analysis and the amount of protein loaded per well was derived from the regression equation. The cytoplasmic and nuclear extract samples were aliquoted and frozen at -80°C.

Western blotting protocol

60 μg of total protein or 20 μg of nuclear extract was boiled in 2X Laemmli sample buffer, separated on a 4-20% SDS-polyacrylamide gradient gel by electrophoresis and transferred to an Immobilon–P PVDF membrane (Millipore, Bedford, MA). Membranes were blocked in blocking solution (Tris-buffered saline-Tween 20: 10 mM Tris-HCl [pH 7.4], 154 mM NaCl, 0.05% Tween 20 [vol/vol]) containing 5 % non-fat dry milk powder [wt/vol] for 1 hour at room temperature, then immunoblotted separately at 4°C overnight. The primary antibody was detected using a suitable secondary horseradish peroxidase-conjugated antibody. The membranes were subjected to chemiluminescence using the SuperSignal West Pico Chemiluminescent Substrate (Pierce, Rockford, IL) according to the manufacture's instructions and intensity of immunoreactivity was measured using NIH ImageJ software (http://rsb.info.nih.gov/nih-image/).

Lung wet-to-dry weight ratio

Since the left lung lobe was handled during the surgical placement of the left atrial catheter, the lower right lobe was sampled and placed in a storage container. The blood wet-to-dry ratio was also determined to calculate the bloodless lung wet-to-dry ratio to exclude contribution of blood [Pearce *et al.*, 1965]. Tissue was weighed and homogenized in a volume of deionized water equivalent to the difference in weight of the storage container. The lung tissue was homogenized and 30 mL of the supernatant was transferred into weigh boats and weighed. 5 mL of blood was weighed supernatant and blood were dried in an oven at 50°C for 1 week. The dry weight of the lung supernatant and blood was recorded and used to determine the contribution of blood to the "wetness" of the tissue. An additional 1.5 mL of the supernatant and blood was transferred to eppendorf tubes and centrifuged for 60 minutes at 15000 rpm. The supernatant was collected and used to measure total hemoglobin. Theoretically, the amount of hemoglobin is directly proportional to the amount of blood in the lung tissue and therefore to the amount of blood water contributing to total lung water. The detailed calculations are listed in the Appendix.

Statistical Analysis

The Prism software (Graphpad Software Inc., San Diego, CA) was used for statistical analysis. Comparison between the experimental groups was conducted using a standard one-way and two-way ANOVA and *post hoc* Newman–Keuls or Tukey-Kramer procedure was performed. Multiple comparisons were performed using a Student's

unpaired t-test. A p-value ≤ 0.05 was considered to be statistical significant. Summary statistics of data are expressed as mean ± SEM.

CHAPTER 3
EFFECT OF BURN AND SMOKE INDUCED LUNG INJURY ON HISTOLOGICAL OUTCOMES AND CYTOKINE EXPRESSION PATTERN IN SHEEP

INTRODUCTION

An excessive inflammatory response is one of the characteristics of ALI and involves a large flux of activated neutrophils that release a variety of pro-inflammatory cytokines such as interleukin -1 beta (IL-1 beta) [Esechie *et al.*, 2008], chemokines such as tumor necrosis factor- alpha [Hartl *et al.*, 2007], proteases such as myeloperoxidase [Schaaf B *et al.*, 2000], and reactive oxygen intermediates [Chen *et al.*, 2003].

The presence of such an array of proteins is detrimental and contributes to microscopic damage to the ultra-structure in the lung tissue as well as altered function. Hamahata and colleagues have recently described the presence of pronounced bronchial airway obstruction, pulmonary edema formation and diminished pulmonary gas exchange in association with elevated pro-inflammatory molecules, IL-8 and IL-6 proteins, at 48 hours post burn and smoke injury in an ovine model of ALI [Hamahata *et al.*, 2008]. Additionally, Soejima *et al.*, observed, in an ovine model of combined burn and smoke injury-induced ALI, a significant increase in pulmonary transvascular fluid flux and excessive lung water content at 48 hours post injury compared with burn alone injury and smoke alone inhalation injury [Soejima *et al.*, 2001]. While the preponderance of evidence using a clinically relevant model of ALI demonstrate causal relationship between this insult and pulmonary dysfunction at 24, 48, 72 and 96 hours, [Murakami *et*

al., 2004; Westphal *et al.*, 2006; Schmalstieg *et al.*, 2007; Enkhbaatar *et al.*, 2008], it remains to be seen whether a similar relationship is present at earlier time points after this dual trauma.

Inhalation injury is classified into upper and lower airway injury, pulmonary parenchyma injury and eventually systemic organ failure. The pathogenesis of ALI is attributed to three notable sequential and overlapping phases: the exudative phase of edema and hemorrhage, the proliferative phase of organization and repair, and the end-stage fibrotic phase [Tomashefski, 2003]. Much of the pathophysiology that occurs with ALI however is related to bronchial and parenchyma edema formation due to increased transvascular fluid flux. This notable fluid transfer between vasculature and extravascular compartments is prominent in the early stages and, in part, triggers the rapid onset organ failure and systemic toxicity. We have previously observed that the histological features of ALI correlate with the duration of injury. Using a clinically relevant ovine model of burn and smoke-induced ALI, Cox [Cox *et al.*, 2003] demonstrated that the degree and location of obstructive material in the airway of sheep occurs in a time-dependent manner. The authors observed that there was distal migration of obstructive cast material in the upper airway into the lower and smaller airways from 24 through 72 hours post injury.

An understanding to the events during the early stages of this injury deserves attention in order to understand ALI. This study was designed to evaluate morphological features associated with the early stages of ALI, 4 through 24 hours post injury and correlate these observations with clinical events. In addition, other standards of outcome

(lung wet-to-dry weight ratio, neutrophil accumulation) were measured. Animals were divided into six groups and sacrificed at various time intervals after the initial injury.

METHODS

Surgical Preparation

Animal surgical preparation is described in detail in Chapter 2.

Burn and smoke inhalation injury

The injury protocol is described in detail in Chapter 2.

Resuscitation protocol

The resuscitation protocol is described in detail in Chapter 2.

Measured Cardiopulmonary Variables

Measured physiological parameters were not considered valid until the animals were fully awake and standing, usually within one hour of injury. Mean arterial (MAP; in mmHg), pulmonary arterial (PAP; in mm Hg); left atrial (LAP; in mm Hg), and central venous (CVP; in mmHg) pressures will be measured with pressure transducers (model P X 3 X 3, Edwards Lifesciences, Irvine, CA) that were adapted with a continuous flushing device. The transducers will be connected to a hemodynamic monitor (model M1205A, Viridia CMS 24/26, Philips Medical Systems, Andover, MA). Zero calibrations were taken at the level of the olecranon joint on the front leg, which

was considered to be the level of the right atrium. Cardiac output was measured with a cardiac output computer (Model COM-1; Edwards Lifesciences, Irvine, CA) by the thermodilution method with 5% dextrose as an indicator solution, for evaluation of cardiac function, cardiac index (CI; in $l.min^{-1}.m^{-2}$), left ventricular stroke work index (LVSWI; in $g.min^{-1}.m^{-2}$), and pulmonary resistance (PVRI; in $dynes.cm^{-5}.m^{-2}$) were calculated with standard equations.

Experimental Groups

Animals were randomly assigned and were sacrificed at various time points conferring to the different experimental groups. Throughout the experimental time period, the animals were allowed free access to food.

Experimental Groups

Group	**Study Length**
Control	No injury; sacrificed 24 hrs study length, n = 5
4 hrs	S+B injury; sacrificed 4 hrs study length, n = 5
8 hrs	S+B injury; sacrificed 8 hrs study length, n = 5
12 hrs	S+B injury; sacrificed 12 hrs study length, n = 5
18 hrs	S+B injury; sacrificed 18hrs study length, n = 5
24 hrs	S+B injury; sacrificed 24 hrs study length, n = 5

Lung tissue preparation

Animals were sacrificed and lung tissue sections immediately frozen in liquid nitrogen and stored at –80°C. The protocol for tissue preparation is described in detail in Chapter 2.

Histological Assessment

A 1 cm thick section was taken from the lower right lobe, fixed with 10% formalin, embedded in paraffin, sectioned into 4 μm pieces, and stained with hematoxylin-eosin. All slides were masked and histological assessment consisted of assigning a semi-quantitative score for congestion, septal edema, and septal inflammation for 24 areas of lung parenchyma in each animal, observed at 10X objective magnification. The sections were graded as follows: 0 = absent, appears normal; 1 = light; 2 = moderate; 3 = strong; 4 = intense.

Measurement of Airway Obstruction

Each slide was masked and systematically scanned at a 4X objective. For each airway, a degree of luminal obstruction was estimated from 0% to 100%. The mean degree of obstruction was determined for each sheep and the cross-sectioned airways were classified as bronchi, bronchioles, or terminal/respiratory bronchioles. Bronchi had associated mucous glands and/or cartilage, bronchioles lacked mucous glands and cartilage, and terminal/respiratory bronchioles had short cuboidal lining epithelial cells and lacked surrounding smooth muscle tissue

Western blotting

A detailed lung tissue preparation and western blotting protocol is detailed in Chapter 2. Briefly, the membranes were immunoblotted at 4°C overnight with primary antibodies diluted in Tris-buffered saline-Tween 20: 10 mM Tris-HCl [pH 7.4], 154 mM NaCl, 0.05% Tween 20 [vol/vol]) containing 1% non-fat dry milk powder [wt/vol]. Rabbit anti-interleukin-8 (Catalog No. AB1840) purchased from Chemicon, Billerica, MA was diluted to 1: 1000 and, rabbit anti-VEGF (Catalog No. sc-507) and goat anti-β-Actin (Catalog No. sc-1616) purchased from Santa Cruz Biotechnology Inc (Santa Cruz, CA) were diluted to 1:500. The primary antibody was detected using a horseradish peroxidase-conjugated goat anti-rabbit diluted to 1:4000 (Catalog No. HAF008) or donkey anti-goat antibody diluted to 1:3000 (Catalog No. HAF109) purchased from R&D Systems (Minneapolis, MN). The membranes were subjected to chemiluminescence using the SuperSignal West Pico Chemiluminescent Substrate (Pierce, Rockford, IL) according to the manufacture's instructions and intensity of immunoreactivity was measured using NIH ImageJ software (http://rsb.info.nih.gov/nih-image/).

Lung wet-to-dry weight ratio

The lower right lobe was sampled to measure bloodless wet-to-dry weight ratio. The injury protocol is described in detail in Chapter 2.

Myeloperoxidase Activity

Myeloperoxidase (MPO), an indicator of PMN accumulation, was determined directly in whole lung homogenates. 50 mg of frozen lung tissue was weighed and homogenized in 0.5 ml hexa-decyl-trimethyl-ammonium bromide buffer (HTAB, Sigma Aldrich, St. Louis, MO) and an additional 0.5 ml of the HTAB buffer was added for a tissue-to-buffer ratio of 50 mg/ml. 20 μl of the lung homogenate was assayed spectrophotometrically using a chromogen, o-dianisidine dihydrochloride, in potassium phosphate (monobasic potassium, dibasic potassium phosphate) and H_2O_2 buffer. Absorbance was measured at 450 nm immediately after addition of chromogen and at 60 seconds intervals for a total of 10 readings. One unit of MPO activity was defined as the degradation of 1 μmole H_2O_2/min at 25°C, which gives a change in absorbance (ΔA) of 0.0113/min.

RESULTS

Since the differences observed between the experimental groups could be attributed to uneven smoke administration, arterial carboxyhemoglobin (COHb) was recorded at the end of the smoke insufflation procedure. As shown in Table 3.1, there was no significant difference in the degree of inhalation injury within the experimental groups.

Table 3.1 Smoke inhalation injury parameter

Group	COHb
Control (n=5)	4.4 ± 0.4
4 hrs (n =5)	63.5 ± 7.5 *
8 hrs (n =5)	67.0 ± 10.9 *
12 hrs (n =5)	68.2 ± 8.1 *
18 hrs (n =5)	71.8 ± 4.2 *
24 hrs (n =5)	76.1 ± 4.8 *

Table 3.1 There was no significant difference in the degree of smoke inhalation in all experimental groups. Data are presented as mean ± SEM for all groups. Experimental groups received 40 % TBSA 3rd degree burn and were insufflated with cotton smoke. The degree of smoke inhalation injury was measured by carboxyhemoglobin in arterial blood. * $p \leq 0.05$ vs. control.

Pulmonary gas exchange

In the present study, we assessed the relationship between the extent of lung parenchymal damage at various time points after burn and smoke (B + S) inhalation injury. As shown in Figure 3.1, the animals developed acute pulmonary dysfunction as

indicated by a progressive decline in PaO_2/FiO_2 ratio after 18 hours and 24 hours post burn and smoke exposure.

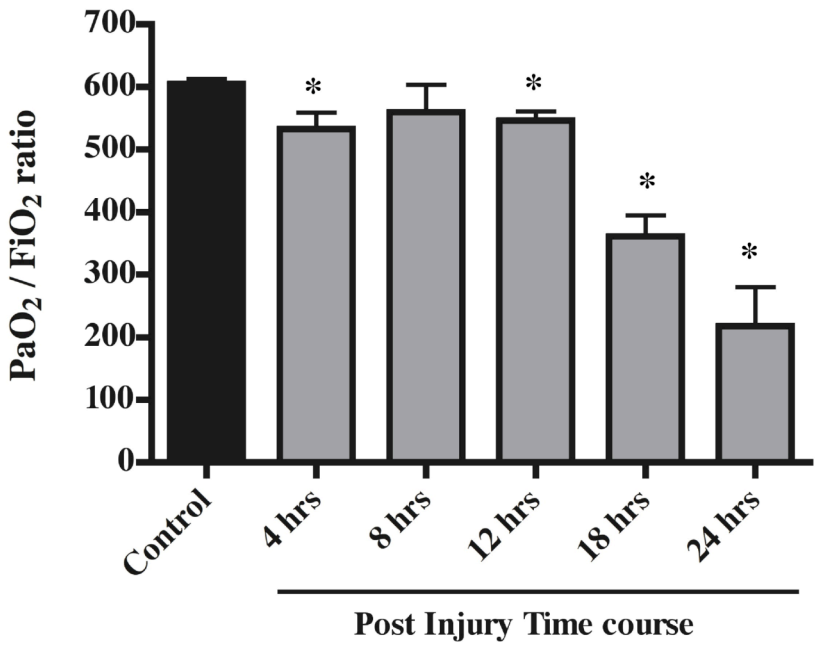

Figure 3.1 Changes in pulmonary gas exchange after burn and smoke injury; PaO_2/FiO_2, partial pressure of oxygen-to-fraction of inspired oxygen ratio. Note that at 4 hours and 12 through 24 hours, the PaO_2/FiO_2 is significantly lower than the control group. Data represented as mean ± SEM. N = 5 per group,* $p \leq 0.05$ vs. control**.**

Cardiopulmonary hemodynamics

The observed differences in hemodynamic variables are shown in Table 3.2. Changes in pulmonary hemokinetics were evident at 4 hours after injury. The onset of pulmonary hypertension, characteristic of ALI, was evident 8 hours through 24 hours after injury; compared to the control group, B + S injured animals showed elevated mean pulmonary artery pressure (MPAP) at 8, 18 and 24 hours.

Table 3.2 Cardiopulmonary Hemodynamics

Group	MAP (mm Hg)	LAP (mm Hg)	MPAP (mm Hg)	PcP (mm Hg)	PVRI ($dyne.s.cm^{-5}/m^2$)	CI ($l.min^{-1}.m^2$)
Control	99 ± 4	8.3 ± 1.1	22.6 ± 0.8	14.3 ± 0.5	127 ± 10	6.5 ± 0.1
4 hrs	103 ± 5	11.4 ± 1.6	23.6 ± 1.5	16.3 ± 1.7	135 ± 11	5.8 ± 0.5
8 hrs	116 ± 6 *	9.6 ± 1.4	27.6 ± 2.1 *	16.8 ± 1.4 *	170 ± 24	5.5 ± 0.2 *
12 hrs	106 ± 3	10.0 ± 1.3	26.2 ± 1.9	16.5 ± 1.4	209 ± 67	5.1 ± 0.5 *
18 hrs	98 ± 4	11.4 ± 0.7 *	29.2 ± 2.4 *	18.5 ± 0.9 *	176 ± 14 *	5.7 ± 0.5
24 hrs	103 ± 5	10.8 ± 1.9	30.0 ± 2.3 *	17.7 ± 0.6 *	223 ± 23 *	5.3 ± 0.6

Table 3.2 Values are presented as mean ± SEM. MAP, mean arterial pressure; LAP, left atrial pressure; MPAP, mean pulmonary arterial pressure; PcP, pulmonary capillary pressure; PVRI, pulmonary vascular resistance index; CI, cardiac index. Comparisons were made using two-way analysis of variance with a Newman-Keuls *post hoc* test. N = 5 per group, * $p \leq 0.05$ vs. control.

In addition, pulmonary capillary pressure (PcP) and pulmonary vascular resistance index (PVRI) significantly increased compared control animals. There was a transient elevation in mean arterial pressure (MAP) and left atrial pressure (LAP) compared to the control animals at 8 hours and 18 hours, respectively.

Lung Histological Assessment

Figure 3.2 shows representative photomicrographs of the lung parenchyma and bronchial airway for each group. The effects of B + S inhalation on lung histopathological changes were quantified based on cumulative scores for alveolar congestion, septal edema and septal inflammation. Although the results show a tendency for septal edema formation after injury, lung sections from sheep in the 8 and 18 hours post injury group were significantly different from the uninjured control group (Control: 0.8 ± 0.2; 8 hrs post B+S: 1.9 ± 0.1; 18 hrs post B+S: 1.6 ± 0.1). There was a significant increase in septal edema at 8 hours ($p = 0.016$) and 18 hours ($p = 0.048$) post B + S inhalation injury. The mean septal inflammation score for 12 hours post injury group (1.5 ± 0.4) was greater than the un-injured control animals (0.6 ± 0.2) but could not be shown to be statistically different (Figure 3.3B). Analysis of mean alveolar congestion showed no significant difference ($p = 0.65$) between the control group and experimental groups at any of the observed time points (Figure 3.3C).

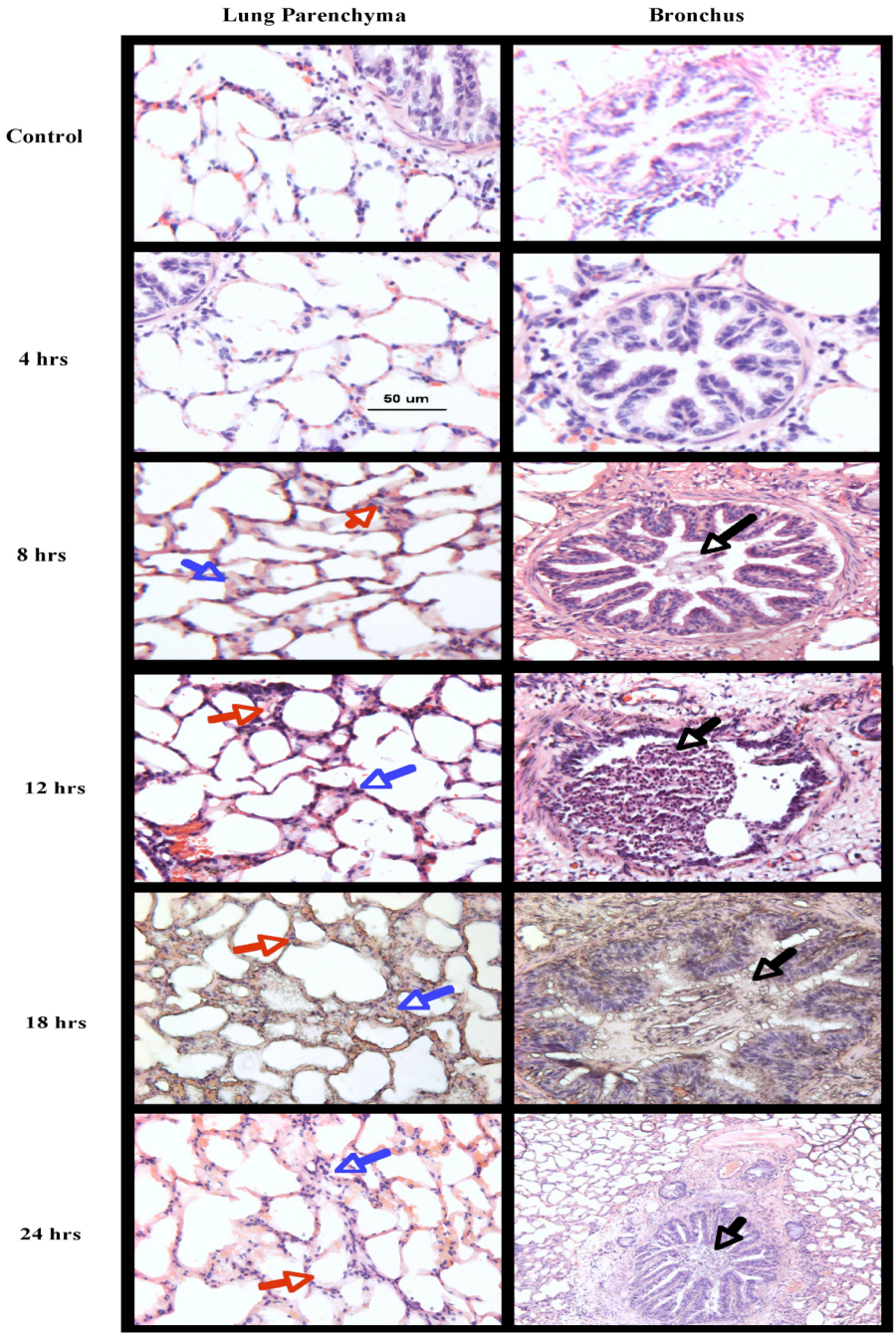

Figure 3.2 Representative photomicrographs of uninjured control and burn and smoke injured animals. Histological sections were paraffin embedded and stained with Hematoxylin and eosin. Images of lung parenchyma (5X magnification) indicates septal thickening and septal edema formation. Obstructive cast material (20X magnification) is present in airway starting at 8 hours post injury through 24 hours.

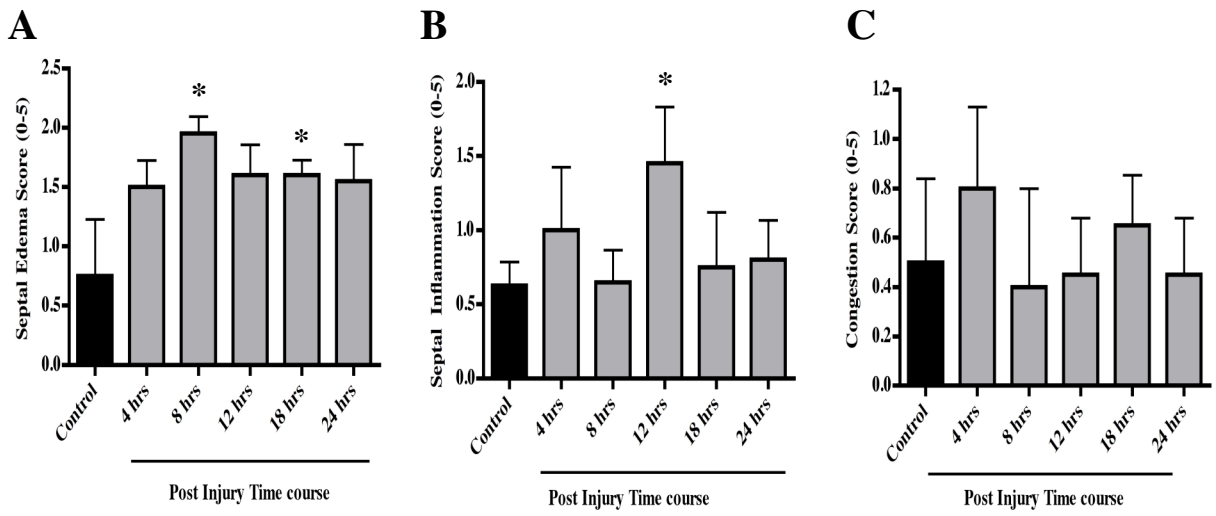

Figure 3.3 Histograms depicting histological changes in the lung after injury. (A, B and C) Histograms of calculated (A) septal edema, (B) septal inflammation, and (C) alveolar congestion in un-injured control sheep and at the indicated time points after combined burn and smoke injury. Note that the presence of septal edema was significant at 8 and 18 hours post injury compared to control animals. Significant septal inflammation was observed 12 hours post injury. Data represented as mean ± SEM; N = 5, $*p \leq 0.05$ vs control.

Temporal assessment of bronchi and bronchioles airway obstruction was determined by estimating the mean luminal obstruction from 0 to 100% (Table 3.3). The mean percentage of the control and the injured sheep (at all time points) was significantly different ($p = 0.0013$). In the experimental groups, there was a steady increase in bronchial obstruction from 4 through 24 hours post injury. In contrast, there was no

significant difference in bronchiolar obstruction between the control and experimental mean.

Table 3.3 Degree of airway obstruction in control and burn and smoke injured sheep

	Airway Level	
Group	**Bronchi**	**Bronchioles**
Control (n =4)	3.7 ± 1.2%	2.6 ± 0.8%
4 hrs (n =5)	7.6 ± 1.4% *	1.9 ± 0.5%
8 hrs (n =5)	11.3 ± 2.3% *	2.0 ± 0.5%
12 hrs (n =5)	22.8 ± 7.9% *	2.8 ± 0.8%
18 hrs (n =5)	22.0 ± 4.3% *	2.3 ± 0.6%
24 hrs (n =5)	31.8 ± 7.3% *	1.6 ± 0.4%

Table 3.3 Changes in airway obstruction after injury. Following tissue sectioning, each slide was masked and systematically scanned at a 4X objective. For each airway, a degree of luminal obstruction was estimated from 0% (no obstructive material in the airway) to 100% (airway is completely obstructed). There was a significant difference in bronchial obstruction post injury. There was no significant difference in bronchiole obstruction. Values are presented as mean ± SEM; *$p \leq 0.05$ vs. control

Lung wet-to-dry weight ratio

Lung water content was evaluated by measuring bloodless lung wet-to-dry weight ratio. Animals sacrificed after 18 hours and 24 hours post injury exhibited significantly greater lung water content compared to the control animals (Figure 3.4). During the first 12 hours post injury, there was no significant difference in lung wet-to-dry weight ratio compared to control sheep. Additionally, there was a significant increase in lung water at the 4 hrs time point compared to the 12 hrs and 24 hrs post injury time points ($p = 0.0083$ and $p = 0.0107$, respectively).

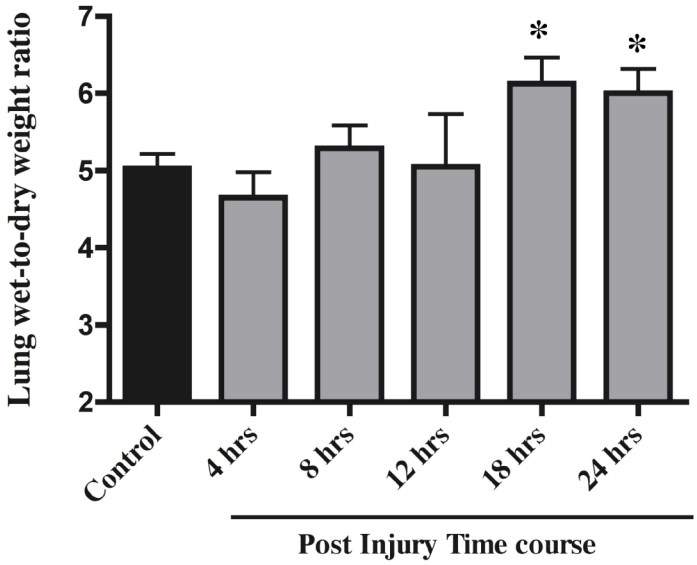

Figure 3.4 Changes in blood free wet-to-dry weight ratio after injury. Values are presented as mean ± SEM. There was a significant difference in lung water content at 18 and 24 hours post injury. N = 5; *$p \leq 0.05$ vs. control.

Myeloperoxidase activity

Infiltration of inflammatory cells (mainly neutrophils) in the lung is associated with the induction of myeloperoxidase (MPO) activity. As shown in Figure 3.5, MPO activity significantly increased in the lung 4 hours post injury and remained elevated through 18 hours post injury. At 24 hours post injury, lung MPO level was not significantly different from the control group.

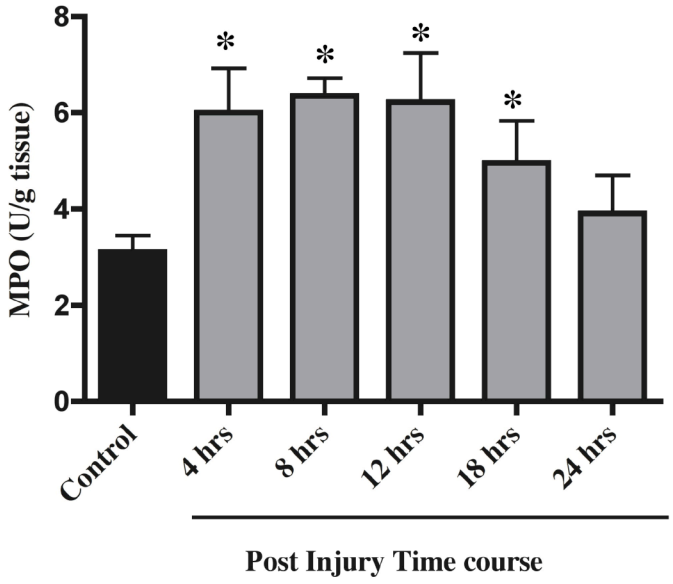

Figure 3.5 Change in lung myeloperoxidase (MPO) in lung tissue homogenate. Burn and smoke inhalation injury significantly increased neutrophil accumulation in the lung from 4 through 18 hours post injury. There was no significant difference in MPO activity at 24 hours post injury. Data is presented as mean ± SEM, N = 5, * $p \leq 0.05$ vs. control.

IL-8 and VEGF-A cytokines in lung homogenate

Figure 3.6 depicts the kinetics of IL-8 and VEGF-A protein expression in the lung. Both IL-8 and VEGF expression significantly increased in the injured group compared to the control animals. The change in IL-8 expression was consistent with the apparent influx of neutrophils after injury (Figure 3.5) while VEGF protein expression was consistent with the lung septal edema formation (Figure 3.3A).

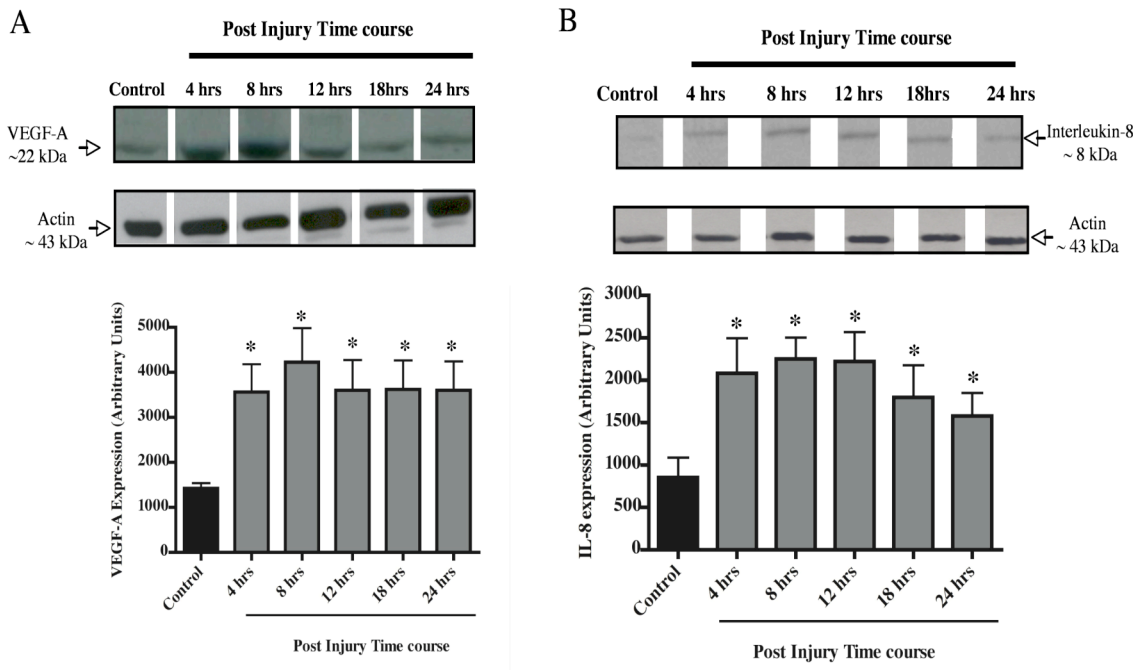

Figure 3.6 Time course of VEGF-A and IL-8 expression in lung homogenate. Following homogenization, the lung lysate was resolved on SDS-polyacrylamide gel elctrophoresis, transferred to a PVDF membrane, and subjected to autoradiography. (A) and (B) Representative immunoblots of lung homogenates using rabbit anti -VEGF antibody or rabbit anti-IL-8 antibody. The histograms demonstrate the integrated intensities quantified by densitometric analysis. Data is presented as mean ± SEM, N = 5, $*p \leq 0.05$ vs. control.

DISCUSSION

In burn victims, the presence of smoke inhalation augments the severity of lung tissue injury. A disruption of the lung structure is a key histological feature that explains the attenuated pulmonary function. This study was designed to examine the time-dependent pulmonary histological changes and functional cardiopulmonary outcomes at earlier time points in a clinically relevant ovine model of burn and smoke inhalation-induced ALI. In the current study we observed that 1) damage to the alveolar septum occurs early in response to smoke inhalation; 2) there was a progressive deterioration of pulmonary hemodynamics (elevated pulmonary vascular resistance and the development of pulmonary hypertension secondary to inhalation injury); 3) rapid accumulation of neutrophils in the lung; 4) pulmonary edema formation (increased lung water content); and 5) progressive loss of pulmonary function as evidenced in attenuated PaO_2/FiO_2.

Clinically, ALI patients develop elevated pulmonary vascular resistance [Brower *et al.*, 2001]. In this study pulmonary artery pressure (PAP) and pulmonary vascular resistance index (PVRI) were elevated 8 hours post injury and remained elevated at 24 hours. The progressive increase in PVRI is likely attributed to inflammatory events in the pulmonary microvasculature. In patients who die of respiratory failure secondary to ALI, there is diffuse alveoli injury such that a majority of the lung is extensively damaged, however there are foci that are remarkably spared [Tomashefski, 2003]. Widespread blockade of the airways with obstructive casting material is a severe problem associated with this injury and significantly impairs ventilation and can lead to ventilator-induced barotraumas [Murakami *et al.*, 2003]. The solid airway cast is mainly composed of shed

bronchial epithelial cells, mucus, fibrin and infiltrated neutrophils. This feature of ALI has been investigated experimentally in injured sheep 24 and 48 hours post smoke inhalation and has been suggested to severely impair pulmonary function [Herndon *et al.*, 1986; Cox *et al.*, 2003]. This study was designed to investigate if the initial decline in physiological variables that determine pulmonary function (gas exchange and elevated airway pressure) could be explained by histological assessment. In Table 3.3, the mean scores from the burn and smoke injured animals showed progressive increase in bronchial obstruction that was maximal at 24 hours after injury. Our data suggests that smoke insufflation produces a significant lesion in the trachea and bronchi is sufficient to produce epithelial sloughing into the airway within the first 4 hours post injury. In contrast, the mean degree of bronchiolar obstruction scores did not display a relationship with the specific time points post injury (Table 3.3). Additionally, the mean bronchiolar obstruction scores were not statistically different from the un-injured control animals. One possible explanation is that during the 4 through 12 hours time period, the amount of obstructive material present is not substantial. Therefore any obstructive material migrating distally from the larger bronchi to the bronchioles and terminal bronchioles, and finally to the alveoli, does not contribute significantly to histological changes in the lung parenchyma after inhalation injury.

In a recent paper on the subject Cox *et al.*, determined that much of the mucous found in the distal bronchioles had been formed in the bronchi [Cox *et al.*, 2003]. The obstruction of the upper airway may have protected the lower airway from being obstructed. On the other hand these obstructed airways most certainly are not ventilated

and the significant hypoxic pulmonary vasoconstriction may play a role in the subsequent hypertension. It is of interest that the fall in PaO_2/FiO_2 at 18 hours corresponded with a sudden increase in lung water also at 18 hours suggesting that there may have been alveolar flooding. This alveolar collapse may have contributed to the greater pulmonary resistances noted at these latter time periods. Westphal *et al*., have reported on the loss of hypoxic pulmonary vasoconstriction with combined burn and inhalation injury. The authors attributed and that this loss of the compensating mechanism may play a role in the fall in PaO_2/FiO_2 [Westphal *et al*., 2003; Westphal *et al.,* 2008].

Although the histological assessment of the lung parenchyma showed that septal edema was observed as early as 8 hour after the initial insult (Figure 3.3A) lung wet-to-dry weight ratio did not increase until 18 hours. Smoke damage is "patchy" and therefore it is possible to observe foci of severely damaged areas adjacent to apparently unaffected areas in the same tissue section. This apparent disparity underscores the heterogeneity of ultra-structural changes in the lung relative to the extent of global parenchymal changes.

ALI is characterized pathologically by neutrophilic alveolitis and destruction of the alveolar epithelial layer leaving denuded membrane by actions of proteases and release of reactive molecules [Weiss *et al*., 1989]. In our study we observed a 2-folds increase in neutrophil accumulation in the lung (as measured by MPO activity assay) 4 hrs post injury which was sustained through 18 hrs post injury. There are 3 lines of evidence that could explain these results. Since neutrophils are thought to be the major effector of cell damage and lung injury [Jinzhou *et al.,* 2008; Perl *et al*., 2008], sequestration of these cells to the lung suggests the presence of inflammatory stimuli

such as cytokines or chemokines [Kuo *et al.*, 1997]. It was of interest to note that an increase in the chemokine IL-8 occurred simultaneous with the rise in MPO. Recent studies showed a correlation between specific time points post smoke and burn injury and expression of interleukin-1a and TNF-α in bronchial gland cells in sheep lung tissue [Cox *et al.*, 2005]. In that study Cox *et al.*, provide supporting evidence that 4 hrs post injury, glandular cells in the lung are active in recruiting acute inflammatory cells. Secondly, the physical property of both the neutrophils and the lung vasculature play an additional role in the accumulation of neutrophils in the lung. Because the diameter of neutrophils are 40-60% [Wiggs *et al.*, 1994] larger in diameter compared to the caliber of pulmonary capillaries, circulating neutrophils must deform in order to pass through this capillary network and in doing so neutrophil trafficking through the lung becomes sluggish. However, upon activation, neutrophils become less deformable due to actin reorganization [Skoutelis *et al.*, 2000; Yoshida *et al.*, 2006]. Seminal studies conducted by Doerschuk [Doerschuk, 1992] demonstrated that activated neutrophils change their shape through redistribution of central globular actin to filamentous actin in the sub-membranous areas of the cell thus preventing deformation and increasing neutrophil sludging through the pulmonary capillary network and contributing to cell and tissue damage. The present data may therefore be interpreted as a large influx of neutrophils into the pulmonary microvasculature beginning at 4 hrs.

The degree in which many of the pro-inflammatory cytokines and chemokines are up-regulated is dependent upon the severity of the injury. In particular, upregulation of IL-8 in the lung after burn and smoke injury stimulates the infiltration phase of

neutrophils which further exacerbates structural loss in the lungs and contributes to sustained inflammation and lung injury [Schmalsteig *et al.*, 2007]. This present study provides a time course of IL-8 protein expression in lung tissue homogenate after injury. IL-8 protein levels were consistent with the increase in neutrophil accumulation into the lung tissue, where high IL-8 levels were associated with greater neutrophil migration and low IL-8 at the 24 hrs time point was associated with reduced migration. Interestingly, VEGF protein expression correlated with the development of lung septal edema post injury (Figure 3.3A and Figure 3.6A).

In conclusion we have determined that severe burn with associated smoke inhalation injury significantly alters lung microscopic structures which leads to deteriorated pulmonary function. Our data demonstrates that in the absence of any therapeutic intervention, there is a rapid accumulation of neutrophils associated with increased IL-8 protein levels alveolar septal thickening (septal edema) in response to inflammatory stimuli and compromised pulmonary function. This appears to be a positive feedback mechanism as a reduction in lung MPO activity towards the end of the study did not correlate with a cessation of cardiopulmonary deterioration or lung histology sparing.

CHAPTER 4
ASSESSMENT OF NITROSATIVE AND OXIDATIVE STRESS AFTER ACUTE LUNG INJURY IN SHEEP

INTRODUCTION

Trauma caused by combined burn and smoke inhalation injury leads to a rapid pathophysiological response and the development of acute lung injury (ALI). It is well accepted that lung injury triggers an exaggerated inflammatory cascade in the pulmonary environment. The presence of inflammatory cells leads to tissue injury through reactive oxidant/ nitrogen species (ROS/RNS), proteases and cytokines. In the previous chapter we reported that neutrophils rapidly accumulate in the lung associated with increased IL-8 protein levels, alveolar septal thickening in response to inflammatory stimuli and compromised pulmonary function.

Nitric oxide (NO) is a ubiquitous signaling molecule formed from the oxidative deamination of L-arginine via the activity of NO synthase (NOS) enzymes. In particular, the inducible isoform of NOS (iNOS) significantly increases the concentration of NO in pathological settings such as ALI [Mizutani *et al*., 2008]. We have previously shown that burn and smoke inhalation resulted in a 3-fold increase in plasma nitrate/nitrite (NOx) production, a stable metabolite of NO [Enkhbaatar *et al.*, 2008]. Additionally, Soejima *et al* [Soejima *et al.*, 2001] recently demonstrated in clinically relevant ovine model, that burn and smoke-induced ALI up-regulated iNOS gene transcription and gene product

(iNOS protein) in the lung. In the study mentioned, the investigators also demonstrated increased formation of ROS associated with ALI.

Superoxide and NO are produced simultaneously and in very high concentration [Liochev *et al*., 2003]. When both molecules are in close proximity, they combine spontaneously to form peroxynitrite (ONOO-), a potent oxidant that reacts with most biological molecules [Huie *et al*., 1999]. Peroxynitrite plays a role in the "suicide hypothesis" [Sims *et al*., 1983; Berger, 1985]. Elevated levels of peroxynitrite causes lesions in DNA by preferentially oxidizing guanine residues [Burney *et al*., 1999; Yu *et al*., 2005; Niles *et al*., 2006]. This fragments DNA and produces singles strand breaks. DNA repair enzymes such as DNA glycosylase and poly (ADP ribose) polymerase (PARP) are triggered to initiate the reparative process. In particular, the involvement of PARP-1 in sepsis induced ALI and burn and smoke induced ALI has recently been described [Shimoda *et al*., 2003; Murakami *et al*., 2004].

A report by Oliver *et al* and others has suggested that PARP-1 is involved in regulating the expression of specific genes through a unique interaction with nuclear factor-κB (NF-κB) [Oliver *et al*., 1999; Chang and Alvarez-Gonzalez, 2001]. NF-κB is pre-synthesized in the cytosol and immediately forms a complex with inhibitory-κB (IκB), sequestering it to the cytosol. Several signal molecules including ROS [Meyer *et al*., 1993] can activate NF-κB in targeted cells. In fact, the addition of micromolar concentrations of H_2O_2 has been reported to activate NF-κB [Schreck *et al*., 1991; Meyer *et al*., 1993]. These signals target IκB for destruction thus liberating NF-κB to translocate

into the nucleus and begin gene transcription. NF-κB activate several genes concerned with inflammatory responses such as iNOS. The suppression of NF-κB activation-dependent transcription of iNOS has been shown in macrophages treated with PARP-1 inhibitors [Le Page *et al*., 1998].

The objective of this study was to assess the development of oxidative stress in the lung at 4, 8, 12, 18 and 24 hours after injury and evaluate the involvement of peroxynitrite-PARP-1 crosstalk during the early stages after injury.

METHODS

Surgical Preparation

Animal surgical preparation is described in detail in Chapter 2.

Burn and smoke inhalation injury

The injury protocol is described in detail in Chapter 2.

Resuscitation protocol

The resuscitation protocol is described in detail in Chapter 2.

Experimental Groups

Animals were randomly assigned and were sacrificed at various time points conferring to the different experimental groups. Throughout the experimental time period, the animals were allowed access to food

Experimental Groups

Group	Study Length
Control	No injury; sacrificed 24 hrs study length, n = 5
4 hrs	S+B injury; sacrificed 4 hrs study length, n = 5
8 hrs	S+B injury; sacrificed 8 hrs study length, n = 5
12 hrs	S+B injury; sacrificed 12 hrs study length, n = 5
18 hrs	S+B injury; sacrificed 18hrs study length, n = 5
24 hrs	S+B injury; sacrificed 24 hrs study length, n = 5

Measurement of nitrate/nitrite (NOx) in plasma

The concentration of NOx in plasma was measured using a NO chemiluminescene detector. Samples to be analysed were converted to NO gas using vanadium (III) and HCl at 90ºC by the NOx reduction assembly prior to entry into the detector. Thereafter, the NO reacted with ozone in the reaction chamber of the detector and the emitted light signal was recorded by dedicated software as the NO content (μM) as compared to standards.

Lung tissue preparation

The protocol for tissue preparation is described in detail in Chapter 2.

Preparation of nuclear protein extracts

The pellet containing the nuclei was thawed on ice and resuspended in 250 μL cold nuclear extraction buffer containing 0.1 M DTT (Sigma Aldrich, Saint Louis, MO) and 1.5 μL stock protease inhibitor cocktail (Sigma Aldrich, Saint Louis, MO) was added to produce a final 1 X concentration (AEBSF 1 mM, aprotinin 800nM, E-64 15 μM, leupeptin 20 μM, bestatin 50 μM, pepstatin A 10 μM). Samples were agitated vigorously for 15 seconds every 10 minutes for 30 minutes. The mixture is again centrifuged at 20,000 X g for 5 minutes. The supernatant containing the nuclear proteins was collected and total protein was quantified in each sample.

Western blotting

60 μg of total protein and 20 μg of the nuclear extract were boiled in 2X Laemmli sample buffer, separated on a 4-20% SDS-polyacrylamide gradient gel by electrophoresis and transferred to an Immobilon–P PVDF membrane (Millipore, Bedford, MA). Membranes were blocked in blocking solution (Tris-buffered saline-Tween 20: 10 mM Tris-HCl [pH 7.4], 154 mM NaCl, 0.05% Tween 20 [vol/vol]) containing 5 % non-fat dry milk powder [wt/vol] for 1 hour at room temperature. The membranes were immunoblotted at 4°C overnight with primary antibodies diluted in Tris-buffered saline-Tween 20: 10 mM Tris-HCl [pH 7.4], 154 mM NaCl, 0.05% Tween 20 [vol/vol]) containing 1% non-fat dry milk powder [wt/vol]. The following antibodies were used: rabbit anti-PAR (Catalog No. 4336-BPC-100) purchased from Trevigen, Gaithersburg, MD was diluted to 1: 1000; rabbit anti-NF-κB p65 (Catalog No. DB033) purchased from

Delta Biolabs, Gilroy, CA was diluted to 1:500; biotinylated mouse anti-nitrotyrosine (Catalog No. 10006966) purchased from Cayman Chemicals, Ann Arbor MI was diluted to 1:1500; and rabbit anti-NOS2 (Catalog No. sc-650) diluted to 1:200 and goat anti-β-Actin (Catalog No. sc-1616) purchased from Santa Cruz Biotechnology Inc (Santa Cruz, CA) was diluted to 1:500. The primary antibody was detected using the following horseradish peroxidase-conjugated secondary antibodies: goat anti-rabbit (Catalog No. HAF008) diluted to 1:4000 or donkey anti-goat (Catalog No. HAF109) antibody diluted to 1:3000 or streptavidin-HRP (Catalog No. DY998) diluted at 1:200 purchased from R&D Systems (Minneapolis, MN). The membranes were subjected to chemiluminescence using the SuperSignal West Pico Chemiluminescent Substrate (Pierce, Rockford, IL) according to the manufacture's instructions and intensity of immunoreactivity was measured using NIH ImageJ software (http://rsb.info.nih.gov/nih-image/).

Poly (ADP-ribose) Immunohistochemistry

For the immunohistochemical detection of poly(ADP-ribose) mouse monoclonal anti-PAR antibody (Calbiochem, San Diego, CA, USA) (1:1000, overnight, 4°C) was used after antigen retrieval [Toth-Zsamboki *et al.*, 2006; Beller *et al.*, 2007]. Secondary labeling was achieved by using biotinylated horse anti-mouse antibody (Vector Laboratories, Burlingame, CA) (30 minutes at room temperature (20-25°C)). Horseradish peroxidase-conjugated avidin (30 minutes, room temperature) and brown colored diaminobenzidine (6 minutes, room temperature) was used to visualize the labeling

(Vector Laboratories, Burlingame, CA). The sections were counterstained with hematoxylin.

The intensity of PAR staining of individual sections was determined by a masked experimenter using the following semi-quantitative PAR-positivity score: 1: no staining, 2: light cytoplasmic staining, 3: few positive nuclei, 4: light nuclear staining in approximately 10% of cells, 5: light nuclear staining in approximately 25% of cells, 6: light nuclear staining in approximately 50% of cells, 7: strong nuclear staining in approximately 50% of cells, 8: approximately 75% of the nuclei are positive, 9: approximately 90% of the nuclei are positive, 10: few negative cells.

Apoptosis Detection in lung tissue

Immunofluorescence staining was performed on frozen sections (15–20 μm) fixed with 4% paraformaldehyde and permeabilized with Triton X-100. Nuclei were stained with Hoechst 33258 (bis-benzamide H, Sigma Aldrich, B2883) and visualized with a Zeiss LSM 510 laser scanning confocal microscope. Volocity software (Improvison, Lexington, MA) was used to construct 3-dimensional models to allow an accurate volume of the tissue examined. The extent of nuclear condensation as measured by the increase in intensity of the nuclear stain Hoechst 33258, a measure of the extent of apoptosis of the cells in the tissue [Nusbaum *et al.*, 2005; Schmalstieg *et al.*, 2007] was analyzed using an Improvision software. The intensities of Hoechst staining were collected and assigned to previously determined ranges (binning).

Reactive oxygen species detection

ROS generation was determined by using immunological reagents to detect carbonyl groups introduced into proteins by oxidative reactions with oxides of nitrogen or by metal catalyzed oxidation [Stadtman, 1993; Shacter, 2000]. This experiment was performed using protein oxidation detection assay [OXYBLOT kit (Millipore, Billerica, MA)]. Lung samples were homogenized in 10 volumes of homogenization buffer containing 50 mM Tris/HCl, 1 mM EDTA, 1% NP-40, 150mM NaCl, 0.25% Na-deoxycholate (pH 7.4), and 1:100 Protease Inhibitor Cocktail. Protein concentration in samples was determined by the Bradford method with bovine serum albumin as standard. The carbonyl groups in proteins were first derivatized with 2,4-dinitrophenylhydrazine (DNPH) in the presence of 6% SDS. The kit used for the oxyblot analysis is sensitive to detect as little as 10 femtomoles of dinitrophenyl residues. To determine specificity, the oxidized proteins provided by the kit were included as a positive control. Treatment of samples with a control solution served as a negative control to the DNPH treatment. After a 15 minutes incubation at room temperature the reaction was stopped. Samples were loaded on 4-20% gradient NuBlu SDS-PAGE (NuSep, Lawrenceville, GA) gels for 60 minutes at 200 volts. Following electroblotting to 0.2 μm nitrocellulose for 1 hour at 100 volts, the membrane was blocked and stained using OxyBlot Kit methods and reagents. Bands were visualized with chemiluminescence and captured on film. The total protein carbonylated was measured by reviewing all the bands in each sample by densitometry. To quantify the amount of oxidation and allow the comparison between the various

samples, oxidative index was defined as the ratio between densitometric values of the total oxyblot bands and β-actin bands.

RESULTS

Changes in plasma NOx and up-regulation of iNOS protein in lung homogenates

There was no significant difference in pre-injury plasma NOx concentration (Figure 4.1 A) between the control group and the B + S injured animals. There was a significant difference observed between the control (4.91 ± 0.59) and the B + S injured animals at 8 hrs (7.21 ± 0.69) ($p < 0.03$) which was sustained to the 12 hrs time point. The plasma NOx concentration was maximal at 12 hrs post B + S injury (14.88 ± 3.96) and was 3-fold higher ($p < 0.03$) than the control group.

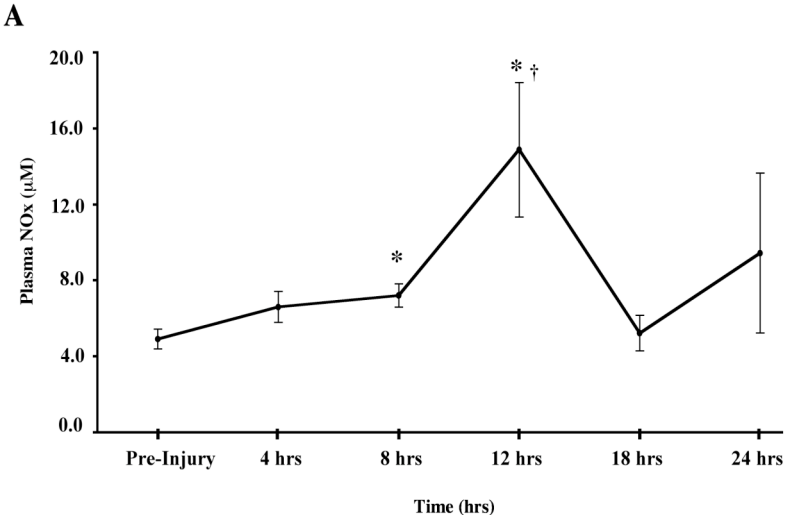

Figure 4.1 Kinetics of plasma nitrite/nitrate (NOx, mM). Sheep were administered a third degree 40% TBSA burn followed by smoke inhalation injury (B+S) and were sacrificed at the indicated times. Blood samples were collected before and after injury and plasma NOx concentration was determined. Results are shown as mean ± SEM. N = 5 per group; † $p \leq 0.05$ vs.4hrs post B+S injury; * $p \leq 0.05$ vs. control.

iNOS protein is significantly up-regulated in sheep lung 8 hrs after injury ($p < 0.005$) and reached a peak at 12 hrs post injury (Figure 4.1 B).

NF-κB (p65) translocates into the nuclear compartment after B + S injury

iNOS transcription is determined by nuclear factor-κB (NF-κB) translocation into the nuclear compartment. We subjected sheep lung nuclear extracts to SDS- polyacrylamide

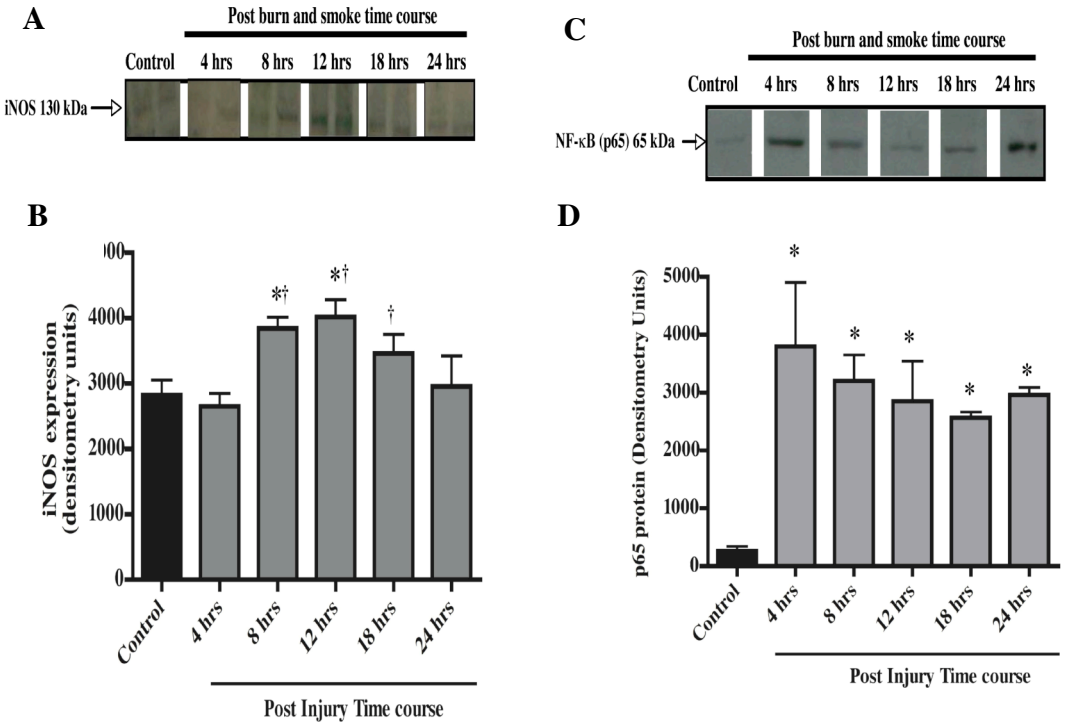

Figure 4.2 Time course of iNOS and p65 protein expression in sheep lung lysate. (A and C) Representative Western blot of lung lysate using rabbit anti-iNOS. (D) Nuclear extracts from lung tissue at the indicated times post burn and smoke injury were resolved on SDS-polyacrylamide gel electrophoresis transferred to a PVDF membrane and immunoblotted using a rabbit anti-p65 antibody. Each lane represents samples from separate animals in each group. (B) and (D) demonstrates the quantitative densitometric analysis of expressed iNOS and p65 bands. Data is represents integrated band intensities obtained from five different samples from each group (mean ± SEM). † $p \leq 0.05$ vs.4hrs post B+S injury; *$p \leq 0.05$ vs. control.

gel electrophoresis followed by immunoblotting to determined amounts of free NF-κB (p65). There was a 14-fold increase in p65 protein 4 hrs after injury compared to the uninjured control animals (Figure 4.2D). This increase in p65 was maintained throughout the experimental time period.

Increased protein oxidation and nitrotyrosine formation after injury

3-nitrotyrosine immunoblotting showed a progressive increase in protein nitration in the lung after B + S injury compared to the uninjured control group ($p < 0.0005$) (Figure 4.3 A and B). At 12 hours post injury, there was a 2-fold increase in protein oxidation compared to the control group ($p < 0.03$), as measured by protein carbonyl formation (Figure 4.3 C and D). This was sustained at 18 through 24 hours post injury ($p < 0.04$ and $p < 0.03$, respectively).

Increased PARP-1 activity in lung tissue post injury

A representative photomicrograph depicting the time course of PARP activity is in Figure 4.4. Immunohistochemical examination of poly (ADP ribose) (PAR) polymers in the lung showed positive staining in the alveoli, airway and pulmonary microvasculature (Figure 4.5 A, B and C). There was progressive and significant increase PAR staining intensity in the airway epithelium, alveoli and endothelial cells. Immunoblotting of the lung nuclear lysate (Figure 4.4 D) showed a significant increase in PAR polymer immunoreactivity at 12 hours post injury and thereafter at 18 and 24 hours.

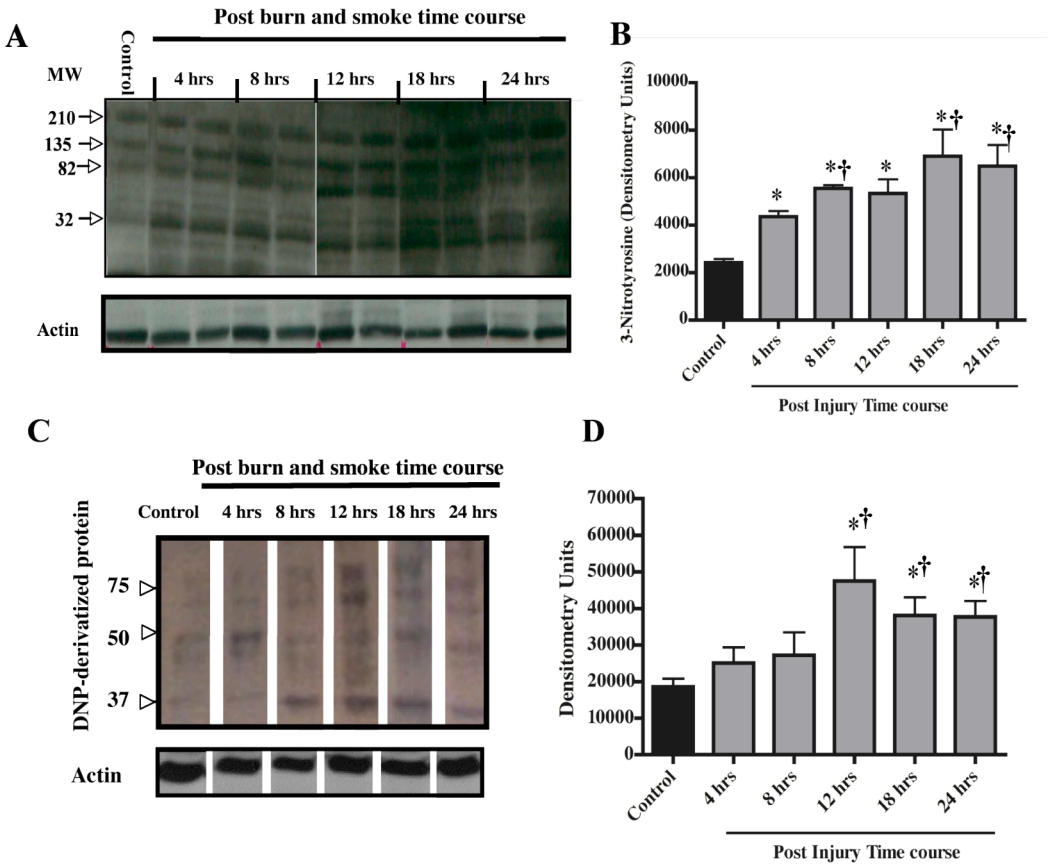

Figure 4.3 Kinetics of 3-nitrotyrosine formation and protein oxidation in sheep lung lysate at the indicated time points after combined burn and smoke injury. Representative Western blots of lung homogenate using (A) mouse ant-3-nitrotyrosine, and (C) rabbit anti-Dinitrophenol (DNP) after protein derivatization with DNP-hydrazone; (B) and (D) represents densitometric analysis of protein bands obtained from five different samples from each experimental group. Arrows indicate protein molecular weight. † $p \leq 0.05$ vs.4hrs post B+S injury; *$p \leq 0.05$ vs. control.

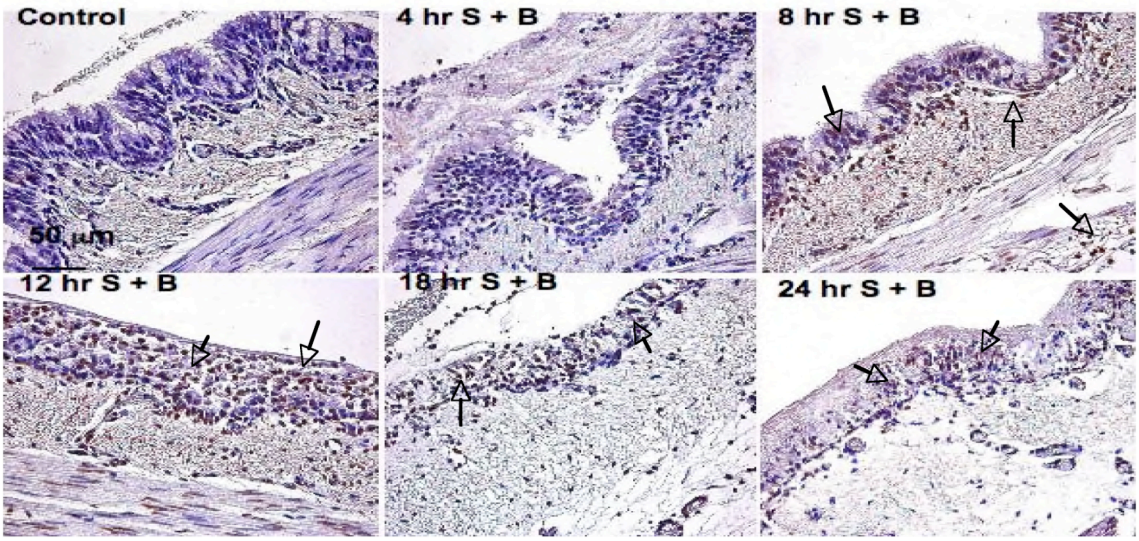

Figure 4.4 Representative photomicrograph depicting the time course of poly(ADP) ribose (PAR) polymers as an index of PARP activity in the lung. The arrows indicate areas in PAR polymer staining; note that intense staining for PAR polymers was observed at 8 hours and 12 hours after injury compared to the uninjured control tissue.

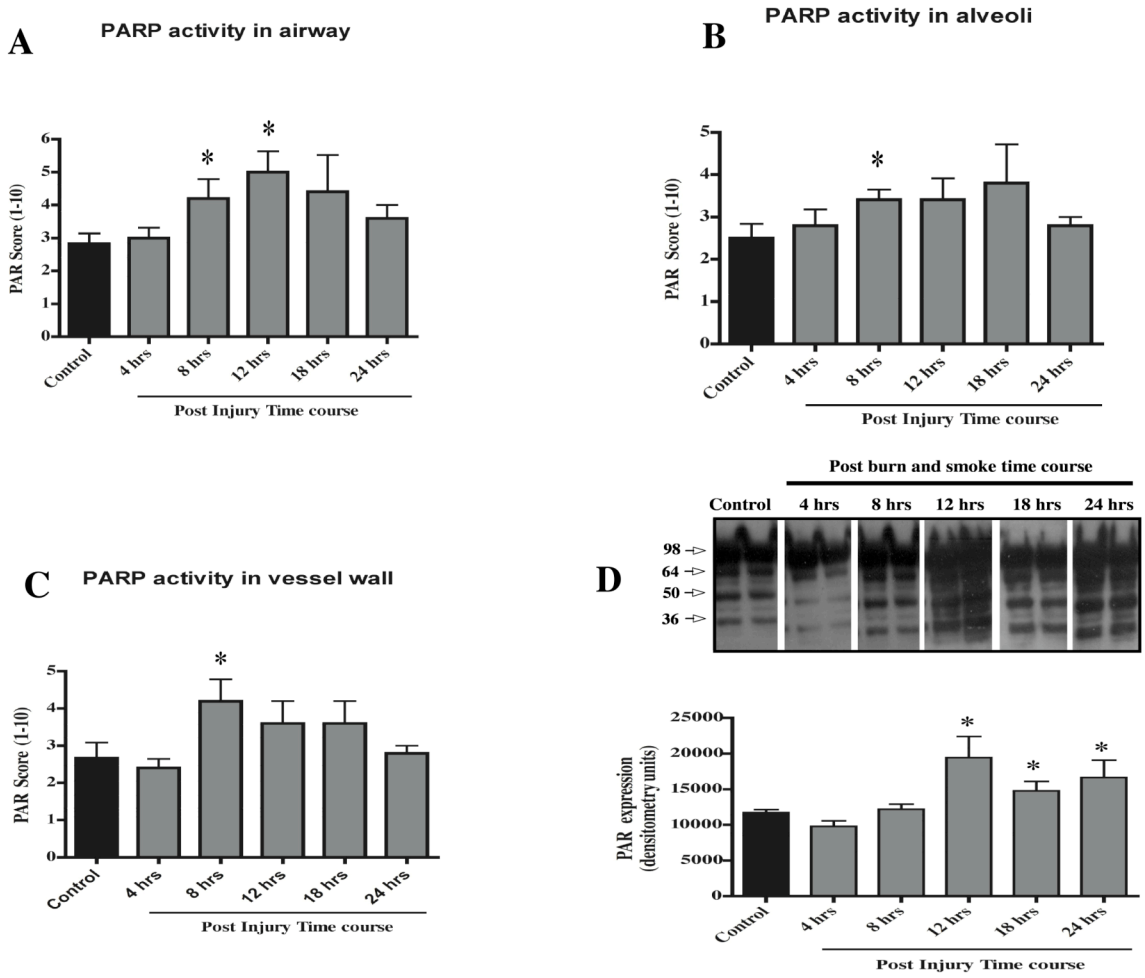

Figure 4.5 Histograms representing PARP activity in lung tissue in uninjured sheep and at multiple time points after injury. (A), (B) and (C) represents integrated semi-quantitative score from five animals in each group. Note that differences in PARP activity is observed at 8 hrs post injury compared to the control animals and at 12 hrs post injury in the airway (A). (D) representative Western blots of nuclear extract using a rabbit anti-PAR antibody and quantitative results after densitometric analysis. Data are presented as mean ± SEM, N=5 per group. *$p \leq 0.05$ vs. control.

Apoptosis detection in the lung

A difference in the degree of Hoechst intensity was apparent between the control un-injured and the injured animals. Increased Hoechst intensity was observed at all times after injury compared with control animal ($p < 0.001$) (Figure 4.6A and B).

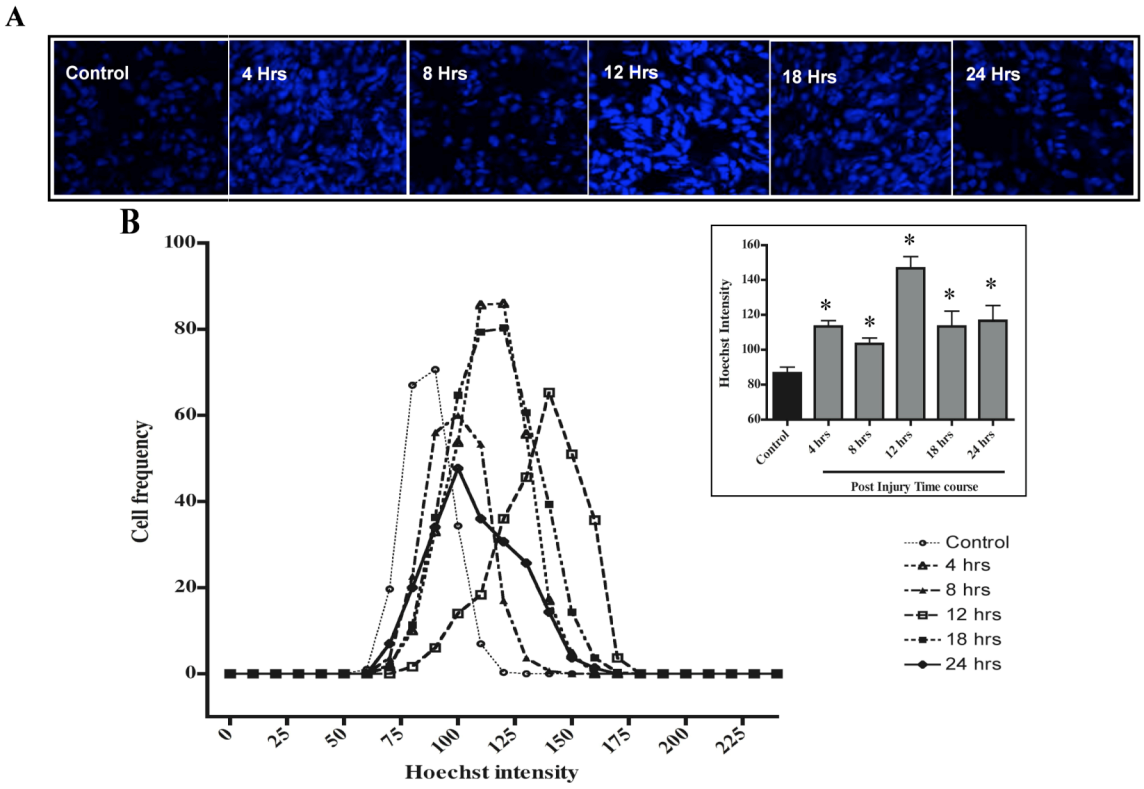

Figure 4.6 (**A**) Apoptosis as detected by fluorescent intensity of Hoechst staining in confocal micrographs of lung tissue. (B) The confocal software counted the number of cells with each Hoechst staining intensity. There was a difference observed in peak fluorescent intensity between the control group versus the burn and smoke injury groups (inset). Data is presented as mean ± SEM, N = 3 per group, $*p \leq 0.05$ vs. control.

DISCUSSION

Trauma due to burn and smoke injury is commonly associated with elevated levels of free radicals such as the ubiquitous signal transduction molecule, nitric oxide (NO) and generation of reactive nitrogen and oxygen species. The results from this study provides evidence for (1) oxidative/nitrosative stress in injured lung tissue (augmented protein oxidation and elevated 3-nitrotyrosine formation), (2) up-regulated iNOS protein and increased plasma NO concentration (shown by Western blotting and chemiluminescence NOx detection), and (3) up-regulated PARP-1 activity in injured lung. Here, we show a time course of the molecular events that occur between the reception of a burn and smoke biological signal and the dissemination of the signal in the lung that eventually leads to nitrosative stress and DNA damage.

Clinical interventions are often performed to decrease airway obstruction and thereby improve pulmonary function. Previous studies from our lab demonstrated a marked increase in PAR polymers and the development of nitrosative stress in injured lung areas 24 and 48 hours post burn and smoke injury [Shimoda *et al*., 2003; Murakami *et al*., 2004]. This present study provides support for a rapid and robust upregulation of iNOS protein in the lung that could contribute substantially to secondary damage (Figure 4.2B).

iNOS is regulated at the transcriptional, posttranscriptional, and post-translational levels. Cellular stimuli such as ROS or RNS can induce airway epithelial cells and invading inflammatory cells such as neutrophils, to transcribe iNOS [Moncada *et al*., 1991; Xie *et al.*, 1994]. In this study, we demonstrated that burn and smoke inhalation

injury significantly up-regulates iNOS protein in the lung and by 12 hours post injury, the enzyme was maximally expressed (Figure 4.2 B, C). This was followed by a gradual decline beginning at 18 hours through 24 hours towards un-stimulated, sham protein level. The expression of iNOS requires several hours as demonstrated in this study. A lag period can be observed before NO production begins. However, once induced, iNOS remained active for hours and produced a significant increase in NO concentration. The plasma NOx data is in agreement with the iNOS expression pattern. Compared to the constitutive NOS isoforms, iNOS derived NO production increases 1000-fold **[**Pacher *et al.*, 2007**].** Although all NOS enzymes may potentially generate O_2-, iNOS is the most likely to produce O_2^- *in vivo.*

Production of NO is highly damaging during pathological challenges such as burn and smoke induced ALI. NO reacts readily with superoxide to form a very potent oxidant, peroxynitrite [Beckman *et al.*, 1990; Kissner *et al.*, 1997]. The large localized production of superoxide in the lungs can serve as a sink to trap NO [Lui *et al.*, 1998]. Lui *et al* have also demonstrated that a modest increase in production of superoxide and NO simultaneously, can greatly stimulate the formation of peroxynitrite; a 10-fold increase in superoxide and NO production will increase peroxynitrite formation 100-fold [Pacher *et al.*, 2007]. Even the generation of a moderate flux of peroxynitrite over long periods of time will result in substantial oxidation and potential destruction of host cellular constituents, leading to the dysfunction of critical cellular processes, disruption of cell signaling pathways, and the induction of cell death through both apoptosis and necrosis [Virág *et al.*, 2003]. Therefore many of the damaging effects are mediated by the

oxidation product, ONOO-, rather than by NO itself. In this study, we observed a progressive post-injury increase in peroxynitrite production and protein oxidation (as measured by 3-nitrotyrosine and protein carbonyl generation, respectively (Figure 4.3)). Consequently, pathological conditions such as severe trauma can greatly increase the production of peroxynitrite by attenuating endogenous antioxidant defenses [Radi *et al., 2002*].

NO, at low concentrations, has been shown to induce IκB phosphorylation, the NF-κB inhibitory subunit. Brüne and others [Brüne, 2000; Connelly *et al.*, 2001] previously reported an inverse relationship between NO concentrations and NF-κB DNA binding. While low NO-donor concentrations increased NF-κB DNA binding, higher NO concentrations inhibited these NF-κB DNA binding activities. These findings are in support of our observations, where as low NO concentration 4 hours post injury was associated with increased NF-κB-p65 nuclear translocation, high NO concentration at 12 hours post injury was associated with a decrease in NF-κB-p65 nuclear translocation. This interaction is most likely due to peroxynitrite formation and nitration of tyrosine residues on the protein rather than elevated NO concentration. Levrand *et al* recently demonstrated that peroxynitrite inactivates NF-κB nuclear translocation by inhibiting upstream phosphorylation of IKK thereby blocking IKK activation and downstream I-κB activation and degradation [Levrand *et al.*, 2005].

Nitrosative and oxidative stress modulate PARP-1 activity in the nucleus. PARP-1 acts to allow DNA repair and cell recovery in conditions associated with a low degree

of DNA damage. However, upon severe DNA injury, over-activation of PARP-1 depletes the cellular stores of NAD+, an essential cofactor of several biochemical pathways in the cell including the mitochondrial electron transport chain [Szabó *et al.*, 1996; Szabó *et al.*, 1998; Liaudet, 2002; Liaudet *et al.*, 2003]. Using immunohistochemical techniques, we show increased positive staining of PAR polymers in the lung, specifically in the alveoli and around the airway and pulmonary microvasculature. These observations were confirmed by immunoblotting the lung nuclear lysate. Several investigators have demonstrated that both exogenous and endogenously generated peroxynitrite potently induce DNA strand breakage leading to PARP-1 activation in a variety of cell types, including pulmonary [Szabó *et al.*, 1997], macrophages [Zingarelli *et al.*, 1996], and cardiomyocytes [Gilad *et al.*, 1997; Pacher *et al.*, 2002]. The formation of DNA single strand breaks represents a critical aspect of peroxynitrite-mediated cytotoxicity, since they represent the obligatory trigger for the activation of PARP-1 [Szabo *et al.*, 1996] a pathway ultimately related to the induction of cell death. In this study, elevated PARP-1 activity was associated with apoptotic cell death.

There are striking similarities between the expression pattern of PARP-1 and the detrimental transcriptional activity of NF-κB. In most tissues and cell types associated with high PARP-1 expression, dysregulated NF-κB activity seems to contribute to cellular dysfunction and cell death during inflammatory disorders. A recent report using drugs to inhibit PARP-1 activity showed a reduction in NF-κB-dependent transcription of IL-1β, iNOS, and TNF-α in glia thus protecting neurons and brain tissue from immune-

induced neurodegeneration [Chiarugi and Moskowitz, 2003]. This PARP-1/ NF-κB relationship is also evident in PARP-1 knockout studies. PARP-1 -/- mice, for example, exhibit an impaired NF-κB-dependent transcription of pro-inflammatory mediators [Oliver *et al.*, 1999; Hassa *et al.*, 2001; Ha *et al.*, 2002].

While peroxynitrite has been associated with apoptosis in various cell types [Taylor *et al.*, 2004; Dickhout *et al.*, 2005; Levrand *et al.*, 2006], our results suggests an early peroxynitrite-mediated cell death in lung tissue after burn and smoke injury. In addition this combined injury leads to the activation of the peroxynitrite-PARP-1 pathway. This early presence provides a possible explanation for the early decline in pulmonary function.

Our data showed that 3-NT formation was detected at 4 hours however NOx concentration was not significantly elevated at that time point compared to the pre-injury level ($p = 0.0864$) although there was a trend towards increased plasma NOx at 4 hours after injury. This disparity could also be explained by differences between the local versus systemic NO response and 3-NT production *in vivo*. In our study, 3-NT was detected in a lung homogenate that contains a heterogeneous cell population including resident alveolar macrophages, pulmonary epithelial cells and vascular endothelial cells. Stimulated alveolar macrophages, for example, produce large amounts of nitric oxide that is accompanied by elevated levels of NOx and may be accompanied by increased synthesis of 3-NT in the lung [Shigenaga *et al.*, 1997; Iijima *et al.*, 2001; Pacher *et al.*, 2007]. Our data are limited in that we did not quantify NOx levels in the tissue homogenate however the early presence of 3-NT suggests the presence of elevated NO

and peroxynitrite formation in response to the injury. Another possible explanation is the paradoxical contribution of superoxide dismutase (SOD) in catalyzing tyrosine nitration. The presence of SOD would be expected to reduce peroxynitrite formation by scavenging superoxide however, by effectively reducing the superoxide scavenging activity Ischiropoulos *et al* demonstrated that a modified and an unmodified SOD could enhance tyrosine nitration through peroxinitrite binding to the preserved copper center active site of both enzymes [Ischiropoulos *et al.,* 1992]. Lastly myeloperoxidase (MPO), contained in neutrophils, has been demonstrated to indirectly catalyze tyrosine nitration via production of nitrogen dioxide [Floris *et al.,* 1993; Sampson *et al.,* 1996]. The contribution of MPO is in keeping with our data in Chapter 3.

Although this study provides evidence to the involvement of iNOS the peroxynitrite generation, we have not ruled out the potential contribution of the other NOS isoforms in the formation of nitrosative stress after injury. NOS-1 or neuronal NOS (nNOS) and NOS-3 or endothelial NOS (eNOS), originally thought to be constitutively expressed, have been recently been demonstrated to be dynamically regulated [Ziesche *et al*., 1996; Iijima *et al*., 2005]. nNOS protein in particular can be up-regulated in response to ovalbumin challenge to mimic allergic airway inflammatory disorder [Iijima *et al*., 2005]. Both enzymes are involved in the catalytic conversion of L-arginine to NO. It is therefore possible that NO production attributed to either nNOS or eNOS contributes to peroxynitrite formation. Our data are limited in that we were unable to detect of these molecules due to the lack of anti-nNOS and anti-eNOS antibodies that cross reacts with the ovine homolog. Nevertheless, our data does demonstrate that during the first 12 hours

post injury the development of nitrosative stress is attributed, at least in part, by iNOS protein expression in the lung.

CHAPTER 5
HYDROGEN SULFIDE ATTENUATES ACUTE LUNG INJURY AFTER SMOKE INHALATION AND BURN INJURY IN SHEEP

INTRODUCTION

As we reported in previous chapters, ALI develops in patients suffering from major trauma such as burn and smoke inhalation injury as well as pneumonia, aspiration of gastric contents and sepsis. Current definitions require the exclusion of left atrial hypertension and heart failure during clinical assessment [Brown, 1998; Abraham *et al*., 2000]. The primary physiological abnormalities are severe arterial hypoxemia as well as marked increase in ventilation and pulmonary hypertension. Most of these patients require assisted ventilation with positive pressure.

Studies from our lab have demonstrated that combined burn and smoke inhalation injury impairs HPV, the vasoconstrictive response to hypoxia, thereby mismatching ventilation with perfusion [Westphal *et al*., 2006]. Gas exchange is affected by increases in the dispersion of both alveolar ventilation and cardiac output because bronchial and vascular functions are altered by disease-related factors, such as the effects of inflammatory mediators on airway and vascular smooth-muscle tone. Because oxygen exchange is determined by alveolar ventilation, areas of high alveolar ventilation / blood flow (V_A/Q) ratio and dead space in ALI increases the ventilation required to keep the arterial partial pressure of oxygen (PaO_2) level constant. Therefore, the work to expand

the lungs to maintain the PaO_2 level must also increase as lung compliance decreases. Additionally, hypoxemia produced by alveolar edema impairs gas exchange by creating areas of low V_A/Q ratio and shunt. A recently published study from our lab described a marked declined in pulmonary gas exchange over time in mice after burn and smoke injury [Mizutani *et al*., 2008]. This is a consistent finding in our large animals studies [Westphal *et al*., 2006; Murakami *et al*., 2007; Enkhbaatar *et al*., 2008]. In previous studies, we have reported that elevated levels of nitric oxide (NO) and reactive nitrogen and oxygen species increases in parallel with this diminished physiological response and increased pulmonary shunting [Westphal *et al*., 2007; Enkhbaatar *et al*., 2008].

The current study used sodium hydrogen sulfide (NaHS) to study the effectiveness of attenuated reactive nitrogen species formation on long-term survival and pulmonary function outcomes, including PaO_2/FiO_2 ratio, pulmonary shunt fraction and inspiratory peak and pause airway pressures. NaHS (Ikaria, Seattle, WA), a H_2S donor compound, has previously been used as a peoxynitrite scavenger [Whiteman *et al*., 2004] and as a modulator of leukocyte mediates inflammation [Zanardo *et al*., 2006]. While significant reduction of iNOS, protein oxidation and PARP-1 was demonstrated in this study, significant reduction in neutrophil accumulation (as measured by myeloperoxidase activity) was not evident. However, we reasoned that a reduction in nitrosative stress would have a significant effect on pulmonary function and survival outcomes. Thus, we wanted to test NaHS treatment in a clinically relevant ovine model of burn and smoke inhalation-induced ALI. As an indirect measure of peroxynitrite formation, we measured protein 3-nitrotyrosine (3-NT) formation in lung homogenates at 96 hours post injury.

Treatment with NaHS after injury significantly reduced 3-NT in the lung. Additionally, treatment with NaHS, a H_2S donor, significantly improved survival outcomes related to the dual insult when compared with the vehicle treated group.

METHODS

Surgical Preparation

The following procedures were approved by the Animal Care and Use Committee of the University of Texas Medical Branch, and were in compliance with the guidelines for the care and use of laboratory animals of the National Institutes of Health and the American Physiological Society. Adult merino ewes, weighing between 31 and 39 kg, were used. All animals were intubated and ventilated during the surgery while under ketamine and halothane anesthesia. Arterial catheters (16-gauge, 24 in., Intracath, Becton Dickinson, Sandy, UT) were placed in the descending aorta via the femoral artery. A Swan-Ganz thermal dilution catheter (Model 93A-131-7F, Edwards Lifesciences, Irvine, CA) was positioned in the pulmonary artery via the right external jugular vein. Through the left fifth intercostal space, a catheter (Durastic Silicone Tubing DT08, I.D.=0.062in, O.D.=0.125in, Allied Biomedical, Ventura, CA) was positioned in the left atrium. The sheep were given 5 to 7 days to recover from the surgical procedure with free access to food and water.

Burn and smoke inhalation injury

The animals were anesthetized using 10 mg/kg of ketamine (KetaVed, Phoenix Scientific, Inc., St. Joseph, MO.) and continued with halothane. A Foley catheter was placed in the urinary bladder to determine urine output after which the animals received a tracheotomy and a cuffed tracheostomy tube (10-mm diameter, Shirley, Irvine, CA) was inserted. The animal's wool was shaved and a 20% total body surface area (TBSA) third-degree flame burn was made on one flank. The burn was administered with a Bunsen burner, and flame applied until the skin is completely contrwacted and the nerve endings destroyed by the heat. Inhalation injury was induced using a modified bee smoker that was filled with 50 g of burning cotton toweling and connected to the tracheostomy tube via a modified endotracheal tube containing an indwelling thermistor from a Swan-Ganz catheter. During the insufflation procedure, the temperature of the smoke was monitored carefully not to exceed 40°C. The sheep was insufflated with a total of 48 breaths of cotton smoke. After smoke insufflation, another 20% TBSA third-degree burn was made on the contra-lateral flank.

Resuscitation protocol

After injury, anesthesia was discontinued and the animals were allowed to awaken but still mechanically ventilated with a Servo Ventilator (Model 900C Siemens-Elema, Solna, Sweden) throughout the experimental period. Ventilation was performed with a positive end-expiratory pressure (PEEP) of 5 cm H_2O and a tidal volume of 15 mL/kg. The respiratory rate set to maintain normocapnia. For the first 3 hrs after the combined

injury, the sheep received an inspired oxygen concentration of 100%; thereafter, oxygen concentration was adjusted to maintain the arterial oxygen saturation above 90%. These settings allow a rapid disappearance of carboxyhemoglobin (CO-Hb) after smoke inhalation. Fluid resuscitation during the experiment was performed with Ringer's lactate solution following the Parkland formula (4 mL / % burned surface area / kg body weight for the first 24 hrs and 2 mL / % burned surface area / kg body weight / day for the next 48 hrs). The Parkland formula was started one hour after injury. One-half of the volume for the first day was infused in the initial 8 hrs, and the rest infused in the next 16 hrs. Urine was collected and urine output recorded every 6 hrs. During this experimental period, the animals were allowed free access to food, but not to water, to allow accurate determination of fluid balance.

Measured Cardiopulmonary Variables

Measured physiological parameters were not considered valid until the animals were fully awake and standing. Mean arterial (MAP; in mm Hg), pulmonary arterial (PAP; in mm Hg); left atrial (LAP; in mm Hg), and central venous (CVP; in mm Hg) pressures were measured with pressure transducers (model P X 3 X 3, Edwards Lifesciences, Irvine, CA). Cardiac output was measured with a cardiac output computer (Model COM-1; Edwards Lifesciences, Irvine, CA) using the thermodilution method with cold 5% dextrose as an indicator solution, for evaluation of cardiac function. The following derived hemodynamic variables were calculated: cardiac index, ventricular stroke work index, vascular resistance index and shunt fraction. The standard equations

used for these variables are described in the Appendix. Arterial and mixed venous blood were measured with a blood gas analyzer (model IL Synthesis 15, Instrumentation Laboratory, Lexington, MA). The data was corrected for the body temperature of the sheep. Oxyhemoglobin saturation and carboxyhemoglobin concentration were analyzed with a CO-oximeter (Model IL482; Instrumentation Laboratory, Lexington, MA). Hematocrit (Ht) was measured in heparinized microhematocrit capillary tubes (Fisherbrand; Fisher, Inc., Pittsburgh, PA).

Hydrogen Sulfide Donor formulation

Na_2S was produced and formulated to pH neutrality and iso-osmolarity by Ikaria Inc (Seattle, WA) using H_2S gas (Matheson, Newark, CA) as a starting material [Elrod *et al.*, 2007]. The NaHS formulation was diluted in normal saline to the desired concentration and used immediately thereafter. All doses were made fresh daily in a rapid fashion and sealed in sterile airtight tubes until use.

Animal model

See Chapter 2 for detailed protocol. The study protocol is shown in Figure 5.1.

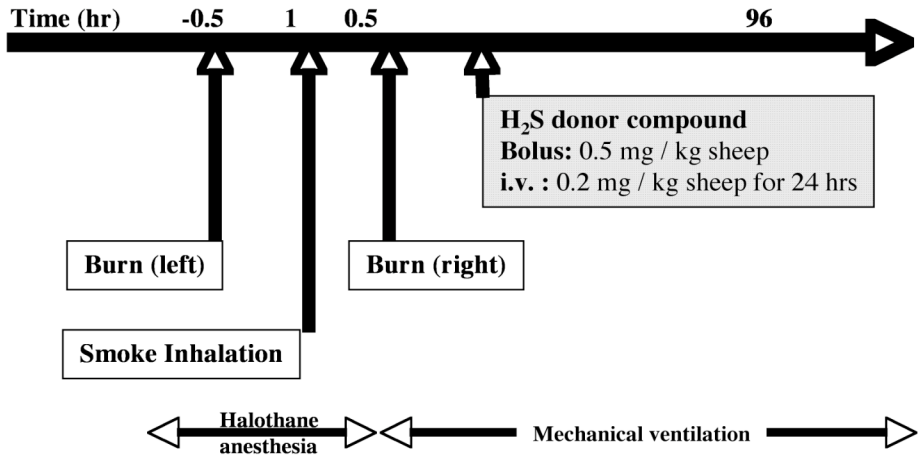

Figure 5.1 Experimental protocol. The H_2S donor was started 1 hour after smoke inhalation injury. Fluid resuscitation using Ringer lactate was started immediately after the injury.

Lung tissue preparation

The protocol for tissue preparation is described in detail in Chapter 2.

Preparation of nuclear protein extracts

The pellet containing the nuclei was thawed on ice and resuspended in 250 µL cold nuclear extraction buffer containing 0.1 M DTT (Sigma Aldrich, Saint Louis, MO) and 1.5 µL stock protease inhibitor cocktail (Sigma Aldrich, Saint Louis, MO) was added to produce a final 1 X concentration (AEBSF 1 mM, aprotinin 800nM, E-64 15 µM, leupeptin 20 µM, bestatin 50 µM, pepstatin A 10 µM). Samples were agitated vigorously for 15 seconds every 10 minutes for 30 minutes. The mixture is again centrifuged at 20,000 X g for 5 minutes. The supernatant containing the nuclear proteins was collected and total protein was determined (Chapter 2).

Preparation of mitochondrial protein extracts

The mitochondrial fraction was isolated using a modified protocol [Cox *et al.*, 2006]. Lung tissue samples were homogenized and the lysate was clarified at 800 x *g* for 15 minutes. The pellet was discarded and the supernatant further clarified at 6000 x *g* for 15 minutes. The supernatant was discarded and the pellet was re-suspended in 10 volumes of a hypotonic lysis buffer for extraction of soluble mitochondrial proteins that consisted of 10 mM HEPES (pH 7.9), 1 mM DTT and 1 mM PMSF. This lysate was again clarified at 11, 000 x *g* for 20 minutes. The supernatant was saved to quantify total protein (Chapter 2).

Western blotting protocol

80 μg of the protein extract was boiled in 2X Laemmli sample buffer, separated on a 4-20% SDS-polyacrylamide gradient gel by electrophoresis and transferred to an Immobilon–P PVDF membrane. Membranes were blocked in blocking solution (Tris-buffered saline-Tween 20: 10 mM Tris-HCl [pH 7.4], 154 mM NaCl, 0.05% Tween 20 [vol/vol]) containing 5 % non-fat dry milk powder [wt/vol] for 1 hour at room temperature. The membranes were immunoblotted at 4°C overnight with primary antibodies diluted in Tris-buffered saline-Tween 20: 10 mM Tris-HCl [pH 7.4], 154 mM NaCl, 0.05% Tween 20 [vol/vol]) containing 1% non-fat dry milk powder [wt/vol]. The following antibodies were used: rabbit anti-PAR (Catalog No. 4336-BPC-100) purchased from Trevigen, Gaithersburg, MD was diluted to 1: 1000; biotinylated mouse anti-nitrotyrosine (Catalog No. 10006966) purchased from Cayman Chemicals, Ann Arbor MI

was diluted to 1:1500; and rabbit anti-NOS2 (Catalog No. sc-650) diluted to 1:200 and goat anti-β-Actin (Catalog No. sc-1616) purchased from Santa Cruz Biotechnology Inc (Santa Cruz, CA) was diluted to 1:500. The primary antibody was detected using the following horseradish peroxidase-conjugated secondary antibodies: goat anti-rabbit (Catalog No. HAF008) diluted to 1:4000 or donkey anti-goat (Catalog No. HAF109) antibody diluted to 1:3000 or streptavidin-HRP (Catalog No. DY998) diluted at 1:200 purchased from R&D Systems (Minneapolis, MN). The membranes were subjected to chemiluminescence using the SuperSignal West Pico Chemiluminescent Substrate (Pierce, Rockford, IL) according to the manufacture's instructions and intensity of immunoreactivity was measured using NIH ImageJ software (http://rsb.info.nih.gov/nih-image/).

Lung Cytochrome C ELISA

The assay was performed according to the manufacturer (R&D Systems, Minneapolis, MN). Briefly, 100 µL of standards or lung mitochondrial extracts were added to each well pre-coated with a monoclonal antibody specific for cytochrome c and incubated for 2 hours at room temperature (20 - 25°C). The plates were aspirated and washed three times with 400 µL of wash buffer. 200 µL of the cytochrome c conjugate antibody was added to each well and incubated for 2 hours. The microplate was washed and 200 µL of substrate solution was added to each well. The microplate was protected from light during this step and incubated for 30 minutes at room temperature. 50 µL of a

stop solution was to each well and the intensity of the color was measured at 450 nm with a wavelength correction at 540 nm using a spectophotometer (MRX, Dynatech Laboratories Inc., Chantilly, VA).

Lung wet-to-dry weight ratio measurement

The lower right lobe was sampled to measure bloodless wet-to-dry weight ratio. The protocol for lung wet-to-dry weight measurement and calculation is described in detail in Chapter 2.

RESULTS

Mortality study and Cardiopulmonary Responses

The number of animals used in the survival analysis was n = 8 for both the control NaHS treated group. The animals in the treated group had 100% survival at the end of the experimental period compared to the untreated control animals that had a 25 % survival (Figure 5.2).

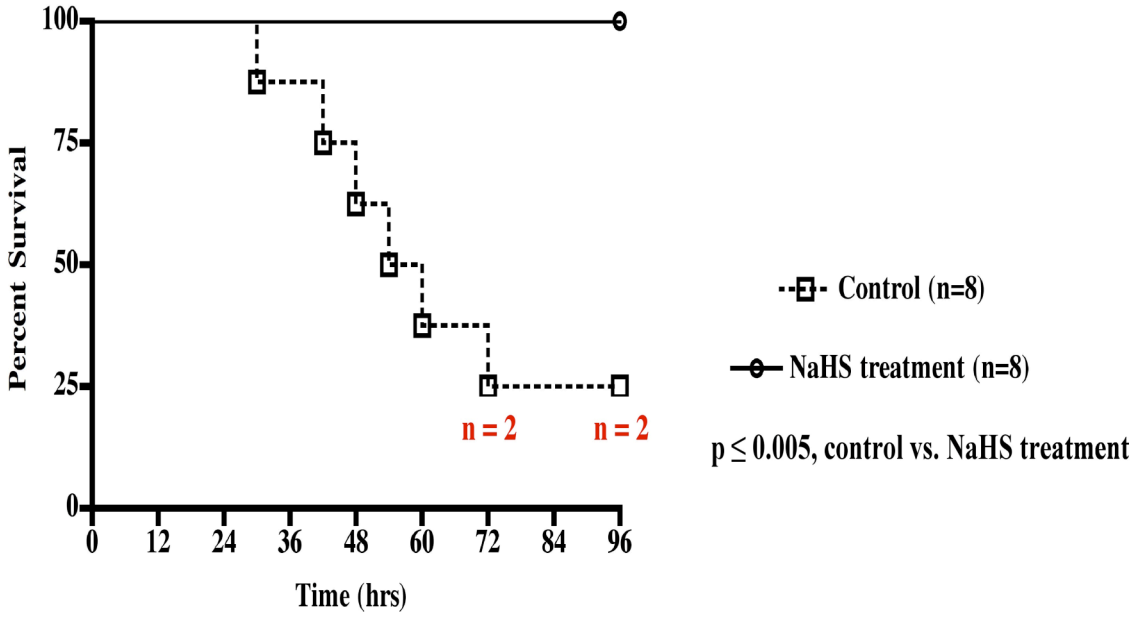

Figure 5.2 Kaplan-Meier curve showing survival over time in the vehicle control group and the NaHS treatment group.

Table 5.1 gives the hemodynamic changes observered during the 96 hr experimental time period. There was no significant difference in cardiac index (CI), mean arterial pressure (MAP) and mean pulmonary artery pressure (MPAP) between the control group and the NaHS treated group. Left atrial pressure (LAP) was reduced in the NaHS treated group at 30 and 36 hours post injury. There was a significant difference in central venous pressure (CVP) at 30 and 72 hours in the NaHS treated animals while pulmonary vascular resistance index (PVRI) was attenuated at 18 hours and at 30 through 60 hours post injury.

Table 5.1 Cardiopulmonary hemodynamics

	Times post injury (hours)										
Parameter	**0**	**12**	**18**	**24**	**30**	**36**	**48**	**60**	**72**	**84**	**96**
CI, l.min.m²											
Vehicle	5.8 ± 0.2	5.5 ± 0.3	5.3 ± 0.4	5.9 ± 0.4	6.1 ± 0.3	6.7 ± 0.5	7.6 ± 0.6	8.1 ± 1.0	7.4 ± 0.9	7.1 ± 1.7	8.2 ± 2.4
NaHS Treatment	6.9 ± 0.2	7.1 ± 0.8	6.8 ± 0.5	6.5 ± 0.2	6.7 ± 0.3	6.4 ± 0.3	7.0 ± 0.6	7.1 ± 0.6	7.0 ± 0.6	7.7 ± 0.6	7.5 ± 0.7
MAP, mmHg											
Vehicle	99 ± 2	108 ± 3	104 ± 4	104 ± 3	103 ± 3	101 ± 3	105 ± 2	105 ± 5	105 ± 8	93 ± 3	88 ± 3
NaHS Treatment	94 ± 2	105 ± 4	108 ± 4	104 ± 3	104 ± 3	105 ± 3	104 ± 3	104 ± 4	102 ± 3	101 ± 4	100 ± 5
MPAP, mmHg											
Vehicle	20.9 ± 0.7	25.9 ± 1.6	28.9 ± 1.4	28.9 ± 1.2	29.9 ± 1.4	29.4 ± 1.4	29.2 ± 1.3	26.3 ± 2.8	25.0 ± 3.0	23.0 ± 1.0	24.0 ± 2.0
NaHS Treatment	19.9 ± 0.5	27.4 ± 1.3	27.4 ± 1.5	28.0 ± 1.3	26.8 ± 1.3	26.6 ± 1.6	28.1 ± 1.0	26.0 ± 1.2	26.6 ± 1.1	26.9 ± 1.3	27.3 ± 1.4
LAP, mmHg											
Vehicle	9.5 ± 0.7	9.6 ± 0.8	10.3 ± 1.1	12.0 ± 0.8	13.3 ± 1.1	13.1 ± 1.1	15.1 ± 1.5	14.0 ± 1.7	14.0 ± 1.0	13.0 ± 2.5	15.0 ± 3.5
NaHS Treatment	8.0 ± 0.6	11.1 ± 1.4	11.4 ± 1.3	11.6 ± 0.8	8.0 ± 0.8 *	11.0 ± 0.6*	12.4 ± 1.2	11.3 ± 1.3	11.0 ± 1.0	12.3 ± 1.2	9.9 ± 1.0
CVP, mmHg											
Vehicle	6.6 ± 0.9	9.0 ± 1.2	11.4 ± 2.6	10.1 ± 0.7	13.4 ± 1.6	11.9 ± 1.4	16.0 ± 5.0	11.3 ± 1.9	12.0 ± 2.1	13.0 ± 4.0	13.5 ± 2.5
NaHS Treatment	5.6 ± 0.6	10.9 ± 0.7	9.5 ± 0.8	9.9 ± 0.6	11.1 ± 1.1 *	10.0 ± 0.8	9.4 ± 1.9	8.4 ± 1.3	6.3 ± 1.0*	9.0 ± 1.0	9.0 ± 1.0
PVRI, dyne.s.cm⁻⁵.m²											
Vehicle	150 ± 7	184 ± 28	227 ± 30	187 ± 20	183 ± 21	162 ± 13	112 ± 14	77 ± 7	136 ± 31	98 ± 35	92 ± 47
NaHS Treatment	120 ± 7	146 ± 21	127 ± 16 *	151 ± 16	127 ± 11 *	135 ± 19 *	149 ± 15 *	137 ± 17*	156 ± 16	135 ± 13	144 ± 19
LVSWI, g.m.m²											
Vehicle	74 ± 4	61 ± 3	51 ± 4	56 ± 5	53 ± 2	57 ± 4	68 ± 4	86 ± 17	82 ± 17	67 ± 16	72 ± 20
NaHS Treatment	83 ± 4	69 ± 7	71 ± 7 *	66 ± 6	69 ± 7 *	67 ± 6	69 ± 7	77 ± 8	65 ± 5	70 ± 4	60 ± 4
Hct, %PCV											
Vehicle	23.0 ± 0.8	25.0 ± 2.0	25.3 ± 2.1	27.3 ± 2.0	29.0 ± 1.5	27.3 ± 1.5	25.0 ± 1.0	22.0 ± 1.2	24.3 ± 0.9	22.0 ± 3.0	24.0 ± 3.5
NaHS Treatment	21.8 ±1.4	23.1 ± 1.6	23.8 ± 1.6	23.4 ± 1.1	24.5 ± 1.2*	23.1 ± 1.5*	24.0 ± 1.8	22.0 ± 1.8	22.0 ± 1.6	22.3 ± 2.1	23.0 ± 2.3
Hb, g/dL											
Vehicle	8.3 ± 0.4	8.7 ± 0.6	9.1 ± 0.7	9.4 ± 0.6	10.0 ± 0.5	9.2 ± 0.5	9.0 ± 0.5	8.0 ± 0.3	8.1 ± 0.1	8.0 ± 0.9	8.9 ± 1.0
NaHS Treatment	7.6 ± 0.6	7.9 ± 0.4	8.3 ± 0.5	8.4 ± 0.5	8.5 ± 0.5*	8.1 ± 0.6	8.1 ± 0.6	8.3 ± 0.7	7.7 ± 0.7	7.8 ± 0.7	7.9 ± 0.8
FiO_2, %											
Vehicle	0.2 ± 0.0	0.2 ± 0.0	0.3 ± 0.1	0.5 ± 0.1	0.9 ± 0.1	0.9 ± 0.1	1.0 ± 0.0	1.0 ± 0.0	1.0 ± 0.0	0.9 ± 0.1	0.7 ± 0.3
NaHS Treatment	0.2 ± 0.0	0.2 ± 0.0	0.2 ± 0.0	0.4 ± 0.1	0.5 ± 0.1*	0.7 ± 0.1	0.8 ± 0.1	0.8 ± 0.1	0.7 ±0.1	0.6 ± 0.1	0.5 ± 0.1

Table 5.1 Cardiopulmonary hemodynamics. Values are presented as mean ± SEM. CI, cardiac index; MAP, mean arterial pressure; MPAP, mean pulmonary arterial pressure; LAP, left atrial pressure; CVP, central venous pressure; PVRI, pulmonary vascular resistance index; LVSWI, left venticular stroke work index; Hct, hematocrit; Hb, hemoglobin; FiO_2, fraction of inspired O_2. Comparisons were made using two-way analysis of variance with a Tukey-Kramer *post hoc* procedure. * $p \leq 0.05$ *vs*. control

The NaHS treatment was also observed to attenuate the calculated left ventricle stroke work index (LVSWI) at 18 and 30 hours post injury. Although there was a tendency towards hemoconcentration (Hct) in the control animals, a significantly higher Hct value was recorded at 30 and 36 hours in the control animals when compared to the NaHS treated animals. Likewise, hemoglobin (Hb) was significantly lowered at 30 hours post injury in the treated animals.

Pulmonary gas exchange

Pulmonary gas exchange [PaO_2 (arterial partial pressure of oxygen)/FiO_2 (fraction of inspired oxygen) and pulmonary shunt fraction] were calculated in all animals and are shown in Figure 5.3. Panel A and B compares the differences between the two experimental groups with (Figure 5.3A) and without (Figure 5.3B) the animals in the control group that survived the 96 hrs experiment. The combined injury was associated with a deterioration of pulmonary gas exchange, as shown by a reduction in the PaO_2/FiO_2 ratio (*top,* Figure 5.3A) associated with a marked increase in pulmonary shunt fraction (*bottom,* Figure 5.3) in vehicle-treated control animals. The PaO_2/FiO_2 ratio in these animals reached a level below 200 at 24 hrs post injury and steadily declined in the subsequent 72 hrs, indicating the presence of severe ARDS (acute respiratory distress syndrome). Treatment with NaHS, the H_2S donor compound prevented the impaired gas exchange caused by burn and smoke inhalation. The PaO_2/FiO_2 ratio remained above 200 in treated animals for 42 hrs after the initial trauma (*top,* Figure 5.3A). Moreover, we observed an improvement in gas exchange (increase in PaO_2/FiO_2 above 200) in the

treated group beginning at 72 hrs through 96 hrs. The increase in pulmonary shunt fraction was markedly decreased in the animals treated with the H_2S donor compound at 24, 36, 40 and 60 hrs (*bottom,* Figure 5.3A). The PaO_2/FiO_2 ratio in the non-surviving control animals (*top,* Figure 5.3 A) remained below 200.

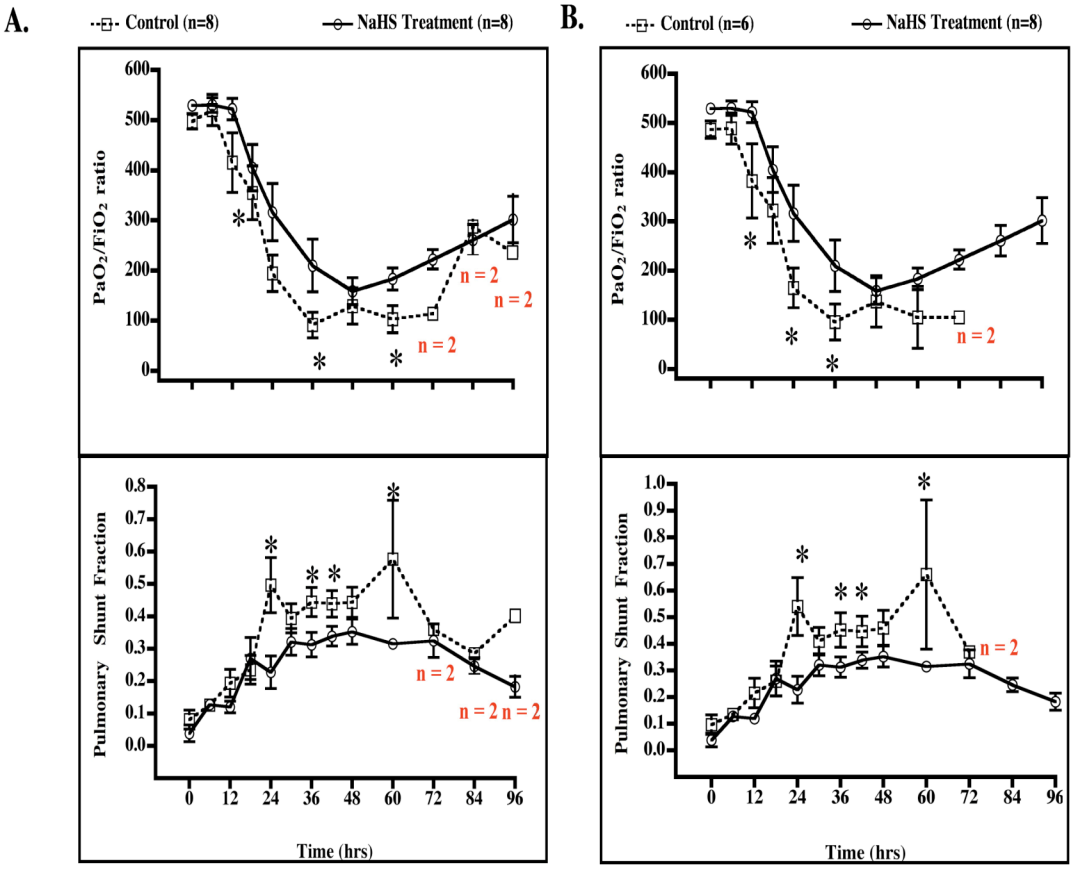

Figure 5.3 Effect of burn and smoke injury and NaHS treatment on pulmonary gas exchange. A) NaHS treatment versus all control animals; B) NaHS treatment versus non-surviving animals during the experimental period. Note that NaHS treatment after combined injury resulted in PaO_2/FiO_2 ratio recovery after 48 hrs. Comparisons were made using two-way analysis of variance with a Tukey-Kramer *post hoc* procedure. * $p \leq 0.05$ *vs*. control

Inspiratory peak and pause airway pressures were recorded from the ventilator readout. Both peak (*top*, Figure 5.4A) and pause (*bottom*, Figure 5.4A) airway pressures were especially pronounced in the control animals compared to the measured airway pressures in the treated animals.

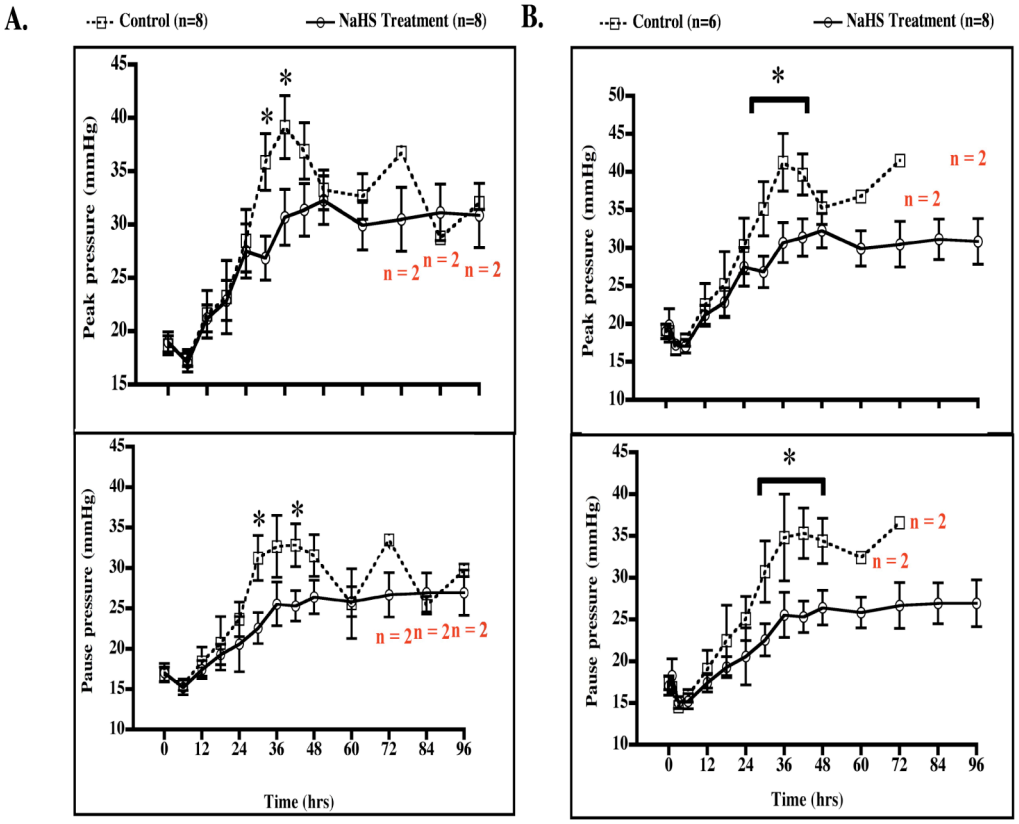

Figure 5.4 Effect of burn and smoke injury and NaHS treatment on airway pressure. A) NaHS treatment versus all control animals; B) NaHS treatment versus non-surviving animals during the experimental period. Comparisons were made using two-way analysis of variance with a Tukey-Kramer *post hoc* procedure. * $p \leq 0.05$ *vs*. control

This increase in ventilatory pressures was markedly increased in the first 48 hrs in both groups, however at 30 hours and 42 hours the peak pressure was significantly higher in the control group compared to the NaHS treated group. The H_2S donor compound had a more significant effect in the first half of the experimental period.

Changes in urine ouput and fluid accumulation

The effect of the H_2S donor compound on urine output is shown in Figure 5.5 B. At 24 and 36 hours post injury and NaHS treatment, the control animals had a significantly lowered urine output compared to the treated animals. Our data shows that the treated animals had a negative fluid balance beginning at 30 hours post injury and this was significantly different from the control animals at 36 hours (*middle,* Figure 5.5 B). A comparison of the control animals that survived versus the non-surviving animals at the 96 experimental study period showed that the H_2S donor compound reduced fluid accumulation in the treated animals compared to the vehicle treated sheep (*bottom,* Figure 5.5 panel C versus *bottom,* Figure 5.5 panel B).

Protein nitration and oxidation in lung homogenate

iNOS protein significantly increased in the lung homogenate of control animals compared with the NaHS treated animals ($p < 0.039$). Moreover, the degree of peroxynitrite formation in the lung tissue (as measured by 3-nitrotyrosine formation) was elevated in the injured control animals.

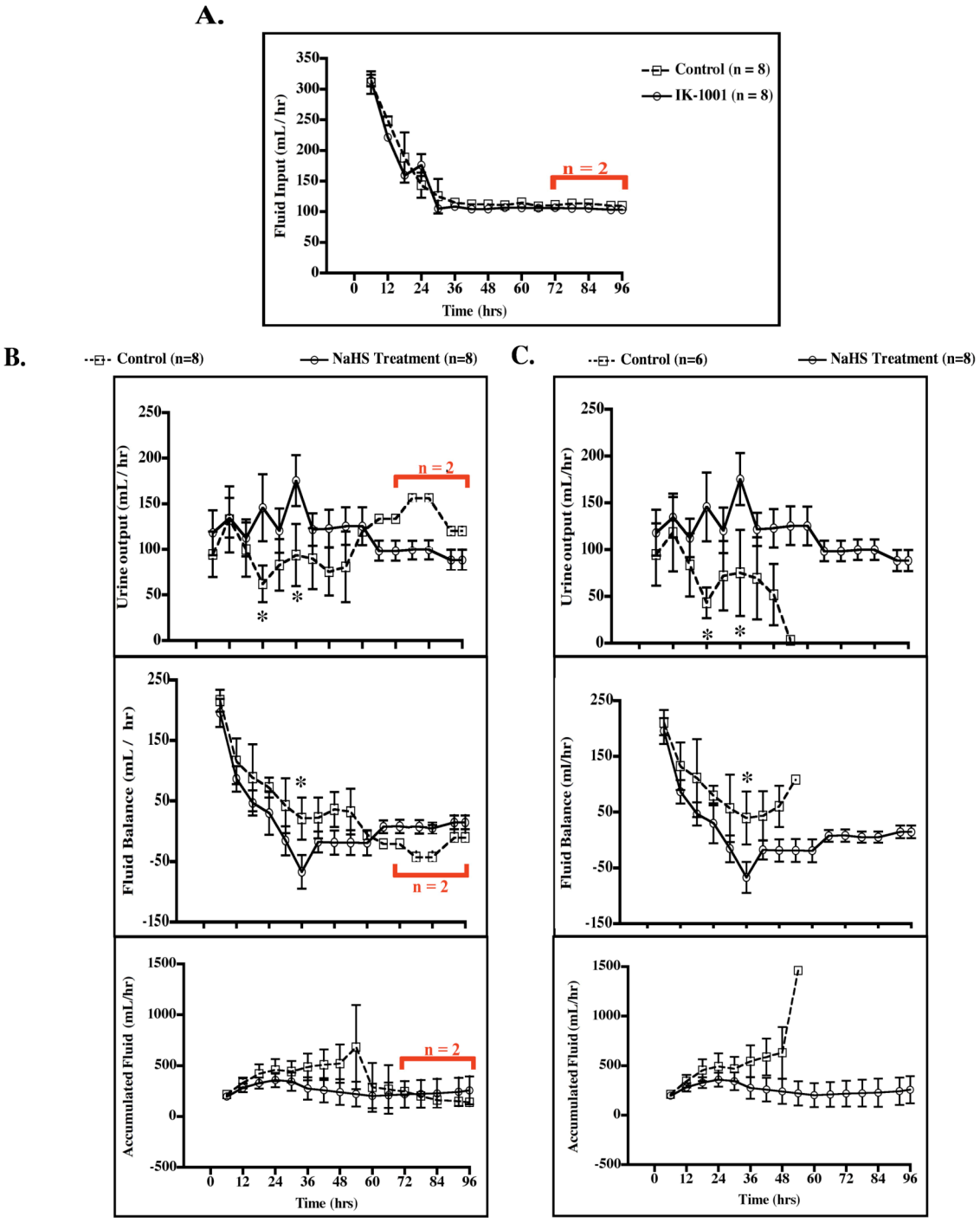

Figure 5.5 Effect of burn and smoke injury and NaHS treatment on fluid intake, urine output, fluid balance and accumulated fluid. A) NaHS did not affect fluid input; B) and C) NaHS treatment versus surviving and non-surviving animals. * $p \leq 0.05$ vs. control.

Treatment with the H_2S donor compound markedly reduced peroxynitrite formation in the lung tissue ($p < 0.043$). Protein oxidation (as measured by protein carbonyl formation) was significantly attenuated in the control animals after concomitant NaHS bolus and intravenous administration (Figure 5.6 D).

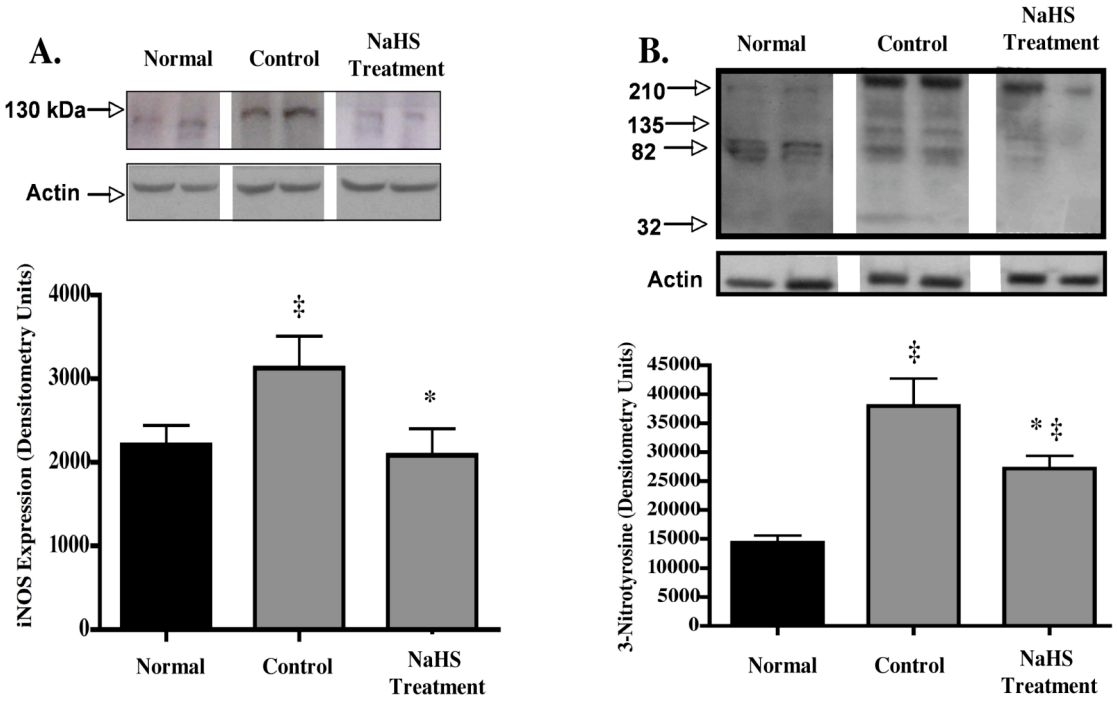

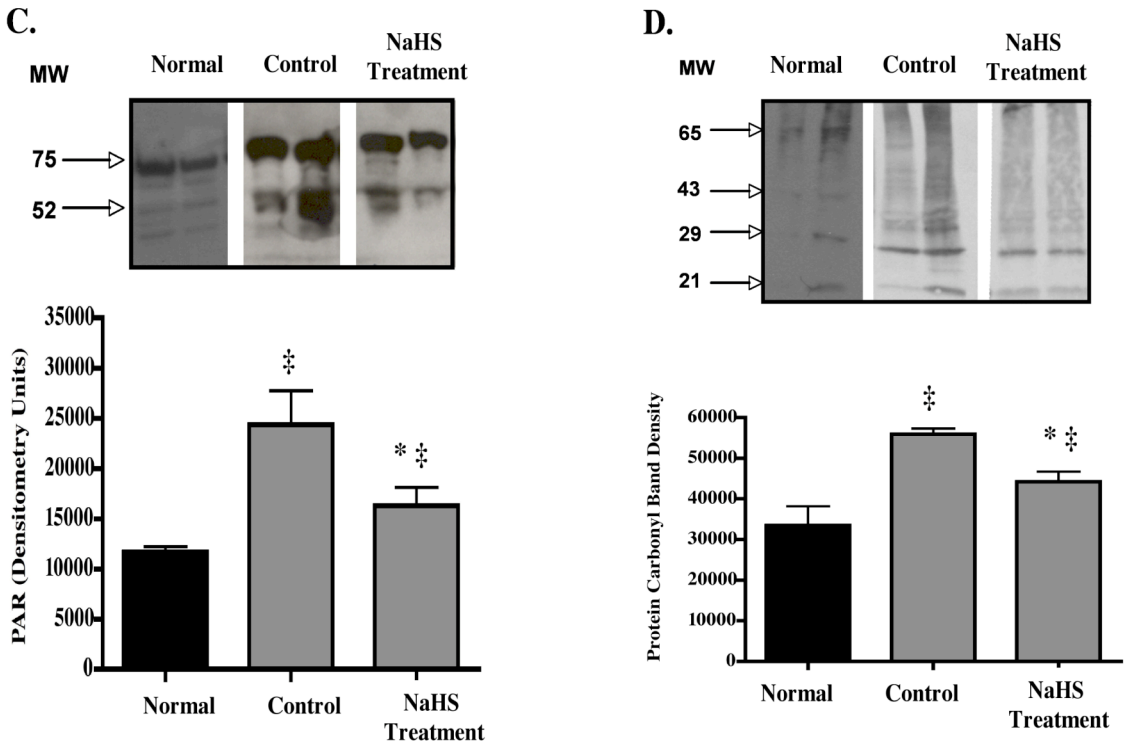

Figure 5.6 iNOS, 3-nitrotyrosine, poly (ADP ribose) polymer and protein oxidation formation in sheep lung lysate after combined burn and smoke injury and NaHS treatment. Representative Western blots of lung homogenate using (A) rabbit anti-iNOS, (B) mouse ant-3-nitrotyrosine, (C) rabbit anti-PAR antibody and (D) rabbit anti-Dinitrophenol (DNP) after protein derivatization with DNP-hydrazone. Histograms represent the integrated band intensities obtained from quantitative results of samples from four separate sheep in each group. Arrows indicate protein molecular weight; ‡ $p \leq 0.05$ vs. Normal; *$p \leq 0.05$ vs. Control.

Lung Cytochrome C ELISA

As shown in Figure 5.7, mitochondrial cytochrome c levels increased significantly in the NaHS treated group ($p = 0.0059$). There was not a significant difference in cytochromre c measurement in the cytoplasmic fraction in the control group compared to the NaHS treated group.

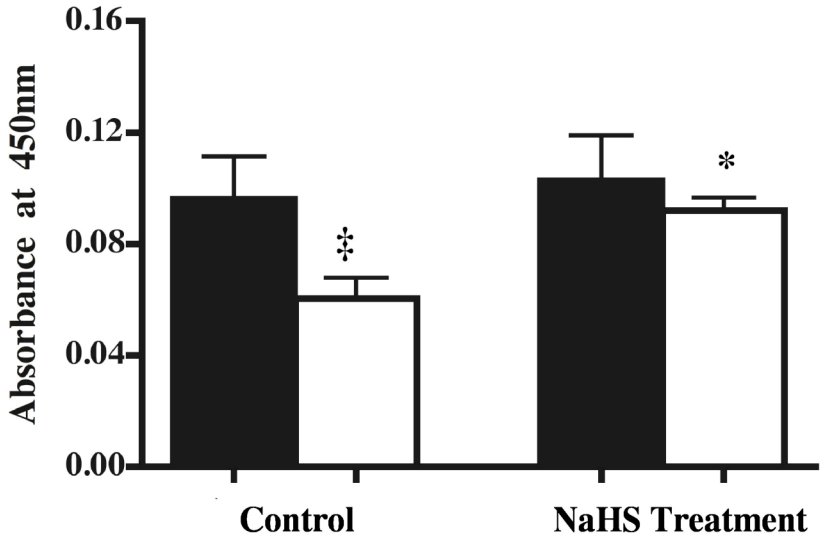

Figure 5.7 Changes in lung Cytochrome C measurement in lung tissue after burn and smoke inhalation injury and NaHS treatment. Solid bars represent cytoplasmic fraction (n = 4) and the open bars represents mitochondrial fraction (n = 4). Lung tissue was homogenized, subjected to centrifugation and the supernatant containing the cytoplamic fraction was withheld for cytochrome C measurement. The mitochondrial fraction was isolated following the protocol described in the Methods section. This experiment was repeated at least four times and the data is presented as mean ± SEM, ‡ $p \leq 0.05$ vs. cytoplasmic cytochrome C; *$p \leq 0.05$ vs. control.

Lung Wet-to-Dry ratios and lung MPO

In this experiment, treatment with the H_2S donor exhibited a trend to decrease lung MPO (4.0 ± 0.3 for control, 2.8 ± 0.5 for treatment). The difference between groups was not significant ($p = 0.059$). Likewise lung wet-to-dry weight ratio in the treated group (6.7 ± 0.6) demonstrated a trend to decrease compared to the control animals (8.9 ± 0.5). These values were not significantly different than the treated group ($p > 0.05$).

DISCUSSION

We have previously described the cytoprotective role of H_2S donor by negatively regulating the pro-inflammatory response associated with burn and smoke induced acute lung injury and increasing an anti-inflammatory response [Esechie *et al*., 2008]. In this study, our objective was to determine if, in a large animal model of ALI, the hydrogen sulfide donor could improve the measured outcomes associated with this trauma. We hypothesized that administration of intravenous NaHS, a H_2S donor compound, after burn and smoke inhalation trauma would attenuate the declining pulmonary function by reducing nitrosative and oxidative stress caused by up-regulation of inducible NOS (iNOS) enzyme. We found that the H_2S donor compound significantly reduced animal mortality compared with the vehicle-treated control animals. Additionally we observed that by 42 hrs post injury the total number of sheep in the control group was reduced by 50%. Furthermore, H_2S treatment was found to not only decrease protein nitration

(decreased 3-nitrotyrosine formation) and oxidation (decreased protein oxidation) in lung tissue after injury, but attenuate iNOS protein expression.

There are several possibilities that might explain the improvement in survival seen with H_2S donor administration. First, the animals that expired early in the control group had severely depressed oxygenation status compared to the 96 hours surviving control animals. The treated animals maintained a better oxygenation status as evidenced in the change in PaO_2/FiO_2 ratio (Figure 5.3). Although the PaO_2/FiO_2 ratio fell significantly from baseline in both groups, the rate of decline was more pronounced in the vehicle treated group suggesting a much more immediate compromise in gas exchange. There is a strong correlation between mean bronchiolar obstruction and PaO_2/FiO_2 ratio in sheep [Cox *et al*., 2003]. Cox *et al* addressed the idea of gravitational migration of obstructive cast material at 72 hours in the absence of therapeutic intervention. They observed that the bronchioles were maximally obstructed at 72 hours post injury while terminal bronchioles were obstructed at 48 hours post injury. It is well known that the obstructive material consists of sloughed airway epithelia cells, mucous and inflammatory cells. However goblet cells only exist in the cartilaginous bronchi. The mucous from goblet cells was found as far down the airway as the alveoli supporting the downward movement of airway secretions and debris.

Moderate increases in the inspiratory airway pressure was observed in the injured untreated animals in our study compared to the treated animals (Figure 5.4). This was paralleled by an increase in pulmonary shunt fraction (Figure 5.3). Our data suggests that H_2S treatment not only improves the ventilatory outcomes after injury but also blunts

HPV associated with this dual trauma. Work from our laboratory has also reported on a loss of HPV after inhalation injury in relation to the vasorelaxation aspects of NO [Westphal *et al*., 2006; Westphal *et al*., 2008].

Several reports describe significant changes in H_2S plasma levels in various disease states. Hui *et al* proposed that the endogenous concentrations of H_2S and NO are markedly increased during inflammatory states such as sepsis and shock in rats suggesting that both molecules may work independently and/or modulate each other's activity in pathological conditions [Hui *et al*., 2003]. However in another study, patients with coronary heart disease, had reduced plasma sulfide levels, from 50 μM to ~25 μM [Chang *et al*., 2008]. In our study, plasma H_2S concentration was not measured. However exogenous administration followed by increased survival and improved pulmonary function suggests a beneficial effect in increasing circulating H_2S levels after combined burn and smoke inhalation injury.

The pathogenesis of burn and smoke inhalation injury is exacerbated by both local and systemic inflammation. As demonstrated in this study, H_2S treatment significantly reduced iNOS protein expression in the lung after injury. This is in agreement with recent work by Oh *et al* who also found that NF-κB was sequestered to the cytosol after H_2S treatment thus decreasing κB dependent transcription [Oh *et al*., 2006]. A reduction in iNOS protein in our study suggests that a similar pattern of NF-κB inhibition might be a probable mechanism in attenuating the negative effects of smoke inhalation with associated thermal injury. A reduction in iNOS was paralleled with a decrease in the peroxynitrite response and protein oxidation that is characteristic of ALI. Although

neutrophil accumulation in this study was not significantly attenuated ($p = 0.059$ versus the control), there was a tendency for lower myeloperoxidase (MPO) activity in the lung after injury.

Interestingly, exogenous H_2S inhibited cytochrome c translocation from the mitochondria into the cytoplasm. Within the inter-mitochondrial space, cytochrome c is actively involved in ATP synthesis through the oxidative phosphorylation pathway. In the mitochondrion, cytochrome c shuttles electrons from the cytochrome c reductase complex to the cytochrome c oxidase complex. This transports excess electrons along the respiratory pathway and generates ATP for energy-dependent processes. However, in response to nitrosative stress, cytochrome c can be released from mitochondria into the cytoplasm as one of the initial steps before cell death [Hong *et al*., 2004]. A recent study by Du *et al* [Du *et al*., 2003] demonstrated that elevated peroxynitrite levels damages mitochondria, that results in: (i) changes in ultrastructural integrity; (ii) a reduction in the mitochondrial membrane potential; and (iii) an increase in reactive oxygen generation. In this study, we detected an increase in peroxynitrite formation and protein oxidation after injury that paralleled our finding of increased cytochrome c translocation. Likewise, we observed a significant reduction in nuclear PAR polymer generation after H_2S treatment. These findings are in contrast to a recent report by Basker *et al* [Basker *et al.*, 2007] that suggested that H_2S might act through cytochrome c and Bax protein to promote DNA damage. It is worth mentioning that the Basker group conducted their studies in an *in vitro* setting. We therefore reasoned that, in relation to the regulation of DNA integrity, factors other than the direct presence of H_2S might be operative *in vivo*, perhaps

explaining the discrepancies observed between the previously mentioned *in vitro* study and our *in vivo* system.

Several studies examining the effect of smoke alone and burn alone injuries on mitochondrial integrity have consistently reported a lower cytoplasmic cytochrome c level compared to cytochrome c mitochondrial levels in an unstimulated state [Ramage *et al.*, 2006; Zang *et al.*, 2007]. These studies, moreover, have shown that after injury with either smoke exposure [Ramage *et al.*, 2006] or thermal injury [Zang *et al.*, 2007], there is an immediate and significant increase in cytoplasmic cytochrome c protein levels within the first 4 hours. The latter study by Zang *et al.* depicted a 72-hour time course whereby cytoplasmic cytochrome c levels was shown to decrease to baseline levels at 72 hours post burn injury. Our data are limited in that they we did not measure cytochrome c in an un-injured normal sheep and we can therefore not determine how combined burn and smoke inhalation injury affect cytochrome c translocation and if the observed changes were restored to normal levels after combined injury and treatment.

In conclusion, we have demonstrated that treatment with NaHS (a H_2S donor) after burn and smoke-induced ALI/ARDS attenuate iNOS expression, peroxynitrite (as measured by 3-nitrotyrosine), protein oxidation (as measured by protein carbonyl formation) and PARP-1 activity *in vivo*. We see here that there is a shift toward survival that is in part mediated by an improvement in gas exchange, a reduction in oxidative lung injury and a decrease in fluid accumulation after burn and smoke inhalation injury.

CHAPTER 6
PROTECTIVE EFFECT OF HYDROGEN SULFIDE IN A MURINE MODEL OF COMBINED BURN AND SMOKE INHALATION-INDUCED ACUTE LUNG INJURY

INTRODUCTION

Acute lung injury (ALI) stems from a severe inflammatory response to toxic compounds such as inhaled smoke. The accumulation of inflammatory cells such as activated neutrophils, lymphocytes and macrophages in the lung is one of the hallmarks of ALI and results in severe tissue damage leading to impaired pulmonary function [Shelton *et al*., 2007]. Oxidative stress resulting from the presence of inflammatory cells contributes largely to the overall pathophysiology of ALI causing the synthesis and secretion of inflammatory mediators such as interleukin-1α (IL-1α), IL-8 [Hirani *et al*., 2001; Miskolci *et al*., 2007] and peroxynitrite [Lamb *et al*., 1999; Sittipunt *et al*., 2001] which in turn may activate other pro-inflammatory signaling pathways and increase synthesis of adhesion molecules.

Several therapeutic interventions exist today to counteract the inflammatory response associated with ALI. Recent data also suggests that hydrogen sulfide (H_2S) may modulate cell viability. For example, significant increases in cell viability were observed in murine macrophage cells pretreated with H_2S and subjected to $ONOO^-$ induced nitrosative stress [Pennings *et al*., 2004]. Additionally, cytotoxcity was attenuated in lipopolysaccharide (LPS) stimulated murine macrophages when they were pre-treated

with H_2S. The cytoprotective effect in this case was linked to attenuated nuclear factor (NF)-κB activation and subsequent nuclear translocation, and decreased κB dependent gene transcription such as inducible NOS [Oh *et al.*, 2006].

Hydrogen sulfide (H_2S) is produced endogenously via the catalytic conversion of L-cystiene by two enzymes: cystathionine β-synthase (CBS) and cystathionine γ-lyase (CSE) [Wang, 2002]. Although both enzymes are required for H_2S synthesis in some tissue, CBS acts mainly in the hippocampal and cerebellar regions of the brain [Dorman *et al* 2002] while CSE is thought to be the primary enzymatic source of H_2S in the ileum [Hosoki *et al.*, 1997], liver [Dorman *et al.*, 2002], vasculature and heart [Zhao *et al.*, 2001]. Recent studies have demonstrated the anti-inflammatory and cytoprotective effects of H_2S [Szabo, 2007]. For instance, in a study using human neuroblastoma cells, Whiteman *et al* reported on the peroxynitrite ($ONOO^-$) scavenging capabilities of H_2S [Whiteman *et al.*, 2004] thereby decreasing intracellular tyrosine nitration as well as attenuating oxidative stress. Other groups have shown that H_2S modulates leukocyte-vascular endothelium [Fiorucci *et al.*, 2005; Zanardo *et al.*, 2006] interactions in vivo, as blockade of CSE enzyme resulted in enhanced leukocyte adhesion and infiltration. Recent data also suggests that H_2S may modulate cell viability.

Although the mechanisms by which H_2S functions in preventing inflammatory cell injury are incompletely understood, Zanardo *et al* demonstrated that in the presence of excess L-cysteine, the precursor of the enzymatic synthesis of H_2S, there was not only a reduction of leukocyte infiltration after inflammatory stimulus, but there was also a

decrease in paw edema formation as a result of decreased vascular permeability in a rat model of inflammation [Zanardo *et al.*, 2006].

The objective of the present study was to investigate the effect of parenteral administration of a hydrogen sulfide donor in the presence of burn and smoke inhalation-induced ALI. We demonstrate that administration of the H_2S donor compound markedly improves survival in this model. This effect is coupled with 1) down-regulation of the concentration of IL-1β in the lung, 2) up-regulation of IL-10, a prototypical anti-inflammatory cytokine, 3) attenuated protein oxidation, and 4) improved lung histology.

METHODS

Hydrogen Sulfide Donor Formulation

Na_2S was produced and formulated to pH neutrality and iso-osmolarity by Ikaria Inc (Seattle, WA) using H_2S gas (Matheson, Newark, CA) as a starting material [Elrod *et al.*, 2007]. The NaHS formulation was diluted in normal saline to the desired concentration and used immediately thereafter. All doses were made fresh daily in a rapid fashion and sealed in sterile airtight tubes until use.

Animal model

This study was approved by the Animal Care and Use Committee of the University Texas Medical Branch in Galveston. All the animals were handled according to the guidelines established by the American Physiology Society and the National Institutes of Health. Female C57BL/6 mice weighing 20 to 26 g (4 to 6 weeks of age)

were purchased from Jackson Laboratory (Bar Harbor, ME). The animals were anesthetized using 4% vaporized isoflurane in air in a chamber, and were intubated using a custom-made endotracheal tube (modified from a 20 gauge angiocatheter, (Baxter, Deerfield, IL)), allowed to breathe spontaneously under 2% isoflurane in air. The backs and flanks of the animals were shaved and 1.0 ml of 0.9% saline was injected subcutaneously to prevent deep tissue injury and spinal cord injury by flame burn under anesthesia. The mice were randomized to 3 groups: 1) a sham group that received no injury, 2) a combined burn/smoke inhalation injury (B/S) group that received both the burn (40% total body surface area (TBSA) third-degree burn) and the smoke inhalation injury (two 30 seconds exposures of cool cotton smoke), 3) a (B/S) group treated with a treatment of sodium sulfide solution at a dose of 2 mg/kg given subcutaneousely (sc).

Burn and smoke inhalation injury

The anesthetized mice were covered with a Zetex cloth containing a rectangular opening corresponding to 40% of the mouse TBSA. A full-thickness flame burn was achieved by a Bunsen burner applied to exposed skin for approximately 10 seconds. Full-thickness injury was confirmed by loss of coloration and lack of bleeding on incision. Smoke inhalation was induced with a hand-made smoker device designed and constructed in our laboratory. The smoker, connected with tubing that provided a constant flow of air, was filled with 20 g of burning cotton toweling, and then attached to the custom-made endotracheal tube via a T connection. A copper condenser coil was placed between the smoker and the endotracheal tube to cool down the hot smoke flow.

Two sets of 30 s exposure of the cool cotton smoke were delivered. The animals were allowed to awaken after they were extubated and anesthesia was discontinued. The animals were either given the vehicle or hydrogen sulfide donor (2 mg/kg; subcutaneously (s.c.)) and were resuscitated with 0.9% saline i.p. (100 mL/kg) immediately after injury, followed by an additional injection of saline (50 mL/kg) every 24 hours during the remainder of the study period. Buprenorphine (2 mg/kg, sc) was given for analgesia in all animals every 24 hours. The animals were then returned to their cages and allowed free access to food and water.

Mortality study

Mice in all groups (n=12) were observed every 12 hours for 120 hours after the injury. No other parameters were measured in these mice.

ELISA

In a separate set of experiments, 18 mice were studied for 12 hours after injury. Lung samples from 3 groups: sham, B/S control, B/S + treatment (n=6 in each group) were collected and frozen immediately in liquid nitrogen. The tissue was homogenized using Tissue-Tearor (BioSpec Products, Inc., Bartlesville, OK) in 30 seconds bursts on ice and the homogenate was centrifuged at 5000 rpm for 30 minutes at 4°C. The supernatant was collected and ELISA kits (R&D Systems, Minneapolis, MN) were used to quantify interleukin-10 (IL-10) and interleukin-1 beta (IL-1β) following the manufacturer's manual. The Bradford assay (Bio-Rad, Hercules, CA) was used to

measure protein content in the homogenate.

Oxyblot detection of protein carbonylation

Lung samples were homogenized in 10 volumes of homogenization buffer containing 50 mM Tris/HCl, 1 mM EDTA, 1% NP-40, 150mM NaCl, 0.25% Na-deoxycholate (pH 7.4), and 1:100 Protease Inhibitor Cocktail (Sigma-Aldrich, St. Louis, MO). Protein concentration in samples was determined by the Bradford method with bovine serum albumin as standard. For detection of protein oxidation an OXYBLOT kit (Millipore, Billerica, MA) was used. The carbonyl groups in proteins were first derivatized with 2,4-dinitrophenylhydrazine (DNPH) in the presence of 6% SDS. The kit used for the oxyblot analysis is sensitive to detect as little as 10 femtomoles of dinitrophenyl residues. To determine specificity, the oxidized proteins provided by the kit were included as a positive control. Treatment of samples with a control solution served as a negative control to the DNPH treatment. After a 15 minutes incubation at room temperature the reaction was stopped.

Western Blotting and Quantification

Samples were loaded on 4-12% gradient NuPAGE Novex Bis-Tris SDS-PAGE (Invitrogen, Carlsbad, CA) gels for 60 minutes at 200 volts. Following electroblotting to 0.2 μm nitrocellulose for 1 hour at 100 volts, the membrane was blocked and stained using OxyBlot Kit methods and reagents. Bands were visualized with chemiluminescence and captured on film. The total protein carbonylated was measured by reviewing all the

bands in each sample by densitometry. Densitometry was performed on scanned films using an Alpha Imager™3400 system with AlphaEaseFC™ software (Alpha Innotech Corporation, San Leandro, CA). To quantify the amount of oxidation and allow the comparison between the various samples, oxidative index was defined as the ratio between densitometric values of the total oxyblot bands and those stained for actin.

Lung Histologic Assessment

Lung samples were fixed by complete immersion in 10% formalin for 3-5 days. Following fixation, samples were paraffin-embedded and sectioned at 5 μm and stained with hematoxylin and eosin (H&E). Masked slides were examined by two observers and patterns of morphological changes were determined by a pathologist who was blinded to the treatment protocol.

RESULTS

Hydrogen sulfide significantly prolonged survival.

Figure 6.1 depicts the results of experiments on survival rate of mice after subjected to 40% third degree burn and smoke inhalation injury. All animals in the sham group survived 120 hours (data not shown). Animals in the control group received saline vehicle alone and the observed median survival was 22 hours after injury. After the first 24 hours, only 33.3% of the control animals were alive. There was a significant increase in median survival in the mice that received hydrogen sulfide treatment (2 mg/kg, sc)

after injury ($p < 0.05$; 75 hours). In the same group, 8 out of 12 of the animals were alive during the first 24 hours.

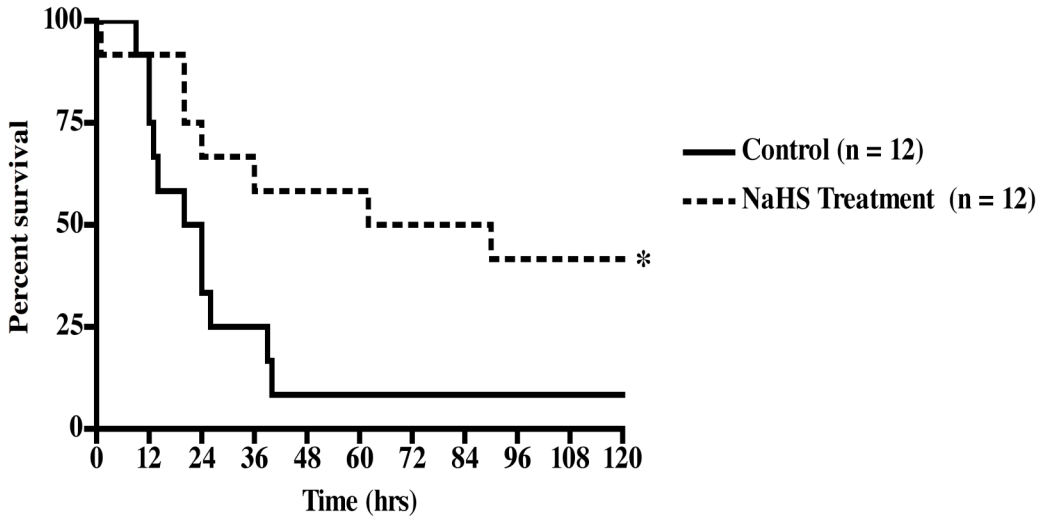

Figure 6.1 Effect of hydrogen sulfide donor on mortality after injury. Both groups received 40% third degree followed by cotton smoke inhalation injury. Compared to the untreated control animals (solid line), treatment with the hydrogen sulfide (2 mg/kg) significantly increased median survival (22 hrs in the control group vs. 76 hours in the NaHS treatment group; *$p = 0.0248$). Animals were observed every 12 hours for 120 hours. All results were combined and presented here.

Hydrogen sulfide attenuates pro-inflammatory cytokine expression and increases anti-inflammatory cytokine concentration in lung tissue.

Figure 6.2 shows the results from experiments using lung tissue to quantify IL-1β concentration after burn and smoke inhalation injury. At twelve hours after injury, the hydrogen donor compound significantly reduced the level of the pro-inflammatory cytokine (pg/mg ± SE) in the lung by 50% when compared with the control animals,

$p < 0.05$. In the presence of acute lung injury and saline treatment, IL-10 concentration was unaffected (mean pg/mg ± SE) compared with the sham group. However, there was a 2-fold increase in IL-10 concentration in the lung after injury and treatment with hydrogen sulfide donor compound compared with both uninjured and burn and smoke injured animals ($p < 0.05$).

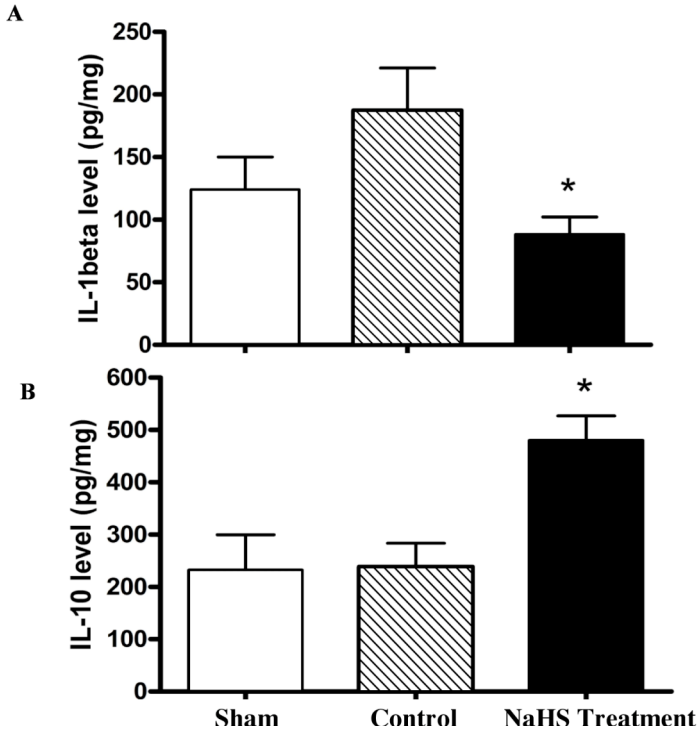

Figure 6.2 Effect of NaHS treatment on A) IL-1β concentration; B) IL-10 cytokine expression in the lung 12 hours post 40% third degree burn and smoke (B+S) inhalation injury. Data are presented as mean ± SEM for all groups of mice. At the end of the study the lungs were harvested and changes in IL -1β and IL-10 protein expression were detected by enzyme immunoassay. The sham animals were intubated but not injured, the control animals were administered the combined B+S injury followed by the saline (vehicle) treatment and the NaHS animals were administered the combined B+S injury followed by the hydrogen sulfide donor compound treatment. Experiments were repeated at least twice and the combined results are shown. *$p \leq 0.05$ vs control.

Hydrogen sulfide attenuates oxidative stress following burn and smoke inhalation.

Burn and smoke inhalation injury significantly increased the presence of protein carbonyl formation in the lung while administration of hydrogen sulfide reversed this effect and reduced protein carbonyl formation, indicative of an overall antioxidant effect.

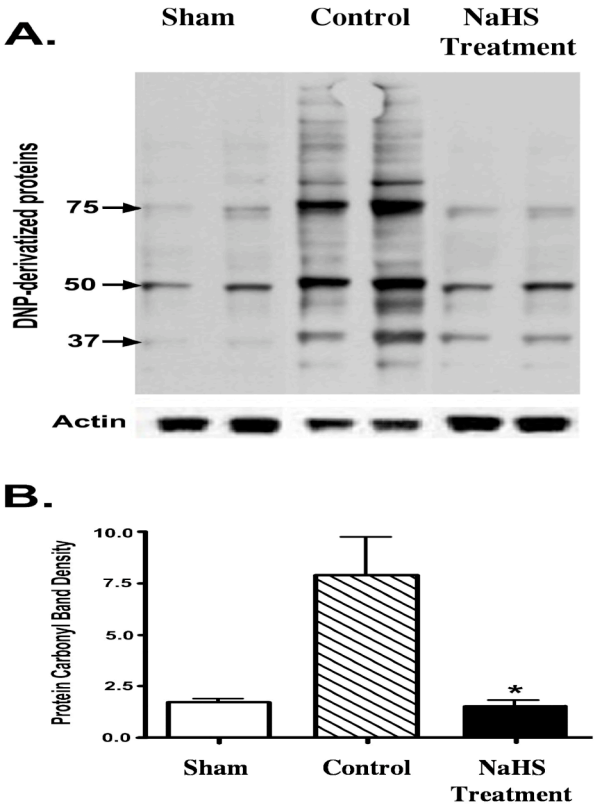

Figure 6.3 NaHS treatment decreased formation of protein carbonyl following burn and smoke inhalation injury. Data are presented as mean ± SE for all groups of mice. (A) Representative Western blots of lung homogenate using rabbit anti-Dinitrophenol (DNP) after protein derivatization with DNP-hydrazone. Each lane represents samples obtained from separate animalsin each group; (B) demonstrates the quantitative results of densitometric analysis of protein carbonyl bands expressed. The change in immunoreactivity was expressed by comparing the integrated intensities obtained with at least five different samples from each group. Arrows indicate protein molecular weight. *$p \leq 0.05$ vs control

Lung histology

Animals in the control group that received injury and vehicle showed a pattern of increased epithelial disorganization, increased presence of airway exudates and edema. Treatment with the H_2S donor attenuated this lung injury.

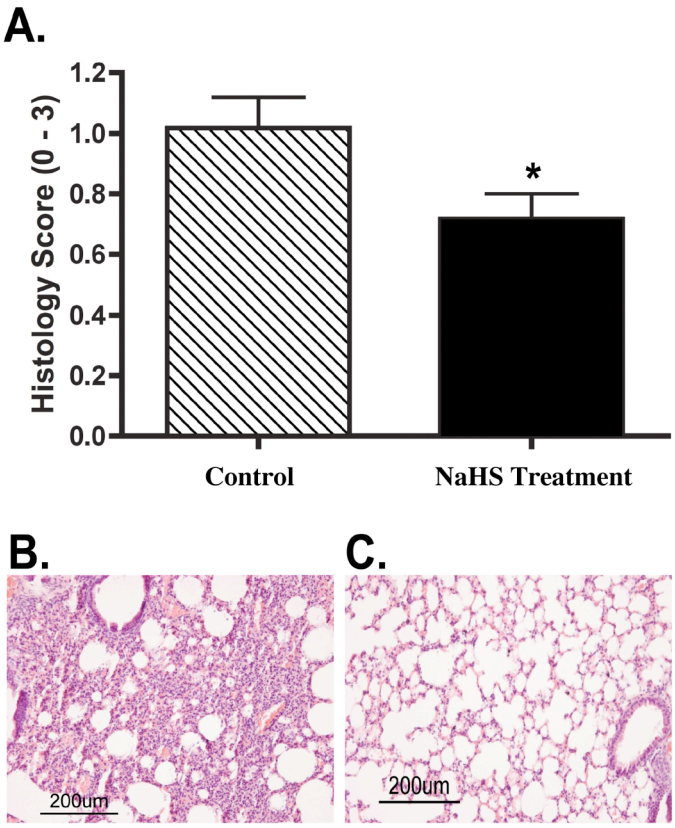

Figure 6.4 Lung histological assessment of control animals compared to NaHS treated animals at 12 hours post third degree 40% total body surface area burn and smoke inhalation injury. (A) demonstrates the quantitative results of the histological scores Representative light micrographs of H&E stained lung sections of (B) Control; (C) NaHS treated animals depict histogram of integrated scores. *$p \leq 0.05$ vs control.

DISCUSSION

This study examined the effect of parenteral administration of NaHS, a H_2S donor in a murine model of burn and smoke inhalation-induced acute lung injury. As demonstrated in this and previous studies, burn and smoke inhalation resulted in increased mortality and synthesis of pro-inflammatory cytokines. However, treatment with hydrogen sulfide improved survival, reduced the lung tissue concentration of IL-1β while the anti-inflammatory cytokine, IL-10, was up regulated. Additionally, we demonstrate that protein oxidation due to smoke inhalation is increased markedly and this effect is attenuated by H_2S administration.

H_2S has previously been shown to exert a cytoprotective effect in several animal models of inflammation and trigger the production of anti-inflammatory molecules. In our study we found that mice exposed to flame burn followed by smoke inhalation injury sustained early and high mortality whereas, H_2S treatment significantly improved survival outcomes. Relevant to our findings may be a study where H_2S was shown to "scavenge" $ONOO^-$ decrease cytotoxicity and improve cell viability in a manner comparable to reduced glutathione (GSH), a known inhibitor of $ONOO^-$ [Whiteman *et al.*, 2004]. H_2S supplementation has also been shown to induce production of GSH in levels in primary cortical neurons and thereby rescue the cells from ROS-mediated cell death [Kimura *et al.*, 2004]. Additionally on exposure to H_2S, LPS stimulated murine macrophages have been shown to not only decrease cytotoxicity but also inhibit the NF-κB transcriptional activity [Oh *et al.*, 2006]. In light of this, it is possible that exogenous

H_2S exerts if protective effects through de novo synthesis of cytoprotective proteins and/or through activation of anti-inflammatory pathways.

Understanding the mechanism by which H_2S regulates key cytokines in the presence of ALI is important as increased synthesis and secretion of inflammatory mediators is thought to contribute to the overall pathology of the injury. In large animal studies, it has previously been reported that smoke inhalation associated with burn injury, triggers the transcriptional activation of several inflammatory genes, which led to increased cellular levels of reactive oxygen species and reactive nitrogen species, and a large number of inflammatory mediators such as cytokines, chemokines and enzymes [Shimoda *et al*., 2003; Westphal *et al*., 2006]. In particular, extensive lung parenchymal damaged was observed in animals subjected to smoke inhalation. In our study, the mice were insufflated with cooled cotton smoke in order to minimize upper airway injury thus mimicking injury observed in human victims of house fires. Impaired oxygenation, as evidenced by attenuated PaO_2/FiO_2 ratios, is characteristic of this injury [Herndon *et al*., 1987].

A marked reduction of pro-inflammatory cytokine, IL-1β occurred in lung tissue of H_2S treated mice after burn and smoke injury suggesting the efficacy of H_2S in regulating neutrophil diapedesis and gene expression of adhesion proteins. A recent report [Li *et al*., 2007] demonstrated similar findings in that slow release of H_2S from a donor compound reduced inflammatory damage to the lung associated with LPS stimulus. Also, the same H_2S donor formulation used in the current study has recently been shown to reduce myocardial IL-1β levels in the heart after myocardial ischemia and

reperfusion in a murine model in vivo [Elrod *et al*., 2007]. Although the mechanistic details of how H_2S attenuates IL-1β concentration is currently unknown, it will be interesting to investigate in future studies how varying concentrations of H_2S in vivo alter the proteolytic cleavage of IL-1β from its 'pro-form' and therefore the activity.

Tissue concentration IL-10 was dramatically increased in mice treated with H_2S versus the untreated group. Although IL-10 signaling is less understood it is however widely accepted that it can inhibit immune function by suppressing adhesion molecules, inflammatory cells such as macrophages and neutrophils as well as pro-inflammatory mediators which are transcriptionally controlled by nuclear factor-κ B (NF-κB) [Asadullah *et al*., 2003]. It is therefore plausible that H_2S controls a central "switch" in the inflammatory pathways which is simultaneously responsible for both the down regulation of IL-1β and the up regulation of IL-10. A similar pattern of response has previously been reported with a number of anti-inflammatory agents including glucocorticoids, beta-receptor agonists [Szabo *et al*., 1997] and anti-inflammatory adenosine receptor ligands [Hasko *et al*., 1996].

Generation of reactive oxygen species (ROS) is a consistent observation following smoke inhalation injury [Demling *et al*., 1994; Nguyen *et al*., 1995]. Because of the potential for ROS (such as hydroxyl radicals) to induce significant damage in vivo, cells and tissues possess antioxidant systems to scavenge and eliminate ROS. However in ALI, this system is significantly overwhelmed by ROS generating cells to the extent that antioxidants such as GSH are reduced in the lung [Bunnell *et al*., 1993]. Oxidative stress

ensues, and can lead to a state of altered cellular metabolism [Ciolino *et al.*, 1997] or disruption of relevant function and systems. The physiological consequences of oxidative modification is seen where protease-antiprotease system may become imbalanced or lung function compromised by surfactant or mucous dysfunction. The extent of pulmonary protein oxidation in ARDS patients has been shown to be five times the level of oxidized proteins in control patients [Bunnell *et al.*, 1993]. In this study, we demonstrated that the H_2S donor compound was able to rescue smoke exposed lungs from oxidative stress by decreasing protein oxidation thereby improving survival. Histological changes in mice that underwent smoke exposure without treatment showed deterioration of airway epithelial organization. Earlier work by Abdi and colleagues [Abdi *et al.*, 1990] and Hubbard' research group [Hubbard *et al.*, 1991] have demonstrated significant sloughing of airway epithelium as early as 15 minutes after smoke insufflation and increased mucus production by 12 hours. In the sham animals there was evidence of damage due to intubation however the treated groups had a markedly lower mean histology score, thus supporting our finding of the cytoprotective effect of H_2S in lung tissue after smoke exposure.

In summary, these data demonstrate the H_2S exerts a protective effect in burn and smoke inhalation-induce lung injury by attenuating tissue concentration of early response pro-inflammatory cytokine and up-regulating anti-inflammatory cytokines. To our knowledge this is the first study to demonstrate the protective effects of H_2S in trauma induced acute lung injury. The current study, in combination with an emerging body of data [Fiorucci *et al.*, 2005; Zanardo *et al.*, 2006; Elrod *et al.*, 2007; Blackstone *et al.*,

2007; Wallace *et al*., 2007; and overviewed in Szabo, 2007] indicates that H_2S releasing compounds may represent a novel pharmacological intervention in the treatment of critical illness such as trauma, ischemia/reperfusion injury and inflammatory disorders [Szabo, 2007].

CHAPTER 7
SUMMARY AND CONCLUSIONS

SUMMARY

Victims of burn trauma frequently have injury to their lungs as a result of inhalation of smoke or toxic gases. Smoke inhalation is a major determinant in the mortality of fire victims. Acute lung injury results in (i) a progressive loss of pulmonary function that severely impacts gas exchange and (ii) an exaggerated inflammatory response that leads to the generation of reactive oxygen and nitrogen species (ROS/RNS).

The initial lung injury is followed by ultra-structural damage to the alveolar epithelium leading to such changes as increased septal thickening due to edema formation, airway obstruction and atelectasis. These microscopic alterations in the lung parenchyma ultimately lead to the onset of pulmonary edema and deteriorated pulmonary function, such that gas exchange becomes progressively impaired in part due to diminished hypoxic pulmonary vasoconstriction is diminished and shunt fraction increases.

The inflammatory response is a broad array of cell signals, chemokines, cytokines and cell infiltration that further stresses the lung parenchyma already undergoing dysfunction due to direct tissue damage. Burn and smoke inhalation induces iNOS protein expression in the lung followed by a cascade of inflammatory events that may persist for several hours beginning with the release of pro-inflammatory cytokines such as IL-1β and IL-8 and a decrease in anti-inflammatory cytokines such as IL-10. This is

then followed by infiltration of leukocytes at the injury site and surrounding tissue. These events create secondary damage to the initial impact and exacerbate the problems and clinical syndromes associated with acute lung injury. Prevention of these events leading to secondary injury ameliorated the decline in pulmonary function associated with ALI.

In the absence of any therapeutic intervention, the injury persists in a feed forward manner. The elevated level of inflammatory proteins is associated with a generation of reactive nitrogen species and increased protein oxidation in lung tissue. In the nuclear compartment, ROS/RNS-dependent DNA damage and activation of DNA repair enzyme poly (ADP ribose) polymerase-1 (PARP-1) is central in initiating cell death after injury. Severe DNA damage and overactivation of PARP-1, as seen in these studies, becomes less compartmentalized and begins to affect other organelles like the mitochondria. Disruption of normal mitochondrial function is evident by increased cytochrome c translocation from the inter-mitochondrial space to the cytoplasm.

CONCLUSION

In these studies, we first demonstrated the effect of burn and smoke injury on the pulmonary and peripheral vasculature in a clinically relevant model of acute lung injury. Inhibition of nitrosative and oxidative stress using NaHS, a H_2S donor compound, improves pulmonary function, attenuates cell death signals and increases survival after acute lung injury. Two possible mechanisms through which H_2S may improve outcomes after acute lung injury are 1) decreasing iNOS protein expression, 2) acting as a molecular switch in the lung such that pro-inflammatory signals are dampened while anti-

inflammatory signals are elevated, 3) decreasing the volume of fluid accumulated in the body after injury. These findings give insight into potential pharmacological interventions to improve severe lung injury.

APPENDIX

Hemodynamic Calculation

Cardiac Index (CI) = cardiac output (L/min) / total body surface area (m^2)

Pulmonary capillary pressure (PcP) = 0.4 X Pulmonary artery pressure (mmHg) + 0.6 X Left atrial pressure (mmHg)

Pulmonary Vascular Resistance Index (PVRI) = Pulmonary artery pressure (mmHg) – Pulmonary capillary wedge pressure (mmHg) X 80 / Cardiac index ($L.min^{-1}. m^2$)

Left Ventricular Stroke Work Index (LVSWI) = Stroke volume index ($ml.m^2$) X mean arterial pressure (mmHg) – central venous pressure (mmHg) X 0.0136

Shunt fraction (Qs/Qt) = $C_AO_2 - C_aO_2 / C_AO_2 - C_VO_2$

Lung wet-to-dry weight ratio calculations

Percentage of water in the blood (R) = 0.5 X dry blood weight / wet blood weight

Index of total water in the tissue (W/D) = wet tissue weight (WHW) / dry tissue weight (DHW)

Index of blood water in total lung water (f) = 2 X tissue lysate absorbance / blood supernatant absorbance

Blood-free wet-to-dry weight ratio (Q) = 0.5 X WHW X (1-f X(1-R)) – DHW / DHW – (0.5 X WHW) X R X f

REFERENCES

Abdi S, Evans MJ, Cox RA, Lubbesmeyer H, Herndon DN, Traber DL. (1990). Inhalation injury to tracheal epithelium in an ovine model of cotton smoke exposure. Early phase (30 minutes). *Am Rev Respir Dis* 142:1436-1439.

Abraham E, Matthay MA, Dinarello CA, Vincent JL, Cohen J, Opal SM, Glauser M, Parsons P, Fisher CJ Jr, Repine JE. (2000). Consensus conference definitions for sepsis, septic shock, acute lung injury, and acute respiratory distress syndrome: time for a re-evaluation. *Crit Care Med* 28:232-235.

Alcorta R. (2004). Smoke inhalation & acute cyanide poisoning. Hydrogen cyanide poisoning proves increasingly common in smoke-inhalation victims. *JEMS* 29:suppl 6-15; quiz suppl 16-17.

Asadullah K, Sterry W, Volk HD. (2003). Interleukin-10 therapy--review of a new approach. *Pharmacol Rev* 55:241-269.

Barrow RE, Spies M, Barrow LN, Herndon DN. (2004) Influence of demographics and inhalation injury on burn mortality in children. *Burns* 30:72-77.

Baskar R, Li L, Moore PK. (2007). Hydrogen sulfide-induces DNA damage and changes in apoptotic gene expression in human lung fibroblast cells. *FASEB J* 21:247-255.

Beckman JS. (1996). Oxidative damage and tyrosine nitration from peroxynitrite. *Chem Res Toxicol* 9:836-844.

Beckman JS, Beckman TW, Chen J, Marshall PA, Freeman BA. (1990). Apparent hydroxyl radical production by peroxynitrite: implications for endothelial injury from nitric oxide and superoxide. *Proc Natl Acad Sci USA* 87:1620-1624.

Beller CJ, Horvath E, Kosse J, Becker A, Radovits T, Krempien R, Berger I, Hagl S, Szabo C, Szabo G. (2007). Opposite effects of vascular irradiation on inflammatory response and apoptosis induction in the vessel wall layers via the peroxynitrite-poly(ADP-ribose) polymerase pathway. *Clin Res Cardiol* 96:8-16.

Berger NA. (1985). Poly(ADP-ribose) in the cellular response to DNA damage. *Radiat Res* 101:4-15.

Blackstone E and Roth MB. (2007). Suspended animation-like state protects mice from lethal hypoxia. *Shock* 27:370-372.

Bradford MM. (1976). A rapid and sensitive method for the quantitation of microgram quantities of protein utilizing the principle of protein-dye binding. *Anal Biochem* 72:248-254.

Brower RG, Ware LB, Berthiaume Y, Matthay MA. (2001). Treatment of ARDS. *Chest* 120:1347-1367.

Brown SD. (1998). ARDS. History, definitions, and physiology. *Respir Care Clin N Am* 4:567-582.

Brüne B, Cantoni O. (2000). Nitric oxide-mediated redox reactions in pathology, biochemistry and medicine. *Cell Death Differ* 7:1018-1020.

Bunnell E, Pacht ER. (1993). Oxidized glutathione is increased in the alveolar fluid of patients with the adult respiratory distress syndrome. *Am Rev Respir Dis* 148:1174-1178.

Burney S, Caulfield JL, Niles JC, Wishnok JS, Tannenbaum SR. (1999). The chemistry of DNA damage from nitric oxide and peroxynitrite. *Mutat Res* 424:37-49.

Chang WJ, Alvarez-Gonzalez R. (2001). The sequence-specific DNA binding of NF-kappa B is reversibly regulated by the automodification reaction of poly (ADP-ribose) polymerase 1. *J Biol Chem* 276:47664-47670.

Chang L, Geng B, Yu F, Zhao J, Jiang H, Du J, Tang C. (2008). Hydrogen sulfide inhibits myocardial injury induced by homocysteine in rats. *Amino Acids* 34:573-585.

Chen Y, Mendoza S, Davis-Gorman G, Cohen Z, Gonzales R, Tuttle H, McDonagh PF, Watson RR. (2003). Neutrophil activation by murine retroviral infection during chronic ethanol consumption. *Alcohol Alcohol* 38:109-114.

Cheng DS, Han W, Chen SM, Sherrill TP, Chont M, Park GY, Sheller JR, Polosukhin VV, Christman JW, Yull FE, Blackwell TS. (2007). Airway epithelium controls lung inflammation and injury through the NF-kappa B pathway. *J Immunol* 178:6504-6513.

Ciesla DJ, Moore EE, Johnson JL, Burch JM, Cothren CC, Sauaia A. (2005). The role of the lung in postinjury multiple organ failure. *Surgery* 138:749-757.

Ciolino HP, Levine RL. (1997). Modification of proteins in endothelial cell death during oxidative stress. *Free Radic Biol Med* 22:1277-1282.

Chiarugi A, Moskowitz MA. (2003). Poly(ADP-ribose) polymerase-1 activity promotes NF-kappaB-driven transcription and microglial activation: implication for neurodegenerative disorders. *J Neurochem* 85:306-317.

Connelly L, Palacios-Callender M, Ameixa C, Moncada S, Hobbs AJ. (2001). Biphasic regulation of NF-kappa B activity underlies the pro- and anti-inflammatory actions of nitric oxide. *J Immunol* 166:3873-3881.

Cooper GM. The Cell: A molecular approach. 2. Washington DC: ASM Press. 2000.

Cooper D, Stokes KY, Tailor A, Granger DN. (2002). Oxidative stress promotes blood cell-endothelial cell interactions in the microcirculation. *Cardiovasc Toxicol* 2:165-180.

Cox B, Emili A. (2006). Tissue subcellular fractionation and protein extraction for use in mass-spectrometry-based proteomics *Nat Protoc* 1:1872-1878.

Cox RA, Burke AS, Oliveras G, Enkhbaatar P, Traber LD, Zwischenberger JB, Jeschke MG, Schmalstieg FC, Herndon DN, Traber DL, Hawkins HK. (2005). Acute bronchial obstruction in sheep: histopathology and gland cytokine expression. *Exp Lung Res* 31:819-837.

Cox RA, Burke AS, Soejima K, Murakami K, Katahira J, Traber LD, Herndon DN, Schmalstieg FC, Traber DL, Hawkins HK. (2003). Airway obstruction in sheep with burn and smoke inhalation injuries. *Am J Respir Cell Mol Biol* 29:295-302.

Demling R, Lalonde C, Picard L, Blanchard J. (1994). Changes in lung and systemic oxidant and antioxidant activity after smoke inhalation. *Shock* 1:101-117.

Dickhout JG, Hossain GS, Pozza LM, Zhou J, Lhoták S, Austin RC. (2005). Peroxynitrite causes endoplasmic reticulum stress and apoptosis in human vascular endothelium: implications in atherogenesis. *Arterioscler Thromb Vasc Biol* 25:2623-2629.

Doerschuk CM. (2001). Mechanisms of leukocyte sequestration in inflamed lungs. *Microcirculation* 8:71-88.

Doerschuk CM. (1992). The role of CD18-mediated adhesion in neutrophil sequestration induced by infusion of activated plasma in rabbits. *Am J Respir Cell Mol Biol* 7:140-148.

Dorman DC, Moulin FJ, McManus BE, Mahle KC, James RA, Struve MF. (2002). Cytochrome oxidase inhibition induced by acute hydrogen sulfide inhalation: correlation with tissue sulfide concentrations in the rat brain, liver, lung, and nasal epithelium. *Toxicol Sci* 65:18-25.

Du L, Zhang X, Han YY, Burke NA, Kochanek PM, Watkins SC, Graham SH, Carcillo JA, Szabó C, Clark RS. (2003). Intra-mitochondrial poly(ADP-ribosylation) contributes to NAD+ depletion and cell death induced by oxidative stress. *J Biol Chem* 278:18426-18433.

Elrod JW, Calvert JW, Morrison J, Doeller JE, Kraus DW, Tao L, Jiao X, Scalia R, Kiss L, Szabo C, Kimura H, Chow CW, Lefer DJ. (2007). Hydrogen sulfide attenuates myocardial ischemia-reperfusion injury by preservation of mitochondrial function. *Proc Natl Acad Sci USA* 104:15560-15565.

Enkhbaatar P, Esechie A, Wang J, Cox RA, Nakano Y, Hamahata A, Lange M, Traber LD, Prough DS, Herndon DN, Traber DL. (2008). Combined anticoagulants ameliorate acute lung injury in sheep after burn and smoke inhalation. *Clin Sci (Lond)* 114:321-329.

Esechie A, Kiss L, Olah G, Horváth EM, Hawkins HK, Szabo C, Traber DL (2008). Protective effect of hydrogen sulfide in a murine model of combined burn and smoke inhalation-induced acute lung injury. *Clin Sci (Lond)* 115:91-97.

Fiorucci S, Antonelli E, Distrutti E, Rizzo G, Mencarelli A, Orlandi S, Zanardo R, Renga B, Di Sante M, Morelli A, Cirino G, Wallace JL. (2005). Inhibition of hydrogen sulfide generation contributes to gastric injury caused by anti-inflammatory nonsteroidal drugs. *Gastroenterology* 129:1210-1224.

Fischer SR, Deyo DJ, Bone HG, McGuire R, Traber LD, Traber DL. (1997). Nitric oxide synthase inhibition restores hypoxic pulmonary vasoconstriction in sepsis. *Am J Respir Crit Care Med* 156:833-839.

Floris R, Piersma SR, Yang G, Jones P, Wever R. (1993). Interaction of myeloperoxidase with peroxynitrite. A comparison with lactoperoxidase, horseradish peroxidase and catalase. *Eur J Biochem* 215:767-775.

Gardiner EE, De Luca M, McNally T, Michelson AD, Andrews RK, Berndt MC. (2001). Regulation of P-selectin binding to the neutrophil P-selectin counter-receptor P-selectin glycoprotein ligand-1 by neutrophil elastase and cathepsin. *Blood* 98:1440-1447.

Gilad E, Zingarelli B, Salzman AL, Szabó C. (1997). Protection by inhibition of poly (ADP-ribose) synthetase against oxidant injury in cardiac myoblasts in vitro. *J Mol Cell Cardiol* 29:2585-2597.

Goodman RB, Strieter RM, Martin DP, Steinberg KP, Milberg JA, Maunder RJ, Kunkel SL, Walz A, Hudson LD, Martin TR. (1996). Inflammatory cytokines in patients with persistence of the acute respiratory distress syndrome. *Am J Respir Crit Care Med* 154:602-611.

Ha HC, Hester LD, Snyder SH. (2002). Poly(ADP-ribose) polymerase-1 dependence of stress-induced transcription factors and associated gene expression in glia. *Proc Natl Acad Sci USA* 99:3270-3275.

Hamahata A, Enkhbaatar P, Kraft ER, Lange M, Leonard SW, Traber MG, Cox RA, Schmalstieg FC, Hawkins HK, Whorton EB, Horvath EM, Szabo C, Traber LD, Herndon DN, Traber DL. (2008). gamma-Tocopherol nebulization by a lipid aerosolization device improves pulmonary function in sheep with burn and smoke inhalation injury *Free Radic Biol Med* 45:425-433.

Hartl D, Latzin P, Hordijk P, Marcos V, Rudolph C, Woischnik M, Krauss-Etschmann S, Koller B, Reinhardt D, Roscher AA, Roos D, Griese M. (2007). Cleavage of CXCR1 on neutrophils disables bacterial killing in cystic fibrosis lung disease. *Nat Med* 13:1423-1430.

Haskó G, Szabó C, Németh ZH, Kvetan V, Pastores SM, Vizi ES. (1996). Adenosine receptor agonists differentially regulate IL-10, TNF-alpha, and nitric oxide

production in RAW 264.7 macrophages and in endotoxemic mice. *J Immunol* 157:4634-4640.

Hassa PO, Covic M, Hasan S, Imhof R, Hottiger MO. (2001). The enzymatic and DNA binding activity of PARP-1 are not required for NF-kappa B coactivator function. *J Biol Chem* 276:45588-45597.

Heck DE, Kagan VE, Shvedova AA, Laskin JD. (2005). An epigrammatic (abridged) recounting of the myriad tales of astonishing deeds and dire consequences pertaining to nitric oxide and reactive oxygen species in mitochondria with an ancillary missive concerning the origins of apoptosis. *Toxicology* 208:259-271.

Herndon DN, Traber LD, Linares H, Flynn JD, Niehaus G, Kramer G, Traber DL. (1986). Etiology of the pulmonary pathophysiology associated with inhalation injury. *Resuscitation* 14:43-59.

Herndon DN, Barrow RE, Traber DL, Rutan TC, Rutan RL, Abston S. (1987). Extravascular lung water changes following smoke inhalation and massive burn injury. *Surgery* 102:341-349.

Hirani N, Antonicelli F, Strieter RM, Wiesener MS, Ratcliffe PJ, Haslett C, Donnelly SC. (2001). The regulation of interleukin-8 by hypoxia in human macrophages--a potential role in the pathogenesis of the acute respiratory distress syndrome (ARDS). *Mol Med* 7:685-697.

Hoag JB, Liu M, Easley RB, Britos-Bray MF, Kesari P, Hassoun H, Haas M, Tuder RM, Rabb H, Simon BA. (2008). Effects of acid aspiration-induced acute lung injury on kidney function *Am J Physiol Renal Physiol* 294:F900-F908.

Hong SJ, Dawson TM, Dawson VL. (2004). Nuclear and mitochondrial conversations in cell death: PARP-1 and AIF signaling. *Trends Pharmacol Sci* 25:259-264.

Hosoki R, Matsuki N, Kimura H. (1997). The possible role of hydrogen sulfide as an endogenous smooth muscle relaxant in synergy with nitric oxide. *Biochem Biophys Res Commun* 237:527-531.

Hubbard GB, Langlinais PC, Shimazu T, Okerberg CV, Mason AD Jr, Pruitt BA Jr (1991). The morphology of smoke inhalation injury in sheep. *J Trauma* 31:1477-1486.

Hui Y, Du J, Tang C, Bin G, Jiang H. (2003). Changes in arterial hydrogen sulfide (H(2)S) content during septic shock and endotoxin shock in rats. *J Infect* 47:155-160.

Huie RE, Padmaja S. (1993). The reaction of NO with superoxide. *Free Radic Res Commun* 18:195-199.

Iijima H, Duguet A, Eum SY, Hamid Q, Eidelman DH. (2001). Nitric oxide and protein nitration are eosinophil dependent in allergen-challenged mice. *Am J Respir Crit Care Med*, 163:1233-1240.

Iijima H, Tulic MK, Duguet A, Shan J, Carbonara P, Hamid Q, Eidelman DH. (2005). NOS 1 is required for allergen-induced expression of NOS 2 in mice. *Int Arch Allergy Immunol* 138:40-50.

Ischiropoulos H, al-Mehdi AB. (1995). Peroxynitrite-mediated oxidative protein modifications *FEBS Lett*. 364:279-282.

Ischiropoulos H, Zhu L, Beckman JS. (1992). Peroxynitrite formation from macrophage-derived nitric oxide. *Arch Biochem Biophys* 298:446-451.

Janeway CA Jr, Travers P, Walport M, and Shlomchik MJ. Gibbs S, editor. Immunobiology: the immune system in health and disease. 5. New York, NY: Garland Publishing. 2001

Jinzhou Z, Tao H, Wensheng C, Wen W, Jincheng L, Qin C, Hailong Z, Weiyong L, Dinghua Y. (2008). Cyclooxygenase-2 suppresses polymorphonuclear neutrophil apoptosis after acute lung injury. *J Trauma* 64:1055-1060.

Johnson D, Hurst T, Wilson T, Murphy F, Saxema A, To T, Mayers I. (1993). NG-monomethyl-L-arginine does not restore loss of hypoxic pulmonary vasoconstriction induced by TNF-alpha. *J Appl Physiol* 75:618-625.

Kimura Y, Kimura H. (2004). Hydrogen sulfide protects neurons from oxidative stress. *FASEB J* 18:1165-1167.

Kissner R, Nauser T, Bugnon P, Lye PG, Koppenol WH. (1997). Formation and properties of peroxynitrite as studied by laser flash photolysis, high-pressure stopped-flow technique, and pulse radiolysis. *Chem Res Toxicol* 10:1285-1292.

Kogaki S, Sawa Y, Sano T, Matsushita T, Ohata T, Kurotobi S, Tojo SJ, Matsuda H, Okada S. (1999). Selectin on activated platelets enhances neutrophil endothelial adherence in myocardial reperfusion injury. *Cardiovasc Res* 43:968-973.

Kuo HP, Hwang KH, Lin HC, Wang CH, Lu LC. (1997). Effect of endogenous nitric oxide on tumour necrosis factor-alpha-induced leukosequestration and IL-8 release in guinea-pigs airways in vivo. *Br J Pharmacol.* 122:103-111.

Kurzius-Spencer M, Foster K, Littau S, Richey KJ, Clark BM, Sherrill D, Goodman RB, Boitano S, Burgess JL. (2008). Tracheobronchial markers of lung injury in smoke inhalation victims. *J Burn Care Res* 29:311-318.

Lamb NJ, Quinlan GJ, Westerman ST, Gutteridge JM, Evans TW. (1999). Nitration of proteins in bronchoalveolar lavage fluid from patients with acute respiratory distress syndrome receiving inhaled nitric oxide. *Am J Respir Crit Care Med* 160:1031-1034.

Lavrovsky Y, Chatterjee B, Clark RA, Roy AK. (2000). Role of redoxregulated transcription factors in inflammation, aging and age-related diseases. *Exp.Gerontol.* 35:521-532.

Levrand S, Pesse B, Feihl F, Waeber B, Pacher P, Rolli J, Schaller MD, Liaudet L. (2005). Peroxynitrite is a potent inhibitor of NF-kappa B activation triggered by inflammatory stimuli in cardiac and endothelial cell lines. *J Biol Chem* 280:34878-34887.

Levrand S, Vannay-Bouchiche C, Pesse B, Pacher P, Feihl F, Waeber B, Liaudet L. (2006). Peroxynitrite is a major trigger of cardiomyocyte apoptosis in vitro and in vivo. *Free Radic Biol Med* 41:886-895.

Li L, Rossoni G, Sparatore A, Lee LC, Del Soldato P, Moore PK. (2007). Anti-inflammatory and gastrointestinal effects of a novel diclofenac derivative. *Free Radic Biol Med* 42:706-719.

Liaudet L, Szabó G, Szabó C. (2003). Oxidative stress and regional ischemia-reperfusion injury: the peroxynitrite-poly(ADP-ribose) polymerase connection. *Coron Artery Dis* 14:115-122.

Liaudet L. (2002). Poly(adenosine 5'-diphosphate) ribose polymerase activation as a cause of metabolic dysfunction in critical illness. *Curr Opin Clin Nutr Metab Care* 5:175-184.

Liochev SI, Fridovich I (2003). Reversal of the superoxide dismutase reaction revisited. *Free Radic Biol Med* 34:908-910.

Liu X, Miller MJ, Joshi MS, Thomas DD, Lancaster JR Jr. (1998). Accelerated reaction of nitric oxide with O_2 within the hydrophobic interior of biological membranes *Proc Natl Acad Sci USA* 95:2175-2179.

Lorenzon P, Vecile E, Nardon E, Ferrero E, Harlan JM, Tedesco F, Dobrina A. (1998). Endothelial cell E- and P-selectin and vascular cell adhesion molecule-1 function as signaling receptors. *J Cell Biol.* 142:1381-1391.

Meyer M, Schreck R, Baeuerle PA. (1993). H_2O_2 and antioxidants have opposite effects on activation of NF-kappa B and AP-1 in intact cells: AP-1 as secondary antioxidant-responsive factor. *EMBO J* 12:2005-2015.

Miller EJ, Cohen AB, Nagao S, Griffith D, Maunder RJ, Martin TR, Weiner-Kronish JP, Sticherling M, Christophers E, and Matthay MA.(1992). Elevated levels of NAP-1/interleukin-8 are present in the airspaces of patients with the adult respiratory distress syndrome and are associated with increased mortality. *Am Rev Respir Dis* 146: 427-432.

Mineta H, Miura K, Ogino T, Takebayashi S, Misawa K, Ueda Y. (2002). Vascular endothelial growth factor (VEGF) expression correlates with p53 and ki-67 expressions in tongue squamous cell carcinoma. *Anticancer Res* 22:1039-1044.

Miskolci V, Rollins J, Vu HY, Ghosh CC, Davidson D, Vancurova I. (2007). NF-kappaB is persistently activated in continuously stimulated human neutrophils. *Mol Med* 13:134-142.

Mizutani A, Enkhbaatar P, Esechie A, Traber LD, Cox RA, Hawkins HK, Deyo DJ, Murakami K, Noguchi T, Traber DL. (2008). Pulmonary changes in a mouse model of combined burn and smoke inhalation-induced injury. *J Appl Physiol* 105:678-684.

Moncada S, Palmer RM, Higgs EA. (1991). Nitric oxide: physiology, pathophysiology, and pharmacology. *Pharmacol Rev* 43:109-142.

Moylan, JP. (1981). Inhalation injury: a primary determinant of survival following major burns. *J Burn Care Rehabil* 2:78-84.

Murakami K, Enkhbaatar P, Shimoda K, Cox RA, Burke AS, Hawkins HK, Traber LD, Schmalstieg FC, Salzman AL, Mabley JG, Komjáti K, Pacher P, Zsengellér Z, Szabó C, Traber DL. (2004). Inhibition of poly (ADP-ribose) polymerase attenuates acute lung injury in an ovine model of sepsis. *Shock* 21:126-133.

Murakami K, Enkhbaatar P, Yu YM, Traber LD, Cox RA, Hawkins HK, Tompkins RG, Herndon D, Traber DL. (2007). L-arginine attenuates acute lung injury after smoke inhalation and burn injury in sheep. *Shock* 28:477-483.

Murakami K, Traber DL. (2003). Pathophysiological basis of smoke inhalation injury. *News Physiol Sci* 18:125-129.

Nguyen TT, Cox CS Jr, Herndon DN, Biondo NA, Traber LD, Bush PE, Zöphel A, Traber DL. (1995). Effects of manganese superoxide dismutase on lung fluid balance after smoke inhalation. *J Appl Physiol* 78:2161-2168.

Niles JC, Wishnok JS, Tannenbaum SR. (2006). Peroxynitrite-induced oxidation and nitration products of guanine and 8-oxoguanine: structures and mechanisms of product formation. *Nitric Oxide* 14:109-121.

Nusbaum P, Lainé C, Bouaouina M, Seveau S, Cramer EM, Masse JM, Lesavre P, Halbwachs-Mecarelli L. (2005). Distinct signaling pathways are involved in leukosialin (CD43) down-regulation, membrane blebbing, and phospholipid scrambling during neutrophil apoptosis. *J Biol Chem* 280:5843-5853.

Oba Y, Salzman GA. (2000). Ventilation with lower tidal volumes as compared with traditional tidal volumes for acute lung injury. *N Engl J Med* 343:813.

Oh GS, Pae HO, Lee BS, Kim BN, Kim JM, Kim HR, Jeon SB, Jeon WK, Chae HJ, Chung HT. (2006). Hydrogen sulfide inhibits nitric oxide production and nuclear factor-kappaB via heme oxygenase-1 expression in RAW264.7 macrophages stimulated with lipopolysaccharide. *Free Radic Biol Med* 41:106-119.

Oliver FJ, Ménissier-de Murcia J, Nacci C, Decker P, Andriantsitohaina R, Muller S, de la Rubia G, Stoclet JC, de Murcia G. (1991). Resistance to endotoxic shock as a consequence of defective NF-kappa B activation in poly (ADP-ribose) polymerase-1 deficient mice. *EMBO J* 18:4446-4454.

Pacher P, Beckman JS, Liaudet L. (2007). Nitric oxide and peroxynitrite in health and disease. *Physiol Rev* 87:315-424.

Pacher P, Mabley JG, Soriano FG, Liaudet L, Szabó C. (2002). Activation of poly(ADP-ribose) polymerase contributes to the endothelial dysfunction associated with hypertension and aging. *Int J Mol Med* 9:659-664.

Park WY, Goodman RB, Steinberg KP, Ruzinski JT, Radella F 2nd, Park DR, Pugin J, Skerrett SJ, Hudson LD, Martin TR. (2001). Cytokine balance in the lungs of patients with acute respiratory distress syndrome. *Am J Respir Crit Care Med* 16:1896-1903.

Pearce ML, Yamashita J, Beazell J. (1965). Measurement of pulmonary edema. *Circ Res* 16:482-488.

Pennings, F.A., Bouma, G.J. and Ince, C. (2004). Direct observation of the human cerebral microcirculation during aneurysm surgery reveals increased arteriolar contractility. *Stroke* 35:1284-1288.

Perl M, Lomas-Neira J, Chung CS, Ayala A. (2008). Epithelial cell apoptosis and neutrophil recruitment in acute lung injury-a unifying hypothesis? What we have learned from small interfering RNAs. *Mol Med* 14:465-475.

Petersen B, Bloch KD, Ichinose F, Shin HS, Shigematsu M, Bagchi A, Zapol WM, Hellman J. (2008). Activation of Toll-like receptor 2 impairs hypoxic pulmonary vasoconstriction in mice. *Am J Physiol Lung Cell Mol Physiol* 294:L300-L308.

Puritt BA Jr, Goodwin CW, Mason AD Jr. and Herndon DN, editor.. Total Burn Care: Epedimiological, demographic and outcome characteristics of burn injury. 16-32. Philadelphia, PA:WB Saunders 2002.

Radi R, Cassina A, Hodara R. (2002). Nitric oxide and peroxynitrite interactions with mitochondria. *Biol Chem* 383:401-409.

Ramage L, Jones AC, Whelan CJ. (2006). Induction of apoptosis with tobacco smoke and related products in A549 epithelial cells in vivo. *J Inflamm* 3:3.

Reeve HL, Michelakis E, Nelson DP, Weir EK, Archer SL. (2001). Alterations in a redox oxygen sensing mechanism in chronic hypoxia. *J Appl Physiol* 9:2249-2256.

Rubenfeld GD, Caldwell E, Peabody E, Weaver J, Martin DP, Neff M, Stern EJ, Hudson LD. (2005) Incidence and outcomes of acute lung injury. *N Engl J Med* 353:1685-1693.

Sakurai H, Schmalstieg FC, Traber LD, Hawkins HK, Traber DL. (1999). Role of L-selectin in physiological manifestations after burn and smoke inhalation injury in sheep. *J Appl Physiol* 86:1151-1159.

Sampson JB, Rosen H, Beckman JS. (1996). Peroxynitrite-dependent tyrosine nitration catalyzed by superoxide dismutase, myeloperoxidase, and horseradish peroxidase. *Methods Enzymol* 269:210-218.

Schaaf B, Wieghorst A, Aries SP, Dalhoff K, Braun J. (2000). Neutrophil inflammation and activation in bronchiectasis: comparison with pneumonia and idiopathic pulmonary fibrosis. *Respiration* 67:52-59.

Schmalstieg FC, Keeney SE, Rudloff HE, Palkowetz KH, Cevallos M, Zhou X, Cox RA, Hawkins HK, Traber DL, Zwischenberger JB. (2007). Arteriovenous CO_2 removal improves survival compared to high frequency percussive and low tidal volume ventilation in a smoke/burn sheep acute respiratory distress syndrome model. *Ann Surg* 246:512-521.

Schreck R, Rieber P, Baeuerle PA. (1991). Reactive oxygen intermediates as apparently widely used messengers in the activation of the NF-kappa B transcription factor and HIV-1. *EMBO J* 10:2247-2258.

Shacter E. (2000). Quantification and significance of protein oxidation in biological samples. *Drug Metab Rev*. 32:307-326.

Shall S, de Murcia G. (2000). Poly (ADP-ribose) polymerase-1: what have we learned from the deficient mouse model? *Mutat Res* 460:1-15.

Sham JS. (2002). Hypoxic pulmonary vasoconstriction: Ups and downs of reactive oxygen species. *Circ Res* 91:649–651.

Shelton JL, Wang L, Cepinskas G, Sandig M, Scott JA, North ML, Inculet R, Mehta S. (2007). Inducible NO synthase (iNOS) in human neutrophils but not pulmonary microvascular endothelial cells (PMVEC) mediates septic protein leak in vitro. *Microvasc Res* 74:23-31.

Shigenaga MK, Lee HH, Blount BC, Christen S, Shigeno ET, Yip H, Ames BN. (1997). Inflammation and NO(X)-induced nitration: assay for 3-nitrotyrosine by HPLC with electrochemical detection. *Proc Natl Acad Sci U S A* 94:3211-3216.

Shimoda K, Murakami K, Enkhbaatar P, Traber LD, Cox RA, Hawkins HK, Schmalstieg FC, Komjati K, Mabley JG, Szabo C, Salzman AL, Traber DL. (2003). Effect of poly(ADP ribose) synthetase inhibition on burn and smoke inhalation injury in sheep. *Am J Physiol Lung Cell Mol Physiol* 285:L240-L249.

Shirani KZ, Pruitt BA Jr, Mason AD Jr. (1987). The influence of inhalation injury and pneumonia on burn mortality. *Ann Surg* 205: 82-87.

Sims JL, Berger SJ, Berger NA. (1983). Poly(ADP-ribose) polymerase inhibitors preserve nicotinamide adenine dinucleotide and adenosine 5'-triphosphate pools in DNA-damaged cells: mechanism of stimulation of unscheduled DNA synthesis. *Biochemistry* 22:5188-5194.

Sittipunt C, Steinberg KP, Ruzinski JT, Myles C, Zhu S, Goodman RB, Hudson LD, Matalon S, Martin TR. (2001). Nitric oxide and nitrotyrosine in the lungs of patients with acute respiratory distress syndrome. *Am J Respir Crit Care Med* 163:503-510.

Skoutelis AT, Kaleridis V, Athanassiou GM, Kokkinis KI, Missirlis YF, Bassaris HP. (2000). Neutrophil deformability in patients with sepsis, septic shock, and adult respiratory distress syndrome. *Crit Care Med* 28:2355-2359.

Soejima K, Schmalstieg FC, Sakurai H, Traber LD, Traber DL. (2001). Pathophysiological analysis of combined burn and smoke inhalation injuries in sheep. *Am J Physiol Lung Cell Mol Physiol* 280:L1233-L1241.

Soejima K, Traber LD, Schmalstieg FC, Hawkins H, Jodoin JM, Szabo C, Szabo E, Virag L, Salzman A, Traber DL. (2001). Role of nitric oxide in vascular

permeability after combined burns and smoke inhalation injury. *Am J Respir Crit Care Med* 163:745-752.

Stadtman ER. (1993). Oxidation of free amino acids and amino acid residues in proteins by radiolysis and by metal-catalyzed reactions. *Ann. Rev. Biochem* 62:797.

Suter PM, Suter S, Girardin E, Roux-Lombard P, Grau GE, Dayer JM. (1992). High bronchoalveolar levels of tumor necrosis factor and its inhibitors, interleukin-1, interferon, and elastase, in patients with adult respiratory distress syndrome after trauma, shock, or sepsis. *Am Rev Respir Dis* 145:1016-1022.

Sutyak JP, Wohltmann CD, Larson J. (2007). Pulmonary contusions and critical care management in thoracic trauma. *Thorac Surg Clin*. 17:11-23.

Szabó A, Hake P, Salzman AL, Szabó C. (1998). 3-Aminobenzamide, an inhibitor of poly (ADP-ribose) synthetase, improves hemodynamics and prolongs survival in a porcine model of hemorrhagic shock. *Shock* 10:347-353.

Szabó C, Saunders C, O'Connor M, Salzman AL. (1997). Peroxynitrite causes energy depletion and increases permeability via activation of poly (ADP-ribose) synthetase in pulmonary epithelial cells. *Am J Respir Cell Mol Biol* 16:105-109.

Szabó C, Zingarelli B, O'Connor M, Salzman AL. (1996). DNA strand breakage, activation of poly (ADP-ribose) synthetase, and cellular energy depletion are involved in the cytotoxicity of macrophages and smooth muscle cells exposed to peroxynitrite. *Proc Natl Acad Sci USA* 93:1753-1758.

Szabó C, Zingarelli B, Salzman AL. (1996). Role of poly-ADP ribosyltransferase activation in the vascular contractile and energetic failure elicited by exogenous and endogenous nitric oxide and peroxynitrite. *Circ Res* 78:1051-1063.

Szabo, C. (2007). Hydrogen sulphide and its therapeutic potential. *Nat Rev Drug Discov* 6:917-935.

Szabó C, Haskó G, Zingarelli B, Németh ZH, Salzman AL, Kvetan V, Pastores SM, Vizi ES. (1997). Isoproterenol regulates tumour necrosis factor, interleukin-10, interleukin-6 and nitric oxide production and protects against the development of vascular hyporeactivity in endotoxaemia. *Immunology* 90:95-100.

Taylor EL, Rossi AG, Shaw CA, Dal Rio FP, Haslett C, Megson IL. (2004). GEA 3162 decomposes to co-generate nitric oxide and superoxide and induces apoptosis in human neutrophils via a peroxynitrite-dependent mechanism. *Br J Pharmacol* 143:179-185.

Tedder TF, Steeber DA, Chen A, Engel P (1995). The selectins: vascular adhesion molecules. *FASEB J* 9:866-873.

Theissen JL, Prien T, Maguire J, Lübbesmeyer HL, Traber LD, Herndon DN, Traber DL. (1989). Respiratory and hemodynamic sequelae of unilateral inhalation injury of the lung. *Anaesthesist* 38:531-535.

Tomashefski JF Jr, and Matthay MA, editor. Acute Respiratory Distress Syndrome: Pulmonary pathology of the acute respiratory distress syndrome. 75-114. New York: Marcel Decker. 2003.

Toth-Zsamboki E, Horvath E, Vargova K, Pankotai E, Murthy K, Zsengeller Z, Barany T, Pek T, Fekete K, Kiss RG, Preda I, Lacza Z, Gero D, Szabo C. (2006). Activation of poly(ADP-ribose) polymerase by myocardial ischemia and coronary reperfusion in human circulating leukocytes. *Mol Med* 12:221-228.

Traber DL, Hawkins HK, Enkhbaatar P, Cox RA, Schmalstieg FC, Zwischenberger JB, Traber LD. (2007). The role of the bronchial circulation in the acute lung injury resulting from burn and smoke inhalation. *Pulm Pharmacol Ther* 20:163-166.

Villard J, Dayer-Pastore F, Hamacher J, Aubert JD, Schlegel-Haueter S, and Nicod LP. (1995). GRO alpha and interleukin-8 in Pneumocystis carinii or bacterial pneumonia and adult respiratory distress syndrome. *Am J Respir Crit Care Med* 152:1549-1554.

Virág L, Szabó E, Gergely P, Szabó C. (2003). Peroxynitrite-induced cytotoxicity: mechanism and opportunities for intervention. *Toxicol Lett* 140-141:113-124.

Wallace JL, Dicay M, McKnight W, Martin GR. (2007). Hydrogen sulfide enhances ulcer healing in rats. *FASEB J* 21:4070-4076.

Wang R. (2002). Two's company, three's a crowd: can H_2S be the third endogenous gaseous transmitter? *FASEB J* 16:1792-1798.

Ware LB, Matthay MA. (2000). The acute respiratory distress syndrome. *N Engl J Med*. 342:1334-1349.

Westphal M, Cox RA, Traber LD, Morita N, Enkhbaatar P, Schmalstieg FC, Hawkins HK, Maybauer DM, Maybauer MO, Murakami K, Burke AS, Westphal-Varghese BB, Rudloff HE, Salsbury JR, Jodoin JM, Lee S, Traber DL. (2006). Combined

burn and smoke inhalation injury impairs ovine hypoxic pulmonary vasoconstriction. *Crit Care Med* 34:1428-1436.

Westphal M, Enkhbaatar P, Schmalstieg FC, Kulp GA, Traber LD, Morita N, Cox RA, Hawkins HK, Westphal-Varghese BB, Rudloff HE, Maybauer DM, Maybauer MO, Burke AS, Murakami K, Saunders F, Horvath EM, Szabo C, Traber DL. (2008). Neuronal nitric oxide synthase inhibition attenuates cardiopulmonary dysfunctions after combined burn and smoke inhalation injury in sheep. *Crit Care Med* 36:1196-1204.

Whiteman M, Armstrong JS, Chu SH, Jia-Ling S, Wong BS, Cheung NS, Halliwell B, Moore PK. (2004) The novel neuromodulator hydrogen sulfide: an endogenous peroxynitrite 'scavenger'? *J Neurochem* 90:765-768.

Wiggs BR, English D, Quinlan WM, Doyle NA, Hogg JC, Doerschuk CM. (1994). Contributions of capillary pathway size and neutrophil deformability to neutrophil transit through rabbit lungs. *J Appl Physiol* 77:463-470.

Wolf SE, Rose JK, Desai MH, Mileski JP, Barrow RE, Herndon DN. (1997). Mortality determinants in massive pediatric burns - an analysis of 103 children with greater - than - or- equal - to 80% TBSA burns (greater - than - or - equal- to 70% full thickness). *Ann Surg* 225:554-565.

Xie QW, Kashiwabara Y, Nathan C. (1994). Role of transcription factor NF-kappa B/Rel in induction of nitric oxide synthase. *J Biol Chem* 269:4705-4708.

Yoshida K, Kondo R, Wang Q, Doerschuk CM. (2006). Neutrophil cytoskeletal rearrangements during capillary sequestration in bacterial pneumonia in rats. *Am J Respir Crit Care Med* 174:689-698.

Yu H, Venkatarangan L, Wishnok JS, Tannenbaum SR. (2005). Quantitation of four guanine oxidation products from reaction of DNA with varying doses of peroxynitrite. *Chem Res Toxicol* 18:1849-1857.

Zanardo RC, Brancaleone V, Distrutti E, Fiorucci S, Cirino G, Wallace JL. (2006). Hydrogen sulfide is an endogenous modulator of leukocyte-mediated inflammation. *FASEB J* 20:2118-2120.

Zang Q, Maass DL, White J, Horton JW. (2007). Cardiac mitochondrial damage and loss of ROS defense after burn injury: the beneficial effects of antioxidant therapy. *J Appl Physiol* 102:103-112.

Ziesche R, Petkov V, Williams J, Zakeri SM, Mosgöller W, Knöfler M, Block LH. (1996). Lipopolysaccharide and interleukin 1 augment the effects of hypoxia and inflammation in human pulmonary arterial tissue. *Proc Natl Acad Sci U S A* 93:12478-12483.

Zhao W, Zhang J, Lu Y, Wang R.. (2001) The vasorelaxant effect of H_2S as a novel endogenous gaseous K(ATP) channel opener. *EMBO J* 20:6008-6016.

Zingarelli B, O'Connor M, Wong H, Salzman AL, Szabó C. (1996). Peroxynitrite-mediated DNA strand breakage activates poly-adenosine diphosphate ribosyl synthetase and causes cellular energy depletion in macrophages stimulated with bacterial lipopolysaccharide. *J Immunol* 156:350-358.

Vita

Aimalohi Esechie was born in Benin City, Nigeria on May 17th, 1981 to Dr. Humphrey and Jovita Esechie. In 2002, after completing her bachelor's degree in Biomedical Science at Texas A&M University in College Station, she attended The Pennsylvania State University where she graduated with a master's degree in Physiology in 2004. This solidified her decision to pursue a doctorate in Physiology with an academic focus in clinical research.

The move to Galveston marked the beginning of her studies at the University of Texas Medical Branch in the Ph.D. program in August 2004. While at graduate school, Aimalohi has demonstrated herself to be a leader amongst her peers and within the Galveston community. At the University of Texas Medical Branch, she has served as a *co-chair* in the International Student Organization. She has been an active volunteer in the Luke Society (2005-2008), an organization that provides free medical assistance to the disadvantaged in the Galveston community. In 2007, she was invited to serve on the Board of the Luke Society. As a graduate student, Aimalohi has received several honors. She was given a travel award in 2007 to present her research at the 13th Annual Shock Society Conference in Baltimore, Maryland. In the same year, she received the Young Investigator Award at the 14th Annual Society of Free Radical Biology and Medicine Conference held in Washington D.C. She is also a recipient of an NIH pre-doctoral supplement grant.

Aimalohi can be contacted at 20406 Cajon Canyon Ct, Katy, Texas 77450

Education

Ph.D. Cell Physiology and Molecular Biophysics, The University of Texas Medical Branch, Galveston, Texas, mentor: Dr. Daniel L. Traber, expected graduation December 2008

M.S Physiology, Pennsylvania State University, University Park, Pennsylvania, mentor: Dr. Norman R. Harris, May 2004

B.S Biomedical Science, Texas A&M University, College Station, Texas, August 2002

Publications

Articles in Peer-Reviewed Journals

Esechie A, Jacob S, Jonkam C, Hamahata A, Enkhbaatar P, Zhu Y, Schmalstieg FC, Traber LD, Traber D, Hawkins HK and Cox RA Histological Assessment of Lung Parenchymal Injury in Sheep after Burn and Inhalation Injury (in preparation)

Lange M, Connelly R, Traber DL, Hamahata A, Cox RA, Nakano Y, Bansal K, **Esechie A**, von Borzyskowski S, Traber LD, Hawkins HK, Herndon DN, Enkhbaatar P, Combined neuronal and inducible nitric oxide synthase inhibition in ovine acute lung injury. Crit Care Med. 2008 May (in press).

Mizutani A, Enkhbaatar P, **Esechie A**, Traber LD, Cox RA, Hawkins HK, Deyo DJ, Murakami K, Noguchi T, Traber DL. Pulmonary Changes In a Mouse Model of Combined Burn and Smoke Inhalation-Induced Injury. J Appl Physiol. 2008 Apr 24.

Lange M, Hamahata A, Enkhbaatar P, **Esechie A**, Connelly R, Nakano Y, Jonkam C, Cox RA, Traber LD, Herndon DN, Traber DL. Assessment of vascular permeability in an ovine model of acute lung injury and pneumonia-induced Pseudomonas aeruginosa sepsis. Crit Care Med. 2008 Apr;36(4):1284-9.

Esechie A, Kiss L, Olah G, Horváth EM, Hawkins HK, Szabo C, Traber DL. Protective effect of hydrogen sulfide in a murine model of combined burn and smoke inhalation-induced acute lung injury. Clin Sci (Lond). 2008 Mar

Enkhbaatar P, **Esechie A**, Wang J, Cox RA, Nakano Y, Hamahata A, Lange M, Traber LD, Prough DS, Herndon DN, Traber DL. Combined anticoagulants ameliorate acute lung injury in sheep after burn and smoke inhalation. Clin Sci (Lond). 2008 Feb;114(4):321-9.

Jonkam CC, Enkhbaatar P, Nakano Y, Boehm T, Wang J, Nussberger J, **Esechie A**, Traber LD, Herndon D, Traber DL. Effects of the bradykinin B2 receptor antagonist icatibant on microvascular permeability after thermal injury in sheep. Shock. 2007 Dec;28(6):704-9.

Enkhbaatar P, Murakami K, Traber LD, Cox R, Parkinson JF, Westphal M, **Esechie A**, Morita N, Maybauer MO, Maybauer DM, Burke AS, Schmalstieg FC, Hawkins HK,

Herndon DN, Traber DL. The inhibition of inducible nitric oxide synthase in ovine sepsis model. Shock. 2006 May;25(5):522-7.

Abstracts

Esechie A, Enkhebaatar P, Jonkam C, Horváth E, Szabo C, Traber L, and Traber D Assessment of Nitrosative Stress Using an Ovine Model of Acute Lung Injury. *Society of Free Radical Biology and Medicine, Washington, D.C, October 2007*

Esechie A, Enkhebaatar P, Jonkam C, Traber L and Traber D, Early Nuclear Factor Kappa B and Vascular Endothelial Growth Factor Expression in Acute Lung Injury. *Shock Society, Baltimore, MD, June 2007.*

Jonkam CC, Enkhebaatar P, Boehm T, Traber LD, Nakano YY, Wang J, **Esechie A**, Herndon D and Traber DL. Icatibant improves microvascular leakage after thermal injury in sheep. *International Society of Burn Injury (ISBI), Toronto, Canada, October 2006.*

Esechie A, Enkhebaatar P, Nakano YY, Traber LD, and Traber DL. Relationship between antithrombin (AT) and protein C (PC) after acute lung injury and sepsis. *Shock Society, Denver CO, June 2006.*

Esechie A, Nakano YY, Enkhebaatar P, Traber LD, Herndon DN, and Traber DL. Comparison of plasma concentration of antithrombin (AT) and protein C (PC) in burn and smoke inhalation injury and sepsis. *FASEB, San Francisco, CA, April 2006.*

Enkhbaatar P, Traber LD, Burke AM, Cox R, Murakami K, **Esechie A,** Maybauer MO, Maybauer DM, Huda R, Hawkins HK, Schmalstieg FC, Herndon DN, and Traber DL. Combined antithrombin and heparin therapy reduces microvascular leakage following cutaneous burn and smoke inhalation. *Second International Symposium on Microcirculation and Mitochondrial Dysfunction in Intensive Care Medicine. Amsterdam, The Netherlands, September 2005*.